Report No. 193300-16-P

E73 10899
CR-133556

"Made available under NASA sponsorship in the interest of early and wide dissemination of Earth Resources Survey Program information and without liability for any use made thereof."

Progress Report

ERIM PROGRESS REPORT ON USE OF ERTS-1 DATA

Summary Report on Ten Tasks

Type II Progress Report
1 January through 30 June 1973

F. J. THOMSON, et al.
Infrared and Optics Division

E73-10899) ERIM PROGRESS REPORT ON USE OF ERTS-1 DATA: SUMMARY REPORT OF WORK ON TEN TASKS Progress Report, 1 Jan. - 30 Jun. (Environmental Research Inst. of Michigan) 141 p HC $9.25 CSCL 05B G3/13 N73-29248 Unclas 00899

JULY 1973

ENVIRONMENTAL
RESEARCH INSTITUTE
OF MICHIGAN
FORMERLY WILLOW RUN LABORATORIES,
THE UNIVERSITY OF MICHIGAN

Original photography may be purchased from:
EROS Data Center
10th and Dakota Avenue
Sioux Falls, SD 57198

Prepared for:
Goddard Space Flight Center
Greenbelt, MD 20771
Contract No. NAS5-21783

Reproduced by
NATIONAL TECHNICAL
INFORMATION SERVICE
US Department of Commerce
Springfield, VA. 22151

141 08

TECHNICAL REPORT STANDARD TITLE PAGE

1. Report No.	2. Government Accession No.	3. Recipient's Catalog No.
193300-16-P		

4. Title and Subtitle	5. Report Date
ERIM PROGRESS REPORT ON USE OF ERTS-1 DATA Summary Report of Work on Ten Tasks	20 July 1973
	6. Performing Organization Code
7. Author(s) F. J. Thomson, et. al.	8. Performing Organization Report No. 193300-16-P
9. Performing Organization Name and Address Environmental Research Institute of Michigan Post Office Box 618 Ann Arbor, Michigan 48107	10. Work Unit No.
	11. Contract or Grant No. NAS5-21783
	13. Type of Report and Period Covered Type II Progress Report January-June 1973
12. Sponsoring Agency Name and Address Goddard Space Flight Center Greenbelt, Maryland 20771 E. F. Szajna, GSFC Technical Monitor Code 430	14. Sponsoring Agency Code

15. Supplementary Notes

16. Abstract This second Type II Progress Report under NAS5-21783 describes the ERIM program in utilization of ERTS data as being conducted under a set of ten tasks. These tasks comprise:

I	Water Depth Measurement
II	Yellowstone Park Data
III	Atmospheric Effects (Colorado)
IV	Surveillance of Shoreline Flooding
V	Recreational Land Use
VI	IFYGL (Lake Ontario)
VII	Image Enhancement
VIII	Water Quality Monitoring
IX	Oil Pollution Detection
X	Mapping Iron Compounds

Work to date is reported and research and application plans are presented.

17. Key Words	18. Distribution Statement
ERTS Data Use, Remote Sensing, Environmental Applications, Infrared, Radar, Underflights, MSS Scanner, Ground Truth	

19. Security Classif. (of this report)	20. Security Classif. (of this page)	21. No. of Pages	22. Price
Unclassified	Unclassified	141	

PRECEDING PAGE BLANK NOT FILMED

INTRODUCTION

This Type II report constitutes the second six month summary of work performed under Contract Number NAS5-21783 by the Environmental Research Institute of Michigan (ERIM). The time period covered is from 1 January 1973 to 30 June 1973.

Ten separate and specific tasks are being pursued under the above contract. The progress to be reported for each task varies because some investigators have had suitable data to work on for some time while other investigators have only just received data. Some tasks are near the final report writing phase of their investigation. In addition, the direction taken by the various tasks is not precisely the same because task objectives differ. For these reasons, the following report includes a summary of the previous six month progress as well as results and conclusions on a task by task basis.

Objectives

The overall objective of the ERIM ERTS program is to demonstrate the feasibility of solving natural resources and environmental quality problems using ERTS collected multispectral data. Specifically, the individual task objectives are:

Task I	Detection, location and measurement of the depth of shoal areas,
Task II	Computer mapping of terrain features in the Yellowstone National Park,
Task III	Investigation of atmospheric effects on the accuracy of mapping rock types and land use categories, in Cripple Creek-Canon City, Colorado, area,
Task IV	Surveillance of shoreline flooding and erosion in the Great Lakes with simultaneous MSS and radar imagery.
Task V	Mapping of land uses and physical characteristics in SE Michigan to identify areas for recreational uses and open space preservation,
Task VI	Delineate air-water-land interactions in the Lake Ontario Basin as a contribution to the IFYGL.
Task VII	Development of image enhancement and advanced information extraction techniques for ERTS MSS data,
Task VIII	Detection of water pollution and monitoring of water quality for four ocean areas and two lake areas,
Task IX	Detection and monitoring of oil pollution in coastal areas from ships and barges, industrial discharges and major incidents (tanker break-up and oil well leaks), and
Task X	Detection and mapping of iron compounds and related geologic features in Wyoming (Atlantic City District at SE end of Wind River Range).

Scope

ERTS produced imagery and MSS data (digital tapes) are being studied using human interpretation and computer processing. The resulting mapping and analyses will permit the assessment of satellite produced information in contributing to these specific natural resource and environmental problems. Wherever possible, we are using software previously developed for the analysis of multispectral data collected by aircraft scanners. Formatting programs have been developed to facilitate use of ERTS-CCT's at ERIM.

All tapes are registered in a data management system for reference and to facilitate return of data to NASA when the contract ends. During this reporting period, we began to survey all ERTS imagery in house and enter data about the imagery in the data management system as well. This job is a larger one than the registration of tapes because we have imagery for many frames for which we do not have tapes, and imagery is additionally received from the EROS Data Center at Sioux Falls as well as NASA-Goddard.

SIGNIFICANT RESULTS REPORTED

Several of the tasks have produced significant results in extracting information from ERTS data. These are summarized as follows:

1. Absolute water depth can be calculated from a ratio of signals from bands MSS 4 and MSS 5. The method requires return of a signal from the bottom in the two spectral bands. The technique has been shown to be effective for depths of up to 5 meters at a test site in the Bahamas. The ultimate utility of the ratio method is compromised by the detrimental effect of signal variations (on CCT's) among detectors within a single band. (Polcyn and Lyzenga)

2. A 13 category terrain feature classification map of Yellowstone National Park has been produced using supervised pattern recognition techniques. Precise location of training sets in the data was accomplished using RB-57 photography and a Variscan film viewer (Roller and Thomson). The categories recognized are felt to be significant a) for providing information inputs into National Park Service management policies and b) for ecological studies of wildlife habitat and revegetation patterns following old forest fire burns.

3. ERTS data has been shown to provide a detection and monitoring capability for a number of water quality problems associated with off-shore ocean dumping sites and inland lakes. Locations and extent of acid-iron wastes and other turbidity anomalies associated with variability in suspended solids concentrations can be determined in the New York Bight. In addition, circulation dynamics within Lake Erie have been mapped from ERTS data to provide information on the spread and movement of major tributary sources of pollution (Wezernak).

4. A corrected ratio of bands MSS-5 and MSS-7 signals has been formed. Individual signals are corrected for path radiance by subtracting darkest object signal levels in each band. The ratio is normalized by dividing by the expected ratio of one scene category. This ratio, when appropriately sliced, yields maps of iron deposits, limestones, and vegetated areas. Further, the decision boundaries of the normalized ratio have been shown to be relatively independent of the time of data collection -- a promising result in signature extension (Vincent).

5. A concise format has been devised for storing the ratio signatures of geologic rock and mineral materials determined from laboratory reflectance spectra contained in the NASA Earth Resources Spectral Information System (ERSIS). The data provide a method for assessing the discriminability of natural materials in ERTS spectral regions prior to processing ERTS data. Further work will determine the degree to which laboratory data results can be used to help construct recognition maps from ERTS data (Vincent).

6. Results of work in advanced information extraction techniques demonstrate: a) that a signal variability exists among ERTS detectors in any one spectral band that will impact users doing quantitative analysis on successive ERTS images; b) a newly developed computer-aided procedure for correlating ERTS pixels to ground features, c) the strong influence of atmospheric effects in ERTS data, and d) area estimation accuracies are better using the ERIM proportion estimation algorithm than for conventional recognition techniques (Malila and Nalepka).

RECOMMENDATIONS

During this reporting period, we requested and received a pass at high sensor gain over the New York Bight area. The gain was increased by factors of 3 in bands MSS-4 and MSS-5 to better portray signal variations in the water on a pass of May 13. Preliminary examination of the imagery at the browse facility at Goddard reveals that apparently no land information was lost because of clipping but cloud signals were clipped.

We recommend that NASA give serious thought to collecting other data at high gain and consider doing so for areas smaller than one whole pass. We feel that such operation will enhance the utility of ERTS-MSS data for earth resources investigations.

Second Type II Progress Report
F. C. Polcyn, MMC 063
Task I, Water Depth Measurement

INTRODUCTION

This task objective is to demonstrate feasibility of measuring water depth using the ERTS-1 MSS sensor. Two test sites were chosen, one near Puerto Rico and the second in Upper Lake Michigan. However, since cloud cover has limited the amount of usuable data from both of these sites, an alternate data set from the Little Bahama Bank was selected. This data was used to test the computer model developed for calculation of water depth by ratioing channel 4 and channel 5. This test was successful and depths were calculated [1]. The capability that this test portends will be useful for updating navigational charts, reducing hazards to shipping, aiding location of fishing grounds and in monitoring changes to shoreline topography from storms and currents.

PROGRESS

The use of ERTS-1 digital tape data for October 10, 1972 of the Little Bahama Bank has been successful in showing the feasibility of measuring shallow depths with the four channel MSS. Two depth maps of this area were produced. The first one (see Fig. 1) used the level slicing technique for channel 4 only because light penetration in that band is the best of the four ERTS bands presently in use. This method gives an indication of relative depths within the scene, and is useful for identifying bottom features and locating possible navigation hazards.

A second, more quantitative technique involves taking the ratio of the signals in two MSS channels. If the water attenuation and bottom reflectance are known, this method gives a specific value for the depth of water in those areas where a bottom signal is returned to the sensor in at least two wavelength bands.

This procedure was followed and a color coded digital depth map was constructed as shown in Fig. 2. The maximum depth for which this map is valid is 5 meters. This limitation is due mostly to the light penetration characteristics of band 5, the next best light penetration channel of the MSS. Heavy blue symbols are the deepest waters, reds and light blue tones are the shallower waters and green is the land area.

---

[1] Polcyn, F. C. and D. R. Lyzenga, "Calculations of Water Depth from ERTS-MSS Data", 193301-9-S/S$_a$/J, Presented at the March 5-9, 1973 ERTS-1 Symposium on Significant Results, New Carrollton, Maryland.

One should also note that only every sixth line and every sixth resolution element was used in the construction of this map. This was decided upon the basis of a statistical analysis of the noise variations across the six detectors in each spectral band. The variations from detector to detector within a given band was deemed too large for use in the ratio processing especially within the relatively small integer range of signals presently assigned for ERTS-1 data over water areas.

A request to ERTS-1 Operations personnel for a data set to be taken at the high gain position instead of the normally operated position resulted in a test made when the ERTS-1 passed over the New York Bight area. New details in the water patterns were reported to be visible in the new set of data. Unfortunately, first reports of the length of the test run gave an indication that as the satellite passed over the Bahamas the gain position was returned to normal. Further attempts are being made to obtain the data of the Little Bahama Bank with the ERTS MSS at high gain position for comparison with the October 10, 1972 data previously analyzed.

Data obtained from ERTS-1 for the Upper Lake Michigan test area had previously shown too much cloudiness. On May 5 and again on May 22, 1973, useful clear imagery was obtained for this area so that the investigation can proceed for this freshwater test site.

As is well known, the tape recorder lifetime has been exceeded so that limited useful data for the Puerto Rico test area is forthcoming. Previously obtained data has been hampered by excessive cloudiness.

NEW TECHNOLOGY

Software has been developed for use with ERTS data tapes to produce digital maps of water depth. Water depth is calculated at each point in the scene, from the formula

$$z = \frac{1}{f(\theta,\phi)(\alpha_1-\alpha_2)} \ln \frac{k_1 V_1 H_1 \rho_1}{k_2 V_2 H_2 \rho_2}$$

where
- z = water depth
- α_1, α_2 = extinction coefficients of water at two different wavelengths
- ρ_1, ρ_2 = bottom reflection in two different bands
- k_1, k_2 = constants of the instrument which are known
- H_1, H_2 = incoming solar radiation
- V_1, V_2 = analog signals observed in the multispectral scanning of the shallow features
- $f(\theta,\phi)$ = sec θ + sec ϕ
- θ = scan angle
- ϕ = solar zenith angle

The resulting values of z are then classified into arbitrary intervals, and a different symbol is printed out on the map for each depth interval.

An alternate method of producing depth contour maps is being considered. This would print out symbols only at points where the calculated depth is equal to certain specified values, leaving blanks at all other points. This would result in maps similar in format to Hydrographic Office depth charts, which might be more convenient to some users.

PROGRAM FOR NEXT REPORTING INTERVAL

The first priority is to obtain a high gain MSS data set on computer compatible tape for a suitable test area such as the Little Bahama Bank which is in range for direct readout of ERTS-1 data by the receiving station on the East Coast. Also, a visit to the test site to confirm discoveries of uncharted shallow features is planned for the next period.

The next step would be to analyze the data set for evidence of improvement over the results for October 10, 1972. In addition, a demonstration of mapping water depth on the shoreline of Lake Michigan is planned as representative of the technique capability with different water, bottom, and topography characteristics in order to generalize the results of the technique.

With successful demonstrations obtained, the next step is the transfer of this information to agencies most likely to benefit from such capability. Included in these are NOAA, NAVY, U. S. Lake Survey, U. S. Army Corps of Engineers, EPA and the appropriate State's Water Resources Commissions as well as the International Hydrographic Office which has responsibility for coordinating efforts to update world navigation charts.

CONCLUSIONS AND RECOMMENDATIONS

The multispectral ratio technique for shallow water depth measurements works. Its accuracy needs to be further checked, and the input data refined. With ERTS-1, that means more data should be collected at the high gain setting. Other spectral interval choices can be checked with the Skylab S-192 sensors. User agencies should be alerted to the new potential for updating navigation charts and assessing changes after storms and current action. Cost comparisons of the different measurement techniques should be carried out in order to assess the proper role for satellite-obtained depth maps.

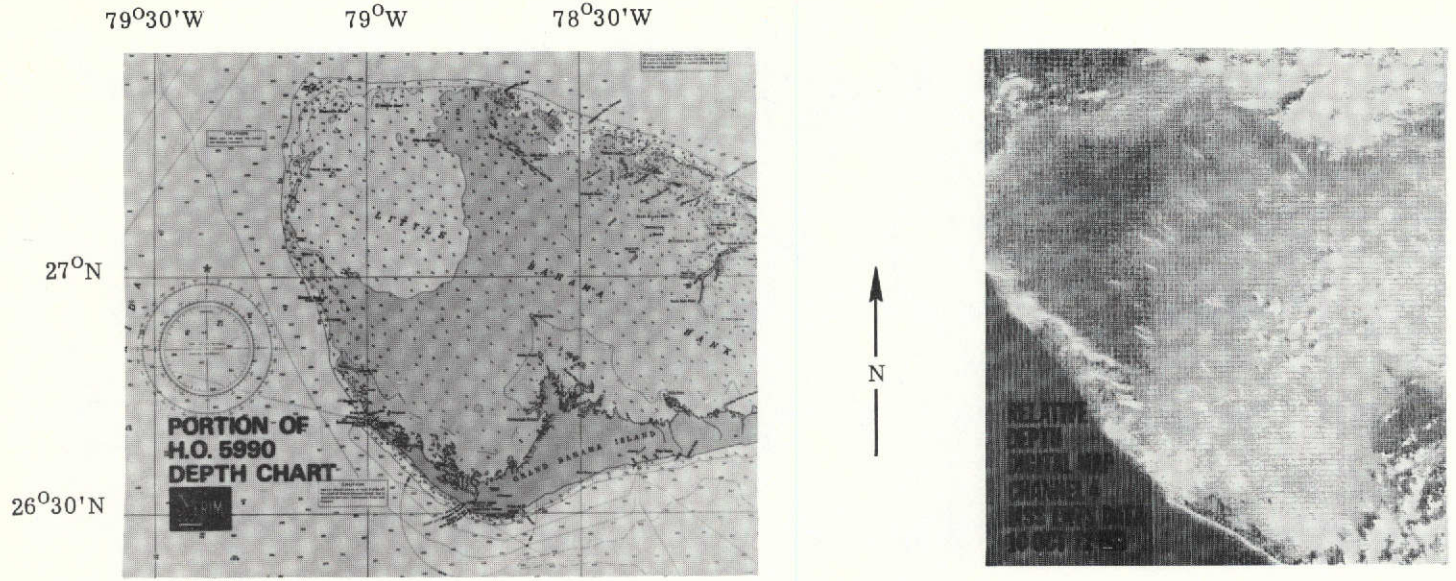

FIGURE 1. RELATIVE DEPTH MAP OF LITTLE BAHAMAS BANK (RIGHT) SHOWING SEVERAL UNDERWATER FEATURES NOT SHOWN ON THE HYDROGRAPHIC OFFICE CHART (LEFT) OF THE SAME AREA

ERIM
FORMERLY WILLOW RUN LABORATORIES, THE UNIVERSITY OF MICHIGAN

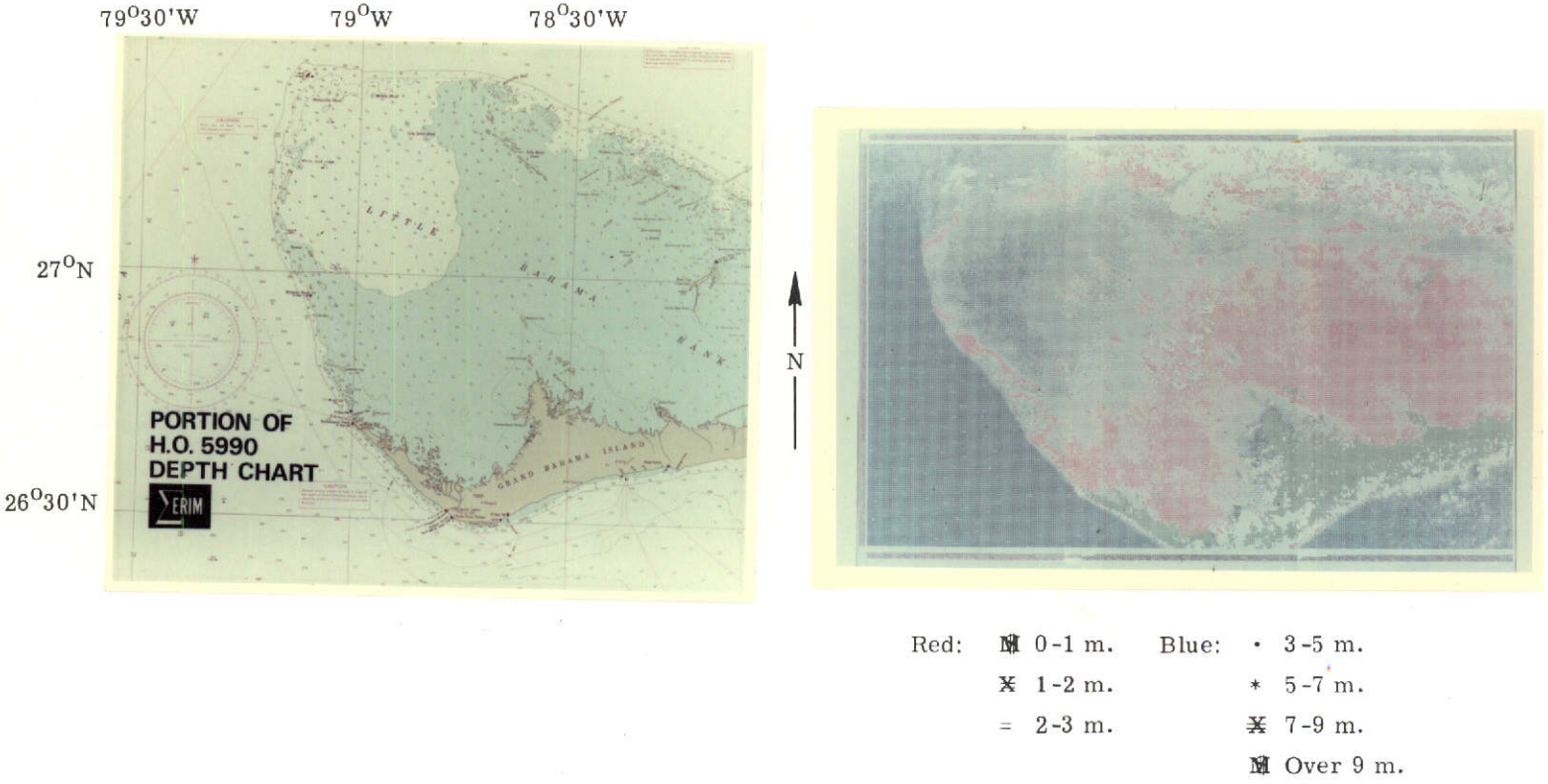

FIGURE 2. COMPUTER-GENERATED ABSOLUTE DEPTH MAP (RIGHT), AND HYDROGRAPHIC OFFICE DEPTH CHART (LEFT) FOR COMPARISON

ERIM
FORMERLY WILLOW RUN LABORATORIES, THE UNIVERSITY OF MICHIGAN

Second Type II Progress Report
Frederick J. Thomson, MMC 077
Task II, Yellowstone Park Data

INTRODUCTION

A fundamental task of the National Park Service under Yellowstone's new Master Plan for park management is that of assigning geographic areas within the park to their optimum role in meeting important multiple-use needs, in accordance with established criteria for protection of the environment. Although specific management measures for accomplishing this goal are to be identified through "mission oriented" research, their implementation is certain to require an organized body of data on the type and distribution of natural resources throughout the park.

The objective of this project is to prepare detailed vegetation and terrain feature maps for Yellowstone suitable for these many purposes using ERTS-A MSS data. The completion of these maps will mark the first time a park-wide environmental inventory of Yellowstone has been available as a basis for management planning. These maps will not only provide an up-to-date record of conditions within the park, but will, in addition, serve as quantitative baseline data for monitoring natural ecosystem development and the ecological consequences of management decisions over extended periods of time.

The project is a cooperative one between ERIM, Dr. Harry Smedes of U.S.G.S. and Mr. Don DeSpain of N.P.S.

PROGRESS

Preliminary 5 Category Cover Type Recognition Map

Computer compatible tapes of bulk processed MSS data for the 7 August 1972 (frame 1015-17404) overflight of the test site were received in early December. The decision to process this data reflected both the fact that this orbit marked the first cloud-free observation of the park, and, from an ecological consideration, occurred during a period of distinctive seasonal differences in vegetation cover type appearance.

ERIM's initial task consisted of converting the data on the ERTS tapes to a format compatible with in-house software programs, and subsequently generating a digital graymap of MSS 5 (red band) for the entire park. A copy of this map was sent to Dr. Smedes in mid-December for his use in transcribing cover type training set locations onto a common base. A list of these training sets, along with their respective environmental parameters and graymap coordinates, was transmitted to ERIM by Dr. Smedes in January. ERIM then began an extensive program centered around the extraction and analysis of multispectral statistical signatures for the training sets, which comprised our effort for February. Based on the environmental complexity of cover types observed during this period, a decision was made to initially produce a basic, 5 category map representing the endpoints of important spectral and environmental cover type continua. We reasoned that

it was important initially to determine the level of recognition accuracy we could attain using spectral categories which were easily distinguishable.

The 5 category map was produced in early March and reported in a paper, "Terrain Classification Maps of Yellowstone National Park," given at the GSFC during the March 5-9 ERTS Symposium. An analysis of recognition accuracy for the five categories resulted in the following hierarchial ranking:

1. water
2. coniferous forest
3. light rock
4. grasslands
5. wet meadows

Estimations of recognition success based on percent area correctly classified indicate overall map accuracy greater than 82 percent.

Final Cover Type Recognition Map

In an attempt to resolve the causes underlying poorer recognition associated with the grassland and lowland meadow types of the 5 category map, refine these and the other categories, and enlarge upon the total number of training sets, Mr. Ralph Root a Colorado State graduate working for Dr. Smedes, spent a week at ERIM in April. During his visit, high altitude RB-57 color and color infrared photography of the park was examined on a VARISCAN. The optical enlarging capability of the VARISCAN permitted us to closely match scales between a scene viewed on the film and the graymaps. Not only was identifying an appropriate training set on the film much easier, but transcription of this location onto the graymaps was far more accurate.

As a result of this analysis, several of the original training sets, especially those in the grasslands and lowland meadows categories were found to be less homogeneous than previously believed. This appears to be the major explanation for the poorer recognition of these types in the preliminary map.

On this premise, we proceeded with another program of signature extraction and analysis for refined versions of original training sets and some representing several new categories. This work occupied our efforts for May. The results of our findings at the end of this period, based solely on training set signature separation, indicated we now had 18 potential categories for inclusion in the final map. The categories were:

1. Lodgepole pine (young-dense type)
2. Lodgepole pine (mature-more open type)
3. Douglas Fir
4. Spruce-Fir
5. 30-45% Conifer cover over rock rubble
6. 30-45% conifer cover over grass
7. 15-30% conifer cover over rock rubble
8. 15-30% conifer cover over grass
9. Wetland shrubs
10. Upland grass
11. Lowland grass
12. Grass-Brush mixture
13. Brush
14. Dark Rock
15. Light Rock
16. Thermal deposits
17. Alpine Meadows
18. Water

Recognition maps of these 18 cover types were generated for restricted test areas within the park and sent to Dr. Smedes for his evaluation of their accuracy.

Based on Dr. Smedes' and Mr. Root's findings, several steps were taken preparatory to more extensive mapping. First, the category alpine meadow was dropped because of excessive recognition commission errors as light rock. Similarly, a disappointing number of recognition commission errors between categories of morphologically similar vegetation types prompted us to combine several similar, categories. Included in this situation were the merging of the two Lodgepole pine types, Douglas Fir and Spruce Fir categories back into a single coniferous forest type, and merging of the upland and lowland grass types into a single grasslands category.

In the case of the forest species, it is possible that many of the recognition commission errors resulted from varying signal contributions of path radiance in MSS 4 and 5. Comparison of signal means in these channels for the various forest species (Table 1) reveals they are rarely more than 1 to 2 data values apart. By our estimations, path radiance at critical altitudes within the park was at least this great. This was determined by comparison of MSS 4 signal levels for deep-pure water from two lakes at elevations of 6000'-7000'. A signal increase of 1.11 data values attributable to path radiance was observed for the water signature at the lower elevation.

Recognition processing of the entire park was completed in June, using the following 13 categories:

1. Coniferous Forest
2. 30-45% conifer cover over rock rubble
3. 30-45% conifer cover over grass
4. 15-30% conifer cover over rock rubble
5. 15-30% conifer cover over grass
6. Wetland shrubs
7. Grasslands
8. Grass-Brush mixture
9. Brush
10. Dark Rock
11. Light Rock
12. Thermal Deposits
13. Water

The classification output was then mapped and sent to Dr. Smedes and Mr. DeSpain.

Dr. Smedes, Mr. Root and Mr. DeSpain are currently concentrating on evaluating the recognition accuracy of this latest product. Additionally, Mr. DeSpain is beginning an assessment of its impact on National Park Service management - decision processes.

B

PROGRAM FOR NEXT REPORTING INTERVAL

Contingent upon Dr. Smedes and Mr. DeSpain finding satisfactory recognition accuracy of cover types, we anticipate immediately proceeding with preparation of the final map. This will be a color product produced on Data Corporation's (Dayton, Ohio) concise-Display Device, yielding a 40" x 60" every data point map for the entire park.

Preparations for report writing are also underway at this point, and generation of this document will occupy the majority of the remainder of ERIM's time on this project.

NEW TECHNOLOGY

None

CONCLUSIONS

This project is expected to contribute much new ecological knowledge about the Yellowstone landscape. In particular, the revegetation patterns of old wildfire burns are being analyzed to determine successional trends occurring in the park. This information should have a significant impact on the Park Service's fire protection and wildlife management programs.

On a more general level, we are working closely with Mr. DeSpain to determine if there are more desirable, or additional formats in which to present data abstracted from the final map, in terms of making it a more effective part of or basis of the "mission oriented" research involving formulation of Yellowstone's future management policies.

One format we are currently experimenting with is the production of thematic maps. Small examples of these have been made illustrating important ecological cover type continuua, e.g., forest to bare rock, and forest to grassland. This type of information on vegetation type boundaries and transitions has considerable value in the management of "edge" species, i.e., plants or animals that depend entirely, or in part, on the ecological character of a transition zone between major cover types for their existance.

We are also interested in investigating a method of automatically computing from the map data the acreage of the various cover types and amount of edge within specified corridors where a land use shift has been proposed. This capability would provide the Park Service with a means of obtaining a timely, specific and detailed data base for assessing the environmental impact of proposed management alternatives.

RECOMMENDATIONS

Many of the most important cover types have signature means in MSS 4 and 5 separated by only 2 percent of the sensor's dynamic range; i.e., 2-3 data values in 127 (Tables 1 and 2). Excepting thermal deposits, which appear essentially white, the brightest natural objects in the scene rarely exceed the data value of 50. This represents only 40 percent of the dynamic range

and indicates that over one half of the scanner's sensitivity is not being used.

Since the danger of clipping important data appears minimal, we believe a pass over the park exercising the high gain option is highly desirable. We anticipate that this data will be extremely useful in assessing the potential separability of important forest species. Using this option the data in MSS 4 and 5 will be expanded 3 times. In effect, the data takes on more significance because now there will be a greater number of quanta within the relative separation of the signatures.

It would also appear that preprocessing the data to remove the effects of path radiance in MSS 4 and 5 is essential to consistent recognition of forest types that occur in interspersion over a wide range of base altitudes.

Table 1. Training Set Signatures of Coniferous Forest Cover Types for ERTS-A Yellowstone Park MSS Data on 6 August 1972

Training Set	Signature Mean and Standard Deviation			
	MSS 4*	MSS 5*	MSS 6+	MSS 7+
Lodgepole Pine (young)	17.23 ± 1.01	12.79 ± 0.98	22.07 ± 1.51	11.76 ± 0.94
Lodgepole Pine (mature)	16.18 ± 0.88	11.01 ± 0.80	21.71 ± 1.37	11.46 ± 0.72
Douglas Fir	16.67 ± 1.00	10.89 ± 1.05	22.26 ± 1.80	11.82 ± 1.61
Spruce - Fir	15.58 ± 0.92	10.09 ± 1.12	20.01 ± 2.22	10.64 ± 1.42

Table 2. Training Set Signatures of Major Terrain Cover Types for ERTS-A Yellowstone Park MSS Data of 6 August 1972

Training Set	Signature Mean and Standard Deviation			
	MSS 4*	MSS 5*	MSS 6+	MSS 7+
Coniferous Forest	17.93 ± 1.96	13.45 ± 2.67	23.54 ± 3.28	12.61 ± 1.98
30-45% Conifer cover over rock rubble	19.15 ± 2.03	15.81 ± 2.74	27.11 ± 3.95	14.87 ± 2.30
30-45% Conifer cover over grass	18.72 ± 1.33	13.50 ± 1.46	31.90 ± 6.26	18.36 ± 4.02
15-30% Conifer cover over rock rubble	25.68 ± 2.97	25.07 ± 4.09	37.07 ± 4.31	19.52 ± 2.15
15-30% Conifer cover over grass	21.24 ± 2.18	16.93 ± 2.99	40.74 ± 6.05	23.74 ± 3.88
Wetland Shrubs	19.33 ± 1.05	13.38 ± 1.31	43.87 ± 3.81	26.35 ± 2.98
Grasslands	22.64 ± 1.55	18.52 ± 1.55	47.62 ± 5.11	29.17 ± 3.83
Grass/Brush	24.17 ± 1.29	21.72 ± 2.30	37.97 ± 3.52	21.52 ± 2.59
Brush	26.32 ± 1.50	25.28 ± 1.88	31.30 ± 2.78	15.64 ± 1.79
Dark Rock	27.72 ± 4.42	26.41 ± 5.32	27.24 ± 3.80	12.51 ± 2.05
Light Rock	37.62 ± 8.29	40.40 ± 11.14	43.57 ± 10.83	19.78 ± 5.54
Thermal Deposits	65.48 ± 9.69	72.52 ± 11.23	71.00 ± 9.31	31.58 ± 3.60
Water	13.65 ± 0.79	5.85 ± 0.87	2.99 ± 0.70	0.27 ± 0.45

*current potential range of 127 data values

+current potential range of 64 data values

Second Type II Progress Report
Frederick J. Thomson, MMC 137
Task III, Atmospheric Effects

INTRODUCTION

The purpose of this task is to demonstrate the effects of the atmosphere on the ability of pattern recognition devices to classify terrain objects. The project is a cooperative one between ERIM personnel, Dr. Harry Smedes and Robert Watson of U.S.G.S., and Mr. Roland Hulstrom of Martin-Marietta Corporation.

PROGRESS

The lack of suitable data has resulted in a low level of effort for this task during the previous six months. Although Frame No. 1009-17075, collected on 1 August 1972, provided good quality coverage of the test site, NDPF at Goddard was unable to provide suitably formatted CCT's until just recently. Tapes for that scene have now been received and will be utilized for the land use mapping phase of the task. It also appears that suitable data has been collected on 17 May and 10 July 1973. Mr. Hulstrom has also made ground measurements on these dates.

Good quality imagery obtained during the winter months has been unusable for land use mapping due to snow cover. However, one such data set is intended for use in investigating the effects of varying base altitude on atmospheric transmission, using snow covered surfaces as standards.

At the Goddard Symposium on 5-9 March, Mr. Thomson presented a paper entitled "Crop Species Mapping in The Sacramento Valley". That paper detailed attempts to map (using maximum likelihood pattern recognition processing of CCT data) 13 crop species and accurately measure crop acreages. Examples of accurate rice acreage recognition were shown. The latter results were also summarized in Dr. Poulton's Thursday paper on significant results in Agriculture.

PROGRAM FOR NEXT REPORTING INTERVAL

Intensive efforts are planned for this task during the upcoming six month period. The acquisition of the 1 August 1972 data will permit the land use mapping activity to begin. Activities related to primary program objectives will commence as CCT's for other scenes are received. The end of this upcoming six month period should see this task at, or finished with, the final reporting writing stage.

NEW TECHNOLOGY

None

CONCLUSIONS AND RECOMMENDATIONS

None

Second Type II Progress Report
M. L. Bryan, MMC 072
Task IV, Lake Ice Surveillance

INTRODUCTION

As discussed in the Fifth Type I report,the period of April/May, 1973 was one during which Task IV, Lake Ice Surveillance, was experiencing a change in plans. The decision was made, concurrent with NASA Houston, that the original ERTS Flight Mission 73M, to be conducted over the Douglas Lake test site on 5 April 1973, was to be cancelled and replaced by ERTS Flight Mission 76M. This latter mission was to collect multispectral radar data over several flooded areas of the eastern portion of the state of Michigan. Figure 1 illustrates the areas imaged, and Table I presents the aircraft flight record.

PROGRESS

Site Description of Radar Imagery Flights

A total of eight sites were imaged. These are outlined on the map. (Figure 1) Sites B and L are in eastern Michigan, bordering on the western portion of Lake Erie. The land here is quite low and, due to the excessive NE winds many businesses and residences had experienced considerable flooding. Site C is in the highly developed NE suburbs of Detroit and bordering on western Lake St. Clair. This area had also experienced flooding. Sites D and I and E and H were selected because of considerable interest at the state level, in the Department of Highways, to collect data concerning the environment assessment of areas in which the development of major highways were being seriously considered. These areas were imaged, not as the prime concern of the flights, but rather because they were along the flight path when traversing from the southern to the northern flooded areas. Sites F and G are the northern flooding areas along the southern end of Saginaw Bay. This area is quite flat, topographically low and covered by an extensive network of drainage ditches. The floods at the time of the flight were primarily the result of strong NE winds which raised the water levels along the shoreline by as much as 12' above the norm. The magnitude and seriousness of these floods, in both the southern and the northern areas may be surmised when it is realized that both of these were later designated as disaster areas and relief monies were made available to residents and business enterprises of the affected areas.

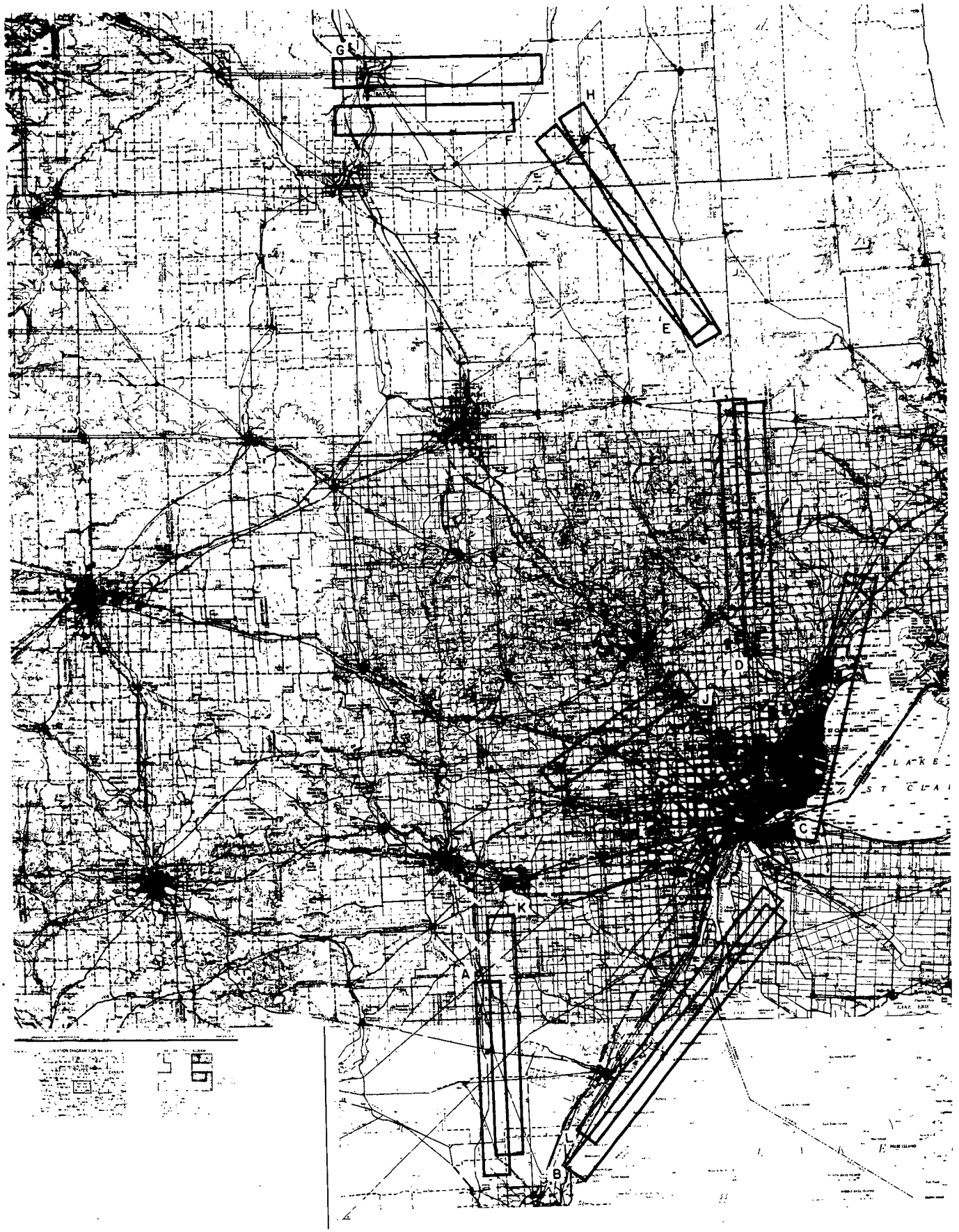

FIGURE 1. AREAS IMAGED X-L IMAGING FLIGHT, APRIL 5, 1973

TABLE 1

MISSION NO. _____ AIRCRAFT ERIM C-46

STAGING BASE WR Airport FLIGHT NO. _____

DATE & DAY 4/5/73 Thursday SITE Southeastern Michigan

TIME TAKE OFF 19:30 EST LAND 22:50 EST

DISPLAY #4 X-Band radar (cross & parallel polarized) DISPLAY #6 L-Band radar (Cross & parallel polarized)

PASS	SWATH	ALTITUDE MSL	STAND OFF RANGE	EVENT NUMBERS	LENGTH OF PASS
1	A	7,500'	14,000'	1-4	23 miles
2	B	7,500'	14,000'	5-9	39 miles
3	C	7,500'	14,000'	10-12	37 miles
4	D	5,600'	12,000'	13-17	29 miles
5	E	5,600'	12,000'	18-21	29 miles
6	F	5,600'	12,000'	22-28	21 miles
7	G	5,250'	12,000'	29-31	24 miles
8	H	4,600'	12,000'	32-35	31 miles
9	I	5,600'	12,000'	36-38	24 miles
10	J	5,600'	12,000'	39-41	20 miles
11	K	5,600'	12,000'	42-46	27 miles
12	L	5,600'	12,000'	47-50	37 miles

NOTE 1: This flight was made after the winter ice had left Whitefish Bay. The area covered included flooded regions along the shores of Lake Erie and St. Clair as well as Saginaw Bay.

NOTE 2: Event Marks identifying key events during the passes are entered simultaneously on all flight records and films.

ERIM Radar Data Collection for ERTS 76M

The ERIM C-46 aircraft took off from the Willow Run Airport, Ypsilanti, Michigan, at 1930 EST on 05 APR 73 (Thursday) and began to make the imaging runs several minutes later. The runs were made in alphabetical order as illustrated in Figure 1 and Table 1. Because all flights were taken during periods of marginal or no solar illumination, no photographic data was taken in conjunction with the radar data. Flight altitudes varied between 4.6 and 7.5 thousands of feet MSL, the stand-off range varied between 12-14 thousands of feet, and a total of 50 separate events were marked simultaneously on both the flight records and the radar films.* A total of 1023 sq. miles were imaged over a distance of 341 miles of imaging runs. The imagery produced from this mission was of excellent quality and clarity.

Consequently, one of the prime objectives, that of comparing ERTS(1) data with simultaneous X, L radar data will be essentially fulfilled - even though the subject under consideration will be shoreline flooding and erosion rather than the originally planned lake ice type and distribution.

Change of Project Program

Following this radar flight, a letter was forwarded to the Technical Monitor, Mr. E. F. Szajna, requesting a change in the project orientation. It had been agreed earlier that one of the major interests in this project is the combination of ERTS(1) imagery and X, L band radar imagery. We had thus completed data collection of this aspect of the original project - hence the methodology if not the earth surface feature had been retained.

Dr. F. Quinn, the technical monitor for this project has approved the change in target type discussed in the letter to Mr. Szajna. This was confirmed in a phone call to Szajna on 29 May 1973. At that time Mr. Szajna stated that it will take about 4-5 weeks to complete the paper work necessary to authorize the change in work plan.

ERTS Imagery and Ground Truth Work

Meanwhile, the Principal Investigator has proceeded to collect the following ERTS imagery.

---

*EVENT = Marking of a known ground reference point or object on the film so that radar film may be collated frequently with surface terrain and its physical features.

1265 - 15480-4
1265 - 15480-5
1265 - 15480-6
1265 - 15480-7

These frames were taken on 14 April 1973 and are for the Lake Erie shoreline of interest, essentially cloud free. Some preliminary photolaboratory work of enlarging the area of particular interest and that covered by the radar imagery of the shoreline has been conducted.

Groundtruthing was conducted in connection with both the radar and the ERTS(1) pass. As indicated in the earlier sections, analysis of these several types of data will be conducted upon receipt of authorization from NASA GSFC concerning the change in the work statement of this task.

PROGRAMMING FOR NEXT REPORTING INTERVAL

The work to be conducted under this task is dependent upon the response to the letter of 17 May 1973 to the Technical Monitor, Mr. E. F. Szajna. If approval of the change of program is received, collating of information from the ERTS imagery, radar tapes and ground truth will be started and comparisons made of the three sources.

NEW TECHNOLOGY - None

CONCLUSIONS AND RECOMMENDATIONS

The ERTS imagery, radar flight data and ground truth information collected are expected to provide a useful series of comparisons in support of the broad objective of comparing ERTS imagery with X, L band radar imagery. Recommendations are deferred until these data sources have been compared and interpretations developed.

Second Type II Progress Report
I. J. Sattinger, MMC 086
Task V, Recreational Land and Open Space

INTRODUCTION

Work performed during the period covered by this report consisted of digital computer analysis of Frame 1067-15463, acquired by ERTS-1 on 28 September, 1972. Intensive study was concentrated on an area within Oakland County approximately nine miles northwest of Pontiac. It includes Big Lake, Pontiac Lake, the Pontiac Lake State Recreation Area, and the Huron Swamp, which is the site for a new 2,000 acre park, the Oakland Metropolitan Park, recently announced by the Huron-Clinton Metropolitan Authority.

PROGRESS

Edited Level Slicing

We began the study of the test area by preparing a four-category computer map, using edited level slicing techniques on Band 5 and Band 7 data. As a basis for preparing this map, we performed a preliminary analysis of training set signatures to determine the spectral bands in which the categories, forest, grass, urban, and water, could be separated on the basis of quanta value only. In Band 5, certain areas, distinguished by their light tone (quanta values above 26), include residential areas with little vegetation, and bare areas, such as sand and gravel pits or major highways. Based on this characteristics, the class of all such developed areas can be mapped from Band 5. If the quanta value of a scene element in Band 5 is 26 or less, the surface is then recognized by reference to Band 7. The signature analysis indicated that by using Band 7 alone, level slicing was able to separate the following categories:

Quanta Value	Category
0 to 11 (dark)	Water
12 to 18 (intermediate)	Grass and Other Vegetation
19 to 26 (light)	Forest
27 to 511	Blank

An evaluation of the resulting four-category map shown in Figure 1 indicates that water areas are consistently mapped. Residential areas with little tree cover are consistently mapped as Urban, but the more developed residential areas with substantial tree and lawn cover tend to be mapped as Other Vegetation. This category also includes a wide variety of vegetative cover in non-urban areas, including some confusion with forested areas. This confusion can be reduced by increasing the lower limit of the range defined as forest, but cannot be completely eliminated, because some areas of forest and grass may have the same quanta level, i.e., radiance, in a single band.

The results obtained in these initial studies are discussed in a paper entitled "Digital Land Use Mapping in Oakland County, Michigan", presented at the Symposium on Significant Results Obtained from ERTS-1, held on March 5-9, 1973, by the Goddard Space Flight Center.

Likelihood Ratio Processing

Following this work with edited level slicing methods, we applied more advanced methods of recognition mapping based on likelihood ratio processing for the same area within Oakland County. Initial efforts at using likelihood ratio processing produced maps in which only about 65% of the scene elements were recognized. The relatively low recognition fractions are caused by the great amount of detail and the high degree of variability of the scene. Many single scene elements contain a mixture of various types of surface. This is particularly true of the urban areas, where individual scene elements contain a varying mixture of asphalt, concrete, roofs, grass, and trees. As a result, the probability that individual scene elements fall within preselected ranges of spectral signatures is low.

To increase the fraction of the scene recognized, we performed additional processing in which we modified the computer program parameters to accept a larger exponent value of the probability density function. Sixteen different land use and land cover categories were recognized, based on spectral signatures taken from five residential areas, two sand and gravel pits, deep and shallow water, three forest areas, and other vegetation-covered areas. In the resulting recognition map, 99% of the scene elements were recognized.

A general check of the result against recent RB-57 photography indicated that we achieved good recognition accuracy. We were able to separate general types of vegetation, such as forest or grasses, into individual classes whose spectral signatures are related to varying species, heights or densities of vegetation. The urban categories were divided into several combinations of roofs, asphalt, concrete, and vegetation. However, spectral signatures which exclusively map urban areas are difficult to define, since urban areas are characteristically mixtures of various surface types. Consequently, some areas of bare soil mixed with grass or forest may be misclassified as urban. Also, older or more affluent residential areas with dense tree cover will not be recognized as urban.

Based on our results, we estimate that in areas similar to the test area appropriate training sets could be selected for twenty different categories of vegetation and urban development which are significant for land resource analysis.

PROGRAM FOR NEXT REPORTING INTERVAL

In accordance with contract requirements, a Data Analysis Plan was submitted on 10 April 1973 describing future plans for technical work throughout the remainder of the contract. Approval of this Data Analysis Plan has now been received.

The Data Analysis Plan indicated that satisfactory cloud-free ERTS-1 coverage of Oakland County during the spring or summer had not yet been obtained. Since that time, Frames 1319-15471 and 1319-15474 were acquired by ERTS-1 on 7 June 1973 under cloud-free conditions. Digital tapes of these frames are being ordered for continuing analysis of Oakland County test areas.

The objective of this work is to further develop the ability to recognize and map features considered significant for the analysis of recreational land and open space. Processing of the frames will be carried to the point of determining the maximum feasible discrimination of such features. Processing techniques may include level slicing, ratio processing, and maximum likelihood ratio processing, as necessary to achieve the best results. Insertion of auxiliary information from other sources by the operator may be used to aid the recognition mapping process. Spectral signatures of various features of interest will be analyzed to guide the computer processing program and evaluate its discrimination capability.

NEW TECHNOLOGY

None

CONCLUSIONS AND RECOMMENDATIONS

A preliminary evaluation of the utility of ERTS data for recreational land studies has been made from the examination of these early results by staff members of the Lake Central Region of the Bureau of Outdoor Recreation and staff members of the Oakland County Planning Commission. They have indicated that general land use and land cover maps similar to those described above can be used in performing conceptual studies for large recreational developments. In particular, applications for which ERTS technology should be considered include the following:

- Delineating open space and determining changes over substantial time intervals.
- Identifying potential recreation sites on the basis of vegetation, water bodies, topography, adjacent land use.
- Studying inland lakes and other water-oriented recreation areas.
- Preparing inventories and assessments of wetlands and woodlands.
- Selecting routes for scenic trails.
- Analyzing scenic and recreation potential of river valleys.

Examples of recent studies conducted by the Lake Central Regional Office of BOR for which ERTS data could have been used, if available, include the Maumee Wild and Scenic River Study (in Northern Ohio and Indiana), study of the recreational potential of the Michigan shoreline of Lake Erie, and selection of corridors for an interstate scenic trail. Members of the regional office are now checking the availability of ERTS coverage of special areas in which they are currently conducting studies.

For studies which require a limited number of land use and land cover categories, the use of edited level slicing is a rapid and economical method for computer processing. Four-category mapping as described above is adequate for certain preliminary studies of river valleys or scenic trail routes. It can also be compared with older photographs or land use maps to detect large areas of changing land use which require more detailed checking. The breakdown can also be used for the selection of training sets for more sophisticated forms of computer processing.

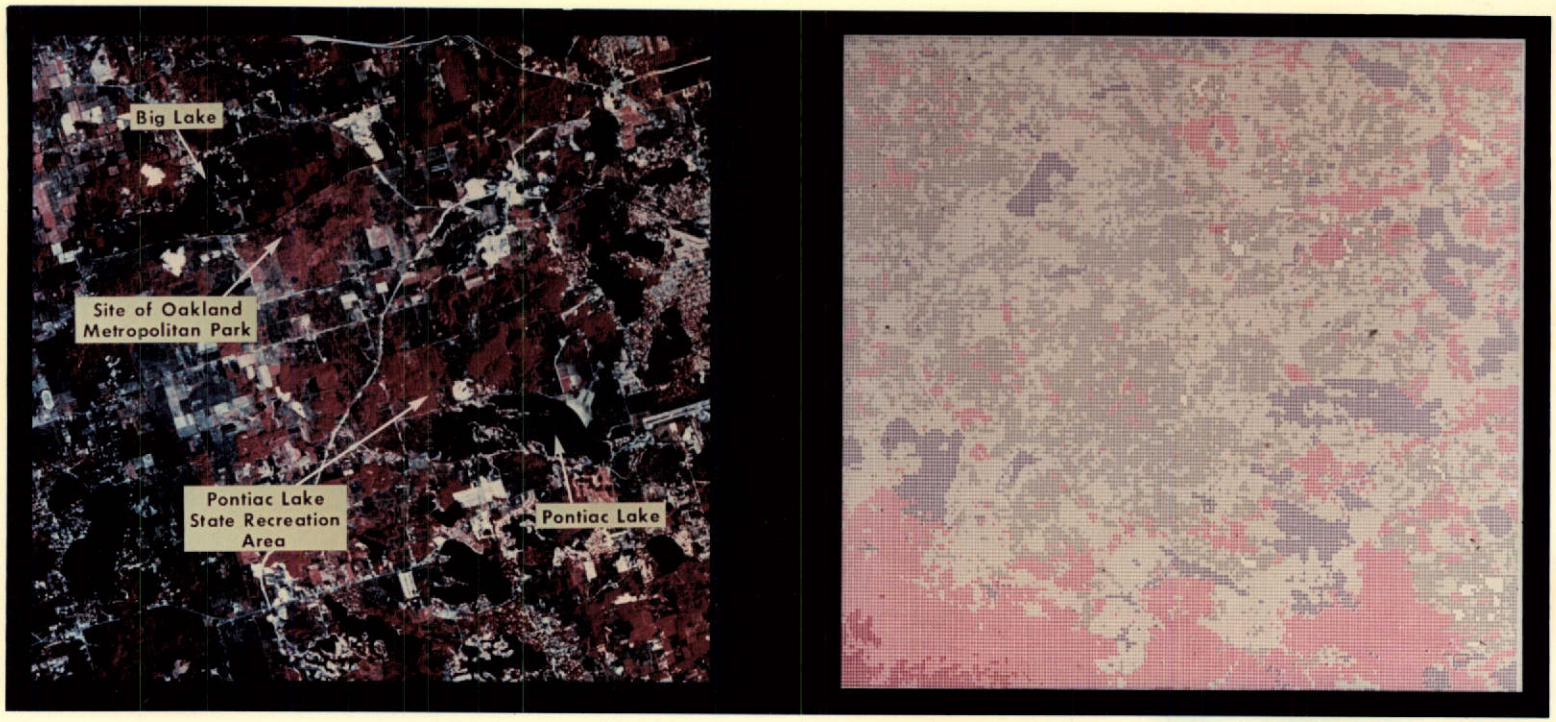

RB-57 Photograph

ERTS-1 Digital Map

N

Blue = Water
Red = Urban
Dk. Green = Forest
Lt. Green = Other Vegetation

FIGURE 1. ERTS-1 DIGITAL MAP, OAKLAND COUNTY, MICHIGAN, 28 SEPTEMBER 1972

ERIM
FORMERLY WILLOW RUN LABORATORIES, THE UNIVERSITY OF MICHIGAN

Second Type II Progress Report
F. C. Polcyn, MMC 114
Task VI, IFYGL (Lake Ontario)

INTRODUCTION

ERTS-1 coverage of the 32,000 square mile Lake Ontario Basin is being used to study temporal and spatial changes which affect many aspects of the hydrology of the Great Lakes. As part of the Internation Field Year for the Great Lakes (IFYGL) -- a coordinated, synoptic study of the Lake Ontario Basin -- processed ERTS-1 imagery is contributing to the data base of synchronized obervations made by investigators from many U. S. and Canadian government agencies and universities.

The objective of this task is to establish quantitative relationships between ERTS-observed features and significant hydrological parameters. Initial correlations are being done on selected representative basins within the Lake Ontario Basin, with the ultimate aim of extending these relationships, through the use of selected hydrologic models, to an analysis of the terrestrial water balance over the entire Lake Ontario Basin.

Data analysis is being concentrated on the August 19, 20, 21, 1972 ERTS imagery (8 Frames) which represent virtually cloud-free coverage of the entire basin, with the exception of the extreme eastern portion. Computer processing is being used to extract those parameters of hydrological and limnological significance. Imagery from subsequent ERTS passes is being manually analyzed.

PROGRESS

Work performed during the period 1 January to 30 June 1973 includes: 1) a review of the literature concerning hydrological models; 2) presentation of a summary paper concerning the objectives and approach of this IFYGL task at Goddard, 6 March 1973; 3) development of the software necessary for the calibration of the eight ERTS digital tapes prior to conversion to analog format for high speed analog processing; 4) documentation and visual analysis of all ERTS imagery (70 mm) of the Lake Ontario Basin received to date. Each of these are briefly discussed below.

Literature Review

During this period a comprehensive search of the literature concerned with hydrologic moddelling, particularly that related to regional or large-scale analyses of water balances, was undertaken. It is recognized that the full potential of the ERTS data acquired for hydrological purposes requires its input into appropriate descriptive models of the dynamic hydrological processes. Only in this way can we utilize ERTS data routinely for optimal water management purposes.

One of the most important results of this literature search (in combination with both visual and computer data analyses) is the determination of which land-use classifications, based on ERTS observable data, are most significant. Under real world conditions a model is only as good as the accuracy of its inputs, and the accuracy of that model for assessment or prediction varies accordingly. ERTS data will be of great value as an input to appropriate models, by virtue of the fact that land use and terrestrial features, such as standing water, can be determined with spatial and temporal accuracy substantially exceeding present means. With increasing emphasis on the study of hydrology on a regional and world-wide basis, the value of ERTS data to such hydrologic modelling is great.

The specific results of this literature search are currently being documented.

Summary Paper*

Two requirements for the successful application of ERTS data to studies of regional hydrology and limnology were examined in this paper -- the kinds of information required and economically feasible methods of obtaining this information for large watersheds (> 100,000 ha). ERTS-1 data is contributing primarily to research in areas of terrestrial water balance and water quality studies. These satellite data are providing quantitative spatial information concerning the condition of the entire Lake Ontario Basin on a seasonal basis. This information is useful to the extent that we know or can discover how surface features, patterns of land use or drainage, or temporal changes affect and are affected by the dynamics of basin hydrology. In addition, a simple processing technique, performed on a rapid throughput computing facility, is required in order to obtain this information in an objective and timely manner. Results of processing data from a twenty by thirty mile test area near Rochester, New York, (ERTS Frames 1027-15233 and 1028-15290) indicate that level slicing ["thresholding"] of normalized ratio values of ERTS Bands 5 and 7 would effectively discriminate diverse terrain classes and land use having significance for water balance studies. In part, the effectiveness of this ratio is based on the negative correlation of the red (chlorophyll absorption) band to the near IR (foliar reflectance) band. This negative correlation effectively enhances slight vegetative differences of drainage basin areas. These vegetative differences in large part determine differences in infiltration of precipitation and rates of runoff, erosion, and evapotranspiration. While use of general purpose digital computers would be too slow and costly for routine (operational) analysis of large amounts of ERTS data, modern special-purpose hybrid and analog systems are ideally suited for such a task. Such a system is the ERIM SPectral Analysis and Recognition Computer (designated by the acronym "SPARC").

---

*Wagner, T. W. and F. C. Polcyn, "Progress of an ERTS-1 Program for Lake Ontario and Its Basin."

Data Conversion

Much of the progress of this reporting period was concerned with the development and exercising of software for the calibration of ERTS MSS digital tapes prior to actual conversion to analog format (and thence to SPARC processing). This subroutine, designated DRKSCL., directly utilizes the 7 track ERTS tape as it comes from NASA.

Conversion of the 19-21 August data tapes has been delayed due to the occurrance in ERTS Band 6 of a striped pattern due to faulty data values (i.e., low values)in every sixth line. We are attempting to ascertain whether the abberations are sufficient to prohibit meaningful recognition during processing.

Documentation of ERTS Imagery

In addition to ERTS MSS coverage of the Lake Ontario Basin from 19-21 August 1972, the following ERTS images have been received and visually analyzed.

Frame No.	Date	Frame No.	Date	Frame No.	Date
1080-15174	11 Oct 72	1243-15235	23 Mar 73	1263-15352	12 Apr 73
1080-15180	11 Oct 72	1243-15242	23 Mar 73	1263-15355	12 Apr 73
		1243-15244	23 Mar 73	1263-15361	12 Apr 73
1190-15291	29 Jan 73	1243-15251	23 Mar 73	1263-15364	12 Apr 73
1190-15293	29 Jan 73				
1190-15300	29 Jan 73	1244-15294	24 Mar 73	1280-15302	29 Apr 73
1190-15302	29 Jan 73	1244-15300	24 Mar 73	1280-15305	29 Apr 73
		1244-15303	24 Mar 73		
1208-15292	16 Feb 73	1244-15305	24 Mar 73	1299-15351	18 May 73
1208-15295	16 Feb 73			1299-15353	18 May 73
1208-15301	16 Feb 73	1260-15181	9 Apr 73	1299-15360	18 May 73
		1260-15183	9 Apr 73	1299-15362	18 May 73
1209-15353	17 Feb 73	1260-15190	9 Apr 73		
1209-15360	17 Feb 73	1260-15192	9 Apr 73	1314-15174	2 June 73
1209-15362	17 Feb 73			1314-15181	2 June 73
				1314-15183	2 June 73
				1314-15190	2 June 73
				1315-15233	3 June 73
				1315-15235	3 June 73
				1315-15242	3 June 73
				1315-15244	3 June 73

Of these data, the March 23-25 sequence appears to be of exceptionally good quality. (While supporting aircraft missions were planned for these ERTS passes, no aircraft data were collected due primarily to unfavorable weather conditions during this period.)

Additional ERTS imagery adjacent to but outside the basin proper has been received and documented.

NEW TECHNOLOGY

New technology developed during this reporting period is chiefly the subroutine DRKSCL, which performs dark level subtraction and scaling on the ERTS data. Dark level subtraction is used to reduce differences between similar targets due to path radiance differences across the lake basin. These differences could be significant for ratio values as well as for single-channel values.

The dark levels are obtained through subroutine ASDRK, which was rewritten in order to operate directly on the ERTS tapes as received from NASA. ASDRK searches the specified area for the ten darkest objects by finding the lowest values of:

$$\sum_{I=1}^{NX} DATUM(I)$$

where: DATUM(I) = voltage at channel I

NX = number of channels

It then prints the resulting dark object voltages for each channel. Simultaneously, ASDRK searches for the five lowest voltage levels in each channel. It then prints the number of occurrences for every level in each channel.

Scaling is done for two reasons. First, noise is generated by the hardware that does the digital to analog (D/A) conversion. The noise is an addition term and scaling up the data by a factor of 4 (channels 4, 5, and 6) or 8 (channel 7) considerably reduces the effect of the noise. Second, the scaling is done to optimally match the D/A converter dynamic range to that of the 7 or 6 bit ERTS data.

PROGRAM FOR NEXT REPORTING INTERVAL

Current plans for the next reporting period include 1) analog processing of ERTS MSS data of the Lake Ontario Basin for the period August 19-21, 1972; 2) documentation of the literature search for hydrologic models with specific application to ERTS data; 3) continued documentation and visual analysis of ERTS imagery of the basin as it becomes available, and 4) continued discussion and evaluation of the results with cooperating IFYGL investigators. Efforts will be made to obtain supporting aircraft coverage of the Basin, although priority commitments for ERIM-MSS aircraft make the obtaining of such aircraft data unlikely in the near future.

CONCLUSIONS AND RECOMMENDATIONS

Several specific conclusions resulted from research during this reporting period -- the major one being that computer-processing of ERTS MSS data for the 32,000 sq mile Lake Ontario Basin should be implemented on a high-speed analog processing facility. This facility (SPARC) is capable of processing data at the rate of 100,000 resolution elements per second. At this data rate,

imagery of the entire Basin (eight frames) may be processed in a matter of hours and printed out in a 70 mm filmstrip image format. Implementation of this processing procedure involves calibration and conversion of NASA-7 track MSS digital tape to analog tape.

NASA may wish to consider the production of analog tapes for delivery to those users involved in combining results from a large number of consecutive ERTS frames. In addition, since the ERTS MSS collects imagery in a continuous strip, the construction of statewide or basin-wide mosaics would be much simplified if the ERTS negatives could be produced in strip imagery format.

Second Type II Progress Report
Period: 1 January - 30 June 1973
W.A. Malila & R. F. Nalepka, MMC 136
Task VII, Image Enhancement and Advanced Information Extraction Techniques

INTRODUCTION

Experience has been gained at ERIM over the past decade in computer processing and extraction of information from airborne multispectral scanner (MSS) data and in modeling atmospheric effects in received radiance signals. The general objective of Task VII is to adapt techniques existing at ERIM for their application to ERTS-1 data, to assess the applicability of these techniques by applying them to selected ERTS-1 data, and to identify any additional problems that might be associated with such processing of satellite multispectral scanner data. Three areas are to be studied: (1) compensation for atmospheric effects in ERTS-1 data, (2) preprocessing for improved recognition performance, and (3) estimation of proportions of unresolved objects in individual resolution elements.

The intensive test site for this investigation is an agricultural area South-West of Lansing, Michigan, and the extensive test area also covers several other counties in South Central Michigan. A variety of agricultural crops and woodlots are in the intensive area. The primary crops are corn and wheat, with field beans, soybeans, and alfalfa also represented. The intensive test area is in an overlap region covered by ERTS-1 on two successive days of each 18-day cycle. Skies were clear on 25 August and ERTS data were collected. Simultaneous multi-altitude underflight coverage was obtained by the Michigan C-47 multispectral scanner aircraft, and ground-based measurements were made of spectral irradiance and sky radiance. RB-57 camera coverage of the region, obtained during June, was received in late September. A second RB-57 flight was made in mid-September, and its photography was received at the end of October.

PROGRESS

The second six months of the contract effort included work on all three interest areas of this task. In addition, there were other, general activities. First, field support was provided for an aircraft MSS underflight, which was only partially completed, and a re-scheduled mission which was aborted because of cloud buildup. A new version of the computer compatible tape (CCT) for Frame 1033-15580 was requested, received, and evaluated. A computer-aided procedure was developed for correlating ERTS CCT data coordinates and Earth coordinates.

Significant Results

The strong influence of atmospheric effects (path radiance and transmittance) on ERTS data has been shown by calculations with a radiative transfer model and by some empirical studies of ERTS-1 MSS data. Part of this work was reported at the "Symposium on Significant Results Obtained from ERTS-1", 5-9 March 1973, in a paper, entitled "Atmospheric Effects in ERTS-1 Data, and Advanced Information Extraction Techniques", by W.A. Malila and R.F. Nalepka. Other work is reported herein.

The use of an advanced information extraction technique to improve area estimates of surface water over those with more standard techniques has been demonstrated. This work also was reported at the March symposium. Additional details and subsequent work are included later in this report.

Another significant result of the work reported here is the development and testing of the above-mentioned computer-aided procedure for correlating ERTS MSS data and Earth coordinate systems. This procedure will greatly facilitate the selection of ERTS pixels in computer compatible tape data to represent areas for training recognition computers and for evaluating recognition results, as well as improve our ability to locate other features in ERTS data. The procedure is discussed in detail in a later subsection.

Support of Aircraft Underflights and ERTS-1 Overpasses

An underflight of ERTS-1 by the ERIM C-46 multispectral scanner (MSS) aircraft was planned for June 8, 1973, in Eaton County, Michigan. It was to consist of two parts -- a set of passes at four different altitudes for atmospheric effects studies and four parallel passes to obtain data for recognition processing studies. The field measurement crew arrived at the site to set up for ground-based measurements. High thin cirrus clouds were present so it was decided to postpone the multi-altitude portion of the mission and fly only two of the four parallel passes. Some planned field measurements were not carried out because of the clouds, but measurements were made of spectral and broad-band irradiances, both global and diffuse. Also, a Radiant Power Measuring Instrument (RPMI) was used to measure irradiances; the instrument was kindly loaned to us by Dr. Robert Rogers (ERTS Investigator PR303) of the Bendix Aerospace Systems Division, Ann Arbor, Michigan.

The site for the multi-altitude flights was moved from Eaton County to the Willow Run Airport to reduce mission costs and minimize conflicts with other planned missions. A mission was planned for June 25th, and standard reflectance panels and field instrumentation were deployed. By the time of the ERTS pass, there was a considerable buildup of clouds, so the mission was aborted. We hope to be able to complete this multi-altitude flight on July 13 or 14, during the next ERTS-1 cycle.

Assessment of ERTS CCT Data Quality

In the first Type II Progress Report (ERIM Report No. 193301-1-P, Jan. 1973), we presented histograms which depicted a problem observed in data for every sixth scan line from ERTS Band 6 on the computer compatible tape (CCT) we received for Frame 1033-15580, Aug 25, 1972. Since this problem necessitated the elimination of either every 6th line of the ERTS data or ERTS Band 6 from computer recognition processing and analysis, we were advised by NASA in March to request the generation of a new version of the CCT from the original data tape. Such a request was made, and the new set of tapes was received during May. An analysis that duplicated that for the original tapes was performed and the results were compared. As is discussed below, the problem in the particular detector channel was corrected but a similar, though less severe, problem appeared in a different detector channel for Band 6. Also, many of the mean values observed for signal channels are slightly different for the new CCT than for the old one, reflecting the revised calibration tables that have been used to produce CCT's since April 13th (according to a GSFC representative).

For the data quality assessment, we used an agricultural area 240 scan lines long and 120 points wide. Six groups, each of 4800 points, were analyzed, one group from scan lines associated with each detector channel. Histograms were produced for each ERTS Band for each group of points. Also, the corresponding means and standard deviations were calculated and are presented in Table 1. In the table, the top value of each pair of entries for a particular channel and group is from the new tape and the bottom value is from the old one.

The Table 1 entry for Group 5, Channel 3 shows the extreme values for both mean and standard deviation on the old tape and the representative values on the new tape. Figure 1 presents a histogram of data points for the old tape and Figure 2 shows the normal histogram produced from the new tape.

As mentioned earlier, the values in Group 4, Channel 3 were normal on the old tape, as can be seen in the histogram of Figure 3, while those on the new tape had a lower than average mean and a 60% greater standard deviation. The greater scanner of points in the latter case is evident on the histogram presented in Figure 4 (note that the x-axis of the histograms have different scales).

Goddard personnel will be consulted about the possibility of obtaining a new set of tapes with reduced variance in the fourth detector channel of Band 6.

TABLE 1. COMPARISON OF SIGNAL CHARACTERISTICS ON ORIGINAL CCT AND NEW CCT FOR FRAME 1033-15580
(Each entry computed for 4800 points from an agricultural scene)

		CHANNEL 1		CHANNEL 2		CHANNEL 3		CHANNEL 4	
GROUP		MEAN	STD. DEV.	MEAN	STD. DEV.	MEAN	STD. DEV.	MEAN	STD. DEV.
1	new	25.56	2.21	18.14	3.54	44.23	6.50	24.90	4.45
	old	24.52	2.17	17.28	3.44	45.07	6.56	24.90	4.45
2	new	24.82	2.00	17.35	3.63	43.91	6.28	25.20	4.46
	old	25.78	1.98	17.62	3.59	44.29	6.33	25.20	4.43
3	new	24.95	2.07	17.38	3.59	43.28	6.17	25.37	4.55
	old	25.20	2.08	17.44	3.65	43.24	5.98	25.37	4.52
4	new	25.38	1.98	17.35	3.74	40.24	9.86	25.49	4.78
	old	25.38	1.91	17.48	3.76	43.73	6.06	25.49	4.76
5	new	25.77	2.23	17.52	3.72	44.09	6.63	25.24	4.73
	old	25.77	2.23	17.52	3.72	17.76	18.78	25.24	4.73
6	new	25.62	2.07	17.78	3.86	45.22	6.47	25.70	4.66
	old	25.58	1.91	17.51	3.58	45.25	6.78	25.71	4.63

GROUP 5 9 JUL 1973

HISTOGRAMS OF DETECTORS 4 AND 5 IN OLD ERTS TAPE TO MATCH NEW
NUMBER OF INTEGERS PER BIN = 1

NUMBER OF POINTS= 4800.0 EACH SYMBOL REPRESENTS .200 PER CENT
CHANNEL= 3

DATA VALUES	FREQUENCY O/O	CUMULATIVE TOTAL	HISTOGRAM IN PER CENT .0 2.0 4.0 6.0 8.0 10.0 12.0 14.0 16.0 18.0 20.0
0	16.67	16.67	=***
1	.40	17.06	=*
2	1.15	18.21	=*****
3	.85	19.06	=*****
4	1.81	20.87	=*********
5	1.81	22.69	=*********
6	2.35	25.04	=************
7	2.96	28.00	=***************
8	4.79	32.79	=************************
9	3.94	36.73	=********************
10	5.17	41.90	=**************************
11	4.62	46.52	=***********************
12	5.23	51.75	=**************************
13	4.94	56.69	=************************
14	2.62	59.31	=*************
15	3.27	62.58	=*****************
16	3.40	65.98	=*****************
17	2.62	68.60	=*************
18	2.12	70.73	=**********
19	2.62	73.35	=*************
20	1.19	74.54	=******
21	1.92	76.46	=**********
22	.65	77.10	=***
23	1.35	78.46	=*******
24	.94	79.40	=*****
25	.65	80.04	=***
26	1.42	81.46	=********
27	.54	82.00	=**
28	1.29	83.29	=*******
29	.12	83.42	=
30	.15	83.56	=
31	.52	84.08	=**
32	.00	84.08	=
33	.42	84.50	=**
34	.06	84.56	=
35	.12	84.69	=
36	.15	84.83	=
37	.15	84.98	=
38	.00	84.98	=
39	.25	85.23	=*
40	.17	85.40	=
41	.21	85.60	=*
42	.35	85.96	=*
43	.54	86.50	=**
44	.44	86.94	=**
45	.92	87.85	=*****
46	.83	88.69	=*****
47	.75	89.44	=****
48	.62	90.06	=***
49	.83	90.90	=*****
50	.46	91.35	=**
51	.75	92.10	=****
52	.79	92.90	=****
53	.19	93.08	=
54	.77	93.85	=****
55	.44	94.29	=**
56	.31	94.60	=*
57	.19	94.79	=
58	.00	94.79	=
59	.17	94.96	=
60	.12	95.08	=
61	.00	95.08	=
62	.12	95.21	=
63	.19	95.40	=
64	.52	95.92	=**
65	.52	96.44	=**
66	.31	96.75	=*
67	.46	97.21	=**
68	.02	97.23	=
69	.04	97.27	=
70	.25	97.52	=*
71	.00	97.52	=
72	.08	97.60	=
73	.29	97.90	=*
74	.25	98.15	=*
75	.02	98.17	=
76	.52	98.69	=**
77	.44	99.12	=**
78	.12	99.25	=
79	.00	99.25	=
80	.19	99.44	=
81	.00	99.44	=
82	.00	99.44	=
83	.00	99.44	=
84	.00	99.44	=
85	.00	99.44	=
86	.00	99.44	=
87	.00	99.44	=
88	.00	99.44	=
89	.12	99.56	=
90	.00	99.56	=
91	.00	99.56	=
92	.08	99.65	=
93	.00	99.65	=
94	.00	99.65	=
95	.00	99.65	=
96	.00	99.65	=
97	.00	99.65	=
98	.00	99.65	=
99	.00	99.65	=
100	.00	99.65	=
101	.00	99.65	=
102	.00	99.65	=
103	.23	99.87	=*
104	.00	99.87	=
105	.00	99.87	=
106	.12	100.00	=

FIGURE 1

HISTOGRAM OF ORIGINAL CCT, GROUP 5, CHANNEL 3

25AUG72 C N43-04/W085-24 N N43-04/W085-18 1033-15580- SUN EL50 AZ137 191-0459-N 0-4-0-1 M ERIM (ERTS DATA)

GROUP 5 15 JUN 1973

HISTOGRAMS OF EACH DETECTOR UNIT IN THE NEW ERTS TAPE SIGNATURE
NUMBER OF INTEGERS PER BIN = 1

NUMBER OF POINTS= 4800.0 EACH SYMBOL REPRESENTS .200 PER CENT
CHANNEL= 3

DATA VALUES	FREQUENCY O/O	CUMULATIVE TOTAL	HISTOGRAM IN PER CENT .0 2.0 4.0 6.0 8.0 10.0 12.0 14.0 16.0
17	.02	.02	=
18	.00	.02	=
19	.04	.06	=
20	.02	.08	=
21	.00	.08	=
22	.04	.12	=
23	.06	.19	=
24	.00	.19	=
25	.08	.27	=
26	.23	.50	=*
27	.00	.50	=
28	.31	.81	=*
29	.00	.81	=
30	.79	1.60	=***
31	1.27	2.87	=******
32	.00	2.87	=
33	1.81	4.69	==========
34	.00	4.69	=
35	3.04	7.73	=***************
36	.00	7.73	=
37	6.33	14.06	=*********************************
38	.00	14.06	=
39	10.52	24.58	=**
40	.48	25.06	=**
41	11.42	36.48	==========
42	1.46	37.94	=*******
43	10.81	48.75	==========
44	11.02	59.77	==========
45	6.31	66.08	=*********************************
46	5.00	71.08	=*************************
47	4.42	75.50	========================
48	4.35	79.85	=======================
49	4.00	83.85	=====================
50	1.87	85.73	==========
51	3.31	89.04	==================
52	.71	89.75	=***
53	2.69	92.44	==============
54	.37	92.81	=*
55	1.71	94.52	=========
56	.00	94.52	=
57	.04	94.56	=
58	1.92	96.48	==========
59	.00	96.48	=
60	1.58	98.06	========
61	.00	98.06	=
62	.00	98.06	=
63	1.12	99.19	======
64	.00	99.19	=
65	.54	99.73	=**
66	.00	99.73	=
67	.00	99.73	=
68	.23	99.96	=*
69	.00	99.96	=
70	.00	99.96	=
71	.04	100.00	=

FIGURE 2

HISTOGRAM OF NEW CCT, GROUP 5, CHANNEL 3

25AUG72 C N43-04/W085-24 N N43-04/W085-18 1033-15580- SUN EL50 AZ137 191-0459-N D-4-D-1 H ERIM (ERTS DATA)

GROUP 4 9 JUL 1973

HISTOGRAMS OF DETECTORS 4 AND 5 IN OLD ERTS TAPE TO MATCH NEW
NUMBER OF INTEGERS PER BIN = 1

NUMBER OF POINTS= 4800.0 EACH SYMBOL REPRESENTS .200 PER CENT
CHANNEL= 3

DATA VALUES	FREQUENCY O/O	CUMULATIVE TOTAL	HISTOGRAM IN PER CENT .0 2.0 4.0 - 6.0 8.0 10.0 12.0 14.0 16.0
18	.02	.02	=
19	.00	.02	=
20	.02	.04	=
21	.00	.04	=
22	.00	.04	=
23	.04	.08	=
24	.04	.12	=
25	.08	.21	=
26	.00	.21	=
27	.17	.37	=
28	.42	.79	=**
29	.00	.79	=
30	.62	1.42	=***
31	.00	1.42	=
32	1.00	2.42	=****
33	.00	2.42	=
34	1.73	4.15	=********
35	1.98	6.12	=**********
36	1.87	8.00	=**********
37	5.62	13.62	=*****************************
38	.00	13.62	=
39	9.25	22.87	=**
40	11.98	34.85	=**
41	.00	34.85	=
42	13.25	48.10	=**
43	.00	48.10	=
44	13.31	61.42	=**
45	3.10	64.52	=****************
46	8.08	72.60	=**
47	8.79	81.40	=***
48	.00	81.40	=
49	6.35	87.75	=*********************************
50	.00	87.75	=
51	.00	87.75	=
52	4.17	91.92	=**********************
53	.00	91.92	=
54	3.06	94.98	=****************
55	.00	94.98	=
56	1.08	96.06	=******
57	.90	96.96	=*****
58	1.29	98.25	=*******
59	.00	98.25	=
60	.00	98.25	=
61	.92	99.17	=*****
62	.00	99.17	=
63	.00	99.17	=
64	.54	99.71	=**
65	.00	99.71	=
66	.06	99.77	=
67	.17	99.94	=
68	.00	99.94	=
69	.06	100.00	=

FIGURE 3

HISTOGRAM OF ORIGINAL CCT, GROUP 4, CHANNEL 3

25AUG72 C N43-04/W085-24 4 N43-04/W085-18 1033-15580- SUN EL50 AZ137 191-0459-N 0-4-0-1 H ERIM (ERTS DATA)

GROUP 4 15 JUN 1973

HISTOGRAMS OF EACH DETECTOR UNIT IN THE NEW ERTS TAPE SIGNATURE
NUMBER OF INTEGERS PER BIN = 1

NUMBER OF POINTS= 4800.0 EACH SYMBOL REPRESENTS .100 PER CENT
CHANNEL= 3

DATA VALUES	FREQUENCY O/O	CUMULATIVE TOTAL	HISTOGRAM IN PER CENT .0 1.0 2.0 3.0 4.0 5.0 6.0 7.0 8.0 9.0 10.0
0	.02	.02	*
1	.10	.12	**
2	.25	.37	***
3	.17	.54	**
4	.06	.60	*
5	.02	.62	*
6	.00	.62	*
7	.00	.62	*
8	.02	.65	*
9	.00	.65	*
10	.15	.79	**
11	.00	.79	*
12	.27	1.06	***
13	.19	1.25	**
14	.35	1.60	****
15	.10	1.71	**
16	.02	1.73	*
17	.17	1.90	**
18	.04	1.94	*
19	.04	1.98	*
20	.15	2.12	**
21	.06	2.19	*
22	.46	2.65	*****
23	.04	2.69	*
24	.46	3.15	*****
25	.27	3.42	***
26	.46	3.87	*****
27	.19	4.06	**
28	.50	4.56	*****
29	.92	5.48	**********
30	1.27	6.75	**************
31	2.04	8.79	**********************
32	1.79	10.58	********************
33	3.73	14.31	**
34	4.62	18.94	**
35	6.15	25.08	**
36	5.10	30.19	***
37	7.15	37.33	***
38	8.46	45.79	**
39	3.62	49.42	**
40	9.31	58.73	**
41	3.87	62.60	***
42	6.71	69.31	**
43	3.62	72.94	***
44	5.50	78.44	**
45	1.83	80.27	********************
46	4.15	84.42	***
47	1.60	86.02	******************
48	2.85	88.87	********************************
49	.54	89.42	******
50	1.29	90.71	**************
51	1.50	92.21	****************
52	.81	93.02	*********
53	1.58	94.60	*****************
54	.50	95.10	*****
55	.48	95.58	*****
56	.81	96.40	*********
57	.29	96.69	***
58	.37	97.06	****
59	.12	97.19	**
60	.25	97.44	***
61	.19	97.62	**
62	.10	97.73	**
63	.27	98.00	***
64	.06	98.06	*
65	.02	98.08	*
66	.15	98.23	**
67	.00	98.23	*
68	.00	98.23	*
69	.10	98.33	**
70	.00	98.33	*
71	.00	98.33	*
72	.06	98.40	*
73	.00	98.40	*
74	.00	98.40	*
75	.27	98.67	***
76	.00	98.67	*
77	.33	99.00	****
78	.00	99.00	*
79	.00	99.00	*
80	.25	99.25	***
81	.00	99.25	*
82	.00	99.25	*
83	.12	99.37	**
84	.00	99.37	*
85	.00	99.37	*
86	.06	99.44	*
87	.00	99.44	*
88	.10	99.54	**
89	.00	99.54	*
90	.00	99.54	*
91	.00	99.54	*
92	.00	99.54	*
93	.00	99.54	*
94	.00	99.54	*
95	.04	99.58	*
96	.00	99.58	*
97	.00	99.58	*
98	.23	99.81	***
99	.00	99.81	*
100	.12	99.94	**
101	.00	99.94	*
102	.00	99.94	*
103	.06	100.00	*

FIGURE 4

HISTOGRAM OF NEW CCT, GROUP 4, CHANNEL 3

D

Correlation of ERTS MSS Data and Earth Coordinate Systems

One serious problem that has been found in computer analyses of ERTS-1 MSS data is the assignment of pixels to individual fields and test plots in the scene. Such assignments are made both for training the recognition computer and for evaluating recognition results. The capability is particularly needed to evaluate results obtained with the ERIM algorithm that estimates proportions of two or more materials in individual resolution elements.

Consequently, we have developed* a computer-aided procedure for correlating ERTS MSS pixels and Earth coordinate systems. In this procedure, a transformation is used to convert field or plot vertices from map or aerial photograph coordinates to ERTS scan line and point numbers. This map transformation is calculated by using selected ground control points and the method of least squares.

The problem of accurately locating field boundaries in ERTS data is primarily a result of the relatively large size of the spatial resolution element on the ground in comparison to field sizes. For example, it is often difficult to distinguish "by eye" the corners of sections and plots of interest on digital displays of ERTS data, and more difficult to locate them accurately. Lack of contrast between materials and any banding or striping in the ERTS data can complicate matters.

We have found that generally some road intersections and other features in the scene around and within the areas of interest can be distinguished readily in digital displays. Fifteen to twenty such points are selected as control points and their ERTS line and point numbers are estimated as well as possible by inspection. Earth coordinates for the same points are determined** from a topographic map and/or an aerial photograph. A least-squares fit of ERTS to Earth coordinates reduces the error in the estimated location of each control point and produces a map transformation that can be used to transfer Earth coordinates of any other point, field, or plot in the vicinity to the corresponding ERTS coordinates. A polynomial transformation is computed, but we thus far have found that terms of higher than first order are not significant.

A companion computer program allows us to define each test area by a polygon with an arbitrary number (≤ 63) of vertices and to compute which ERTS pixel centers lie within the polygon. Further, there is a capability to move the polygon sides in or out by specified distances so as to include or exclude

* Development costs are being shared by this contract and an ERIM subcontract under the Michigan State University ERTS Contract, NAS5-21834.

** Digitization is facilitated by the use of an x-y digitizing machine.

pixels which contain boundaries between scene features. An illustration of the effect of this procedure is presented in Fig. VII- 5. A section (1 mile square) in our test area was arbitrarily divided into 16 40-acre "fields". Part (a) of Figure 5 displays as blanks the pixels selected for these fields. when the acceptance polygon was inset by one-half a resolution element on all sides.* An average of 22 pixels was selected for each 40-acre field. For Part(b), the inset was increased to three-quarters of a resolution element, and the smaller number of acceptable pixels (an average of 16) in each field is apparent. Parts(c) and (d) show the further reduction in the average number of acceptable pixels to 12 and 5 when the inset is increased to 1 and 1-1/2 resolution elements, respectively. Figure 6 presents other sets of fields delineated by the 0.5 resolution element criterion; field sizes of 640, 160, 80, and 10 acres are shown.

The inset of one-half a resolution element is the theoretical minimum needed to exclude pixels that contain boundary effects. A greater inset probably should be used in practice because of errors in the process. Aside from possible errors in the location of the control points on both the ERTS and Earth coordinates and in the location of test plot vertices in the maps or photographs, there are known displacements inherent in the ERTS data which we presently do not take into account.

It is difficult to make a quantitative assessment of the accuracy of our procedure, because of the lack of an absolute knowledge of pixel locations. One attempt, using Gull Lake, Kalamazoo and Barry Counties, Michigan, as imaged in Frame 1033-15580, is presented and discussed below.

A lake was selected because there generally is a large contrast between land and water in ERTS Band 7, so that the accuracy of boundary locations can be assessed. Gull Lake is one of the largest in the area, has a regulated water level, is in a region for which topographic maps were on hand, and has some distinctive shoreline features and an island.

Our goals were (1) to select only those pixels that were completely within the lake and (2) to determine whether map-based coordinates of the shoreline could be accurately placed in the ERTS data. The results discussed below show that a good job was done in selecting only water pixels and that shoreline features were accurately placed around the lake.

Eighteen control points were selected from a 6 x 20 mile area with Gull Lake roughly at the center. None of the control points were on the Gull Lake shoreline and few were near it because of indistinct roads in the immediate vicinity. Latitude and longitude for these points were extracted from three different USGS maps of two different scales. Approximately 90 points along the

* Note that the inset must be greater than one-half a pixel dimension along the scan line since the actual resolution element size is 79 x 79 m even though the sampling rate along the scan line gives an effective pixel width of 57 m.

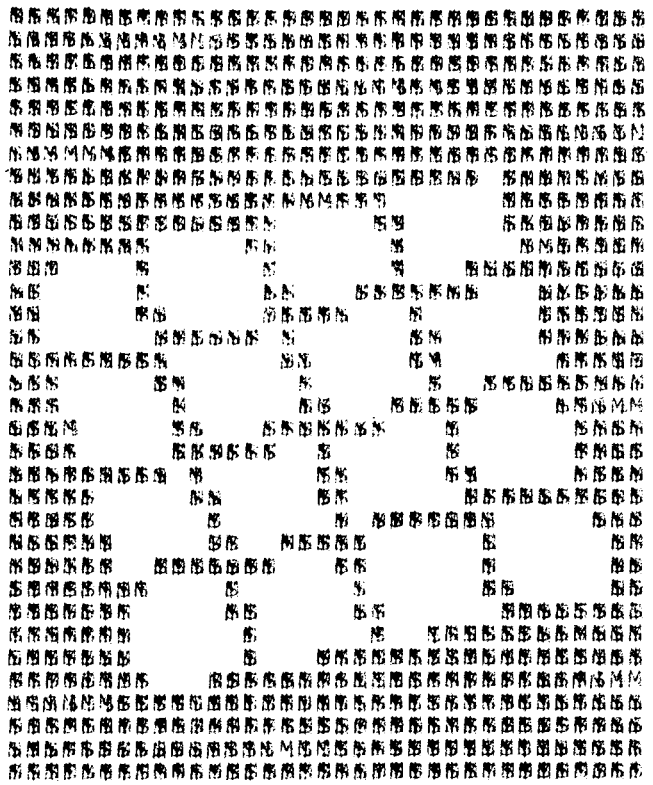

PART(a) 0.5 INSET

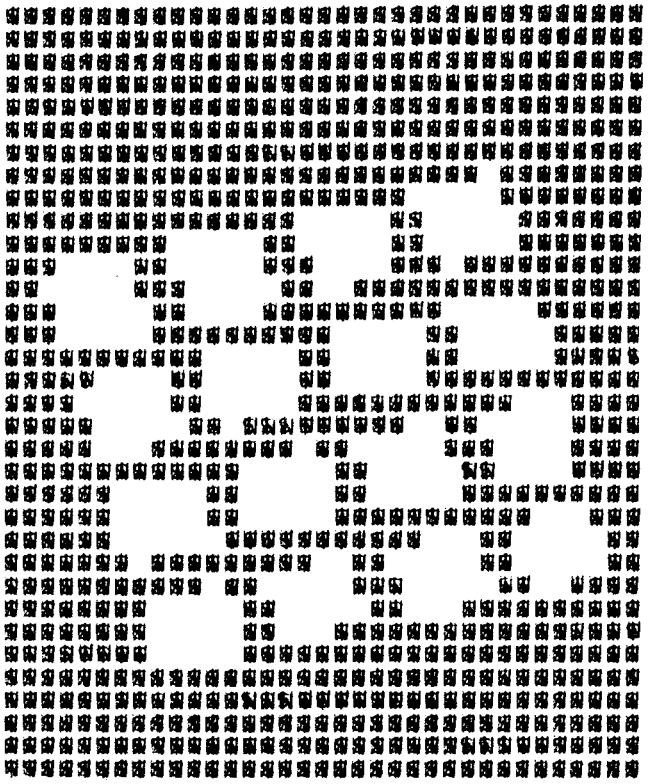

PART(b) 0.75 INSET

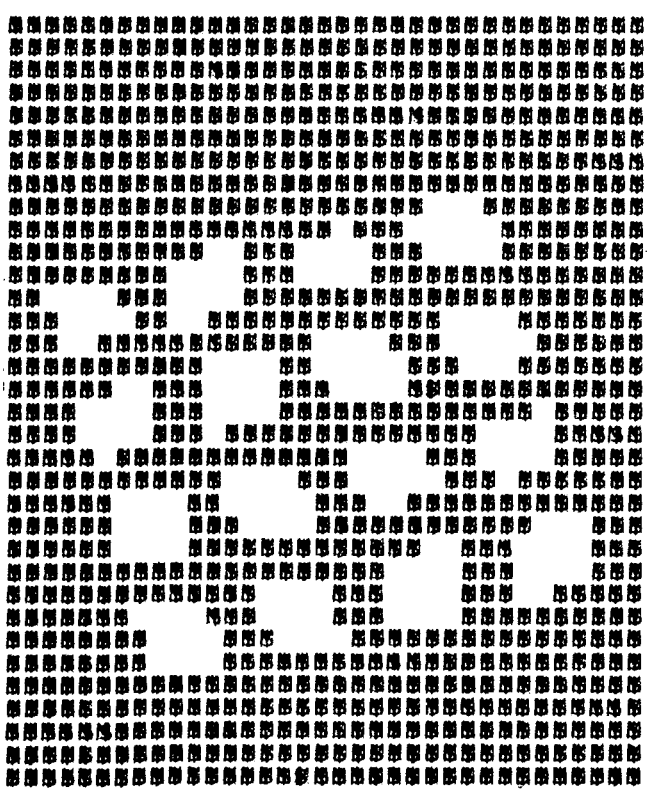

PART(c) 1.0 INSET

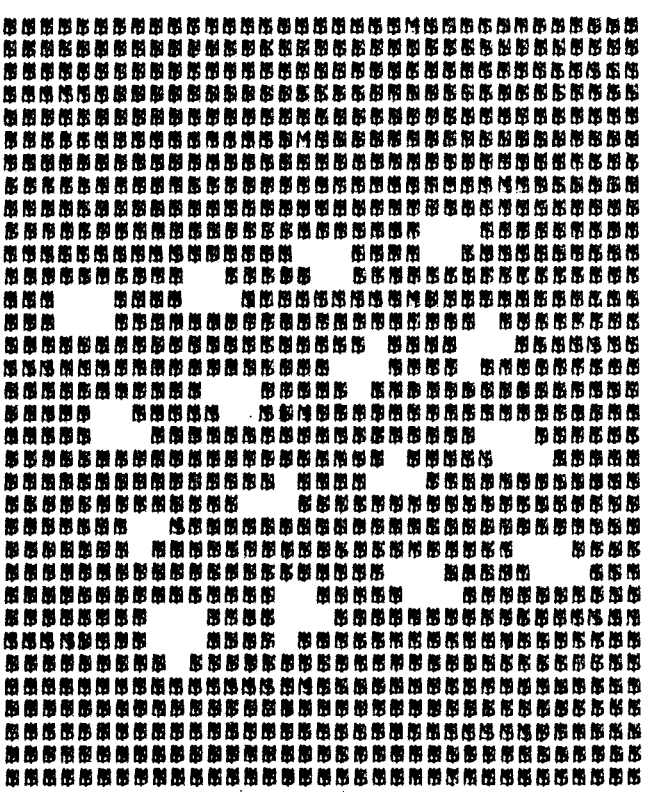

PART(d) 1.5 INSET

FIGURE 5. EFFECT OF INSET PARAMETER ON PIXEL SELECTION FOR 40-ACRE FIELDS

(Inset Parameter is Measured in MSS Resolution Elements)

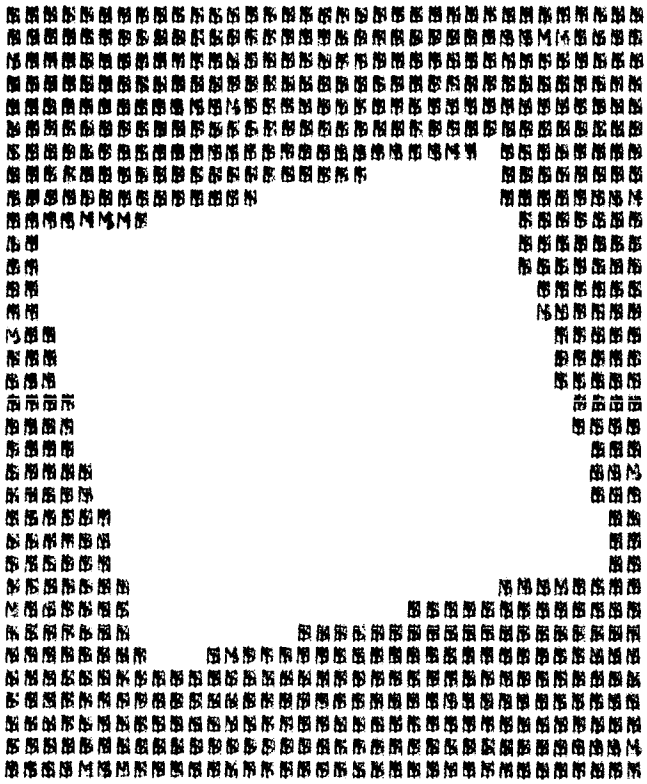

640 ACRE FIELD

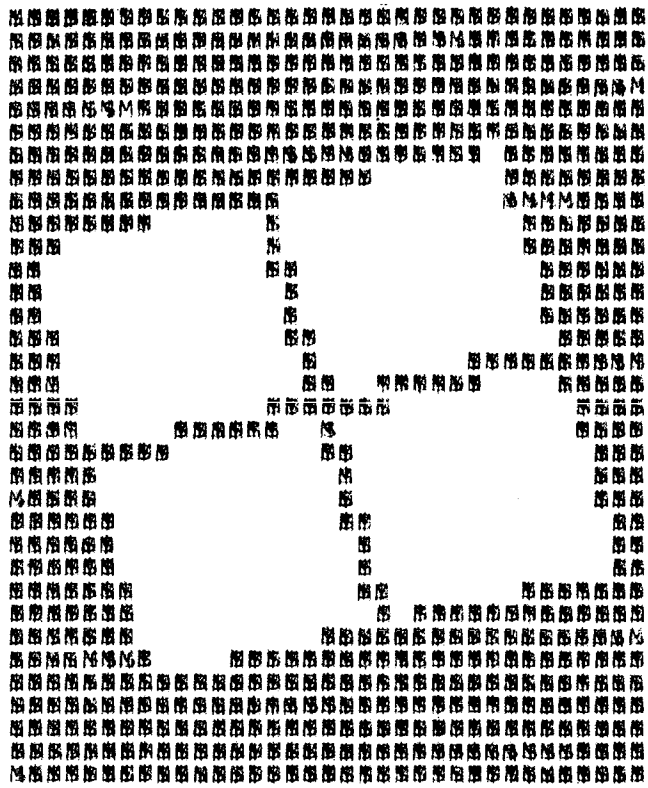

160 ACRE FIELDS

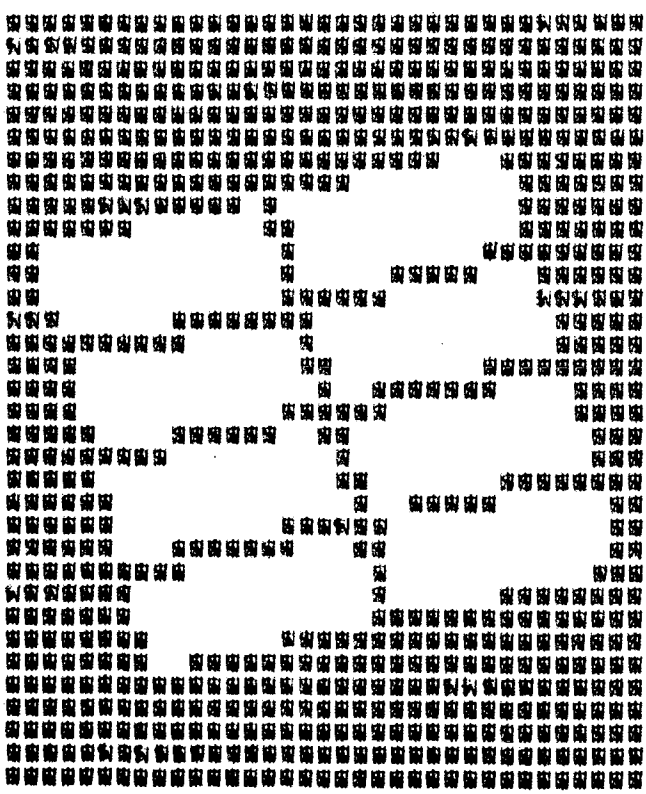

80 ACRE FIELDS

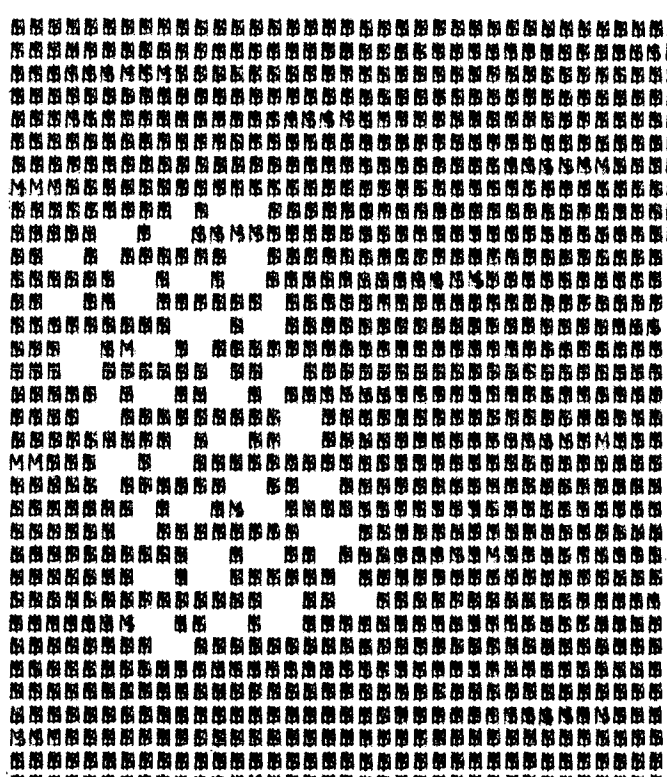

10 ACRE FIELDS

FIGURE 6. EFFECT OF FIELD SIZE ON PIXEL SELECTION FOR 0.5-RESOLUTION-ELEMENT INSET.

shoreline of Gull Lake on the USGS map also were digitized for transformation to ERTS coordinates. An inset of +0.5 resolution elements was used along the major shoreline and -0.5 along the shoreline of the island at the South end of the lake. The negative inset, or outset, was necessary to exclude island shoreline points from the water because the island was the area outlined.

The line printer map in Figure 7 presents the results of the Gull Lake analysis. Five gray levels are displayed, three for values determined by the procedure to be within the lake and two for those outside. The choice of symbols within each of these two groups was determined by the value of the signal in ERTS Band 7. Observation showed that open water points were all at levels of 5 or less, while the surrounding land was generally at levels of 12 or greater; intermediate values were found along the shoreline. For points determined to be within the lake by the procedure, the predominant darkest symbol (M over $) corresponds to the 1554 points with values ≤ 5, the intermediate symbol (X over =) corresponds to the 18 points with values of 6 or 7, and the lightest symbol (*) corresponds to points with values ≥ 8. Only 9 points with values ≥ 8 were said to be within the lake, and the highest of these values was 9. Since land values generally are ≥ 12, the lighter pixels included at most only partial land observations. Further some of them might even have been caused by the presence of weeds near the shore; current aerial photography is not available to check for the presence of weeds. In summary, <1% of the lake points, or <3% of the shoreline points, seem to have been misclassified (*) as being open water.

On the other side of the computed shoreline, 93 points with values ≤ 5 were placed (symbol θ). These points correspond to open water values that were excluded from Gull Lake. This result was not unexpected since the shoreline is irregular and was approximated by a multi-sided polygon. All shoreline undulations on the map were not followed exactly and vertices were chosen to exclude all land from the polygon, leaving some water areas on the outside. Vertices around the island were all placed in the water.

Upon comparing the ERTS data of Figure 7 to the USGS map in Figure 8 one can see that the inlets and peninsulas around the lake are accurately positioned by the procedure. The average accuracy of positioning is clearly less than one pixel, but at this time we cannot quantitatively determine how much less. The results encourage use of the procedure on subsequent processing of ERTS data, and we plan to use it.

An abstract was prepared for a paper that will describe the procedure and discuss results such as those presented here. Entitled "Correlation of ERTS MSS Data and Earth Coordinate Systems" and authored by William A. Malila, Ross H. Hieber, and Arthur P. McCleer of ERIM, the paper is scheduled for presentation at the Conference on Machine Processing of Remotely Sensed Data, to be held at Purdue University on October 16-18, 1973. A copy of the abstract is included as Appendix I.

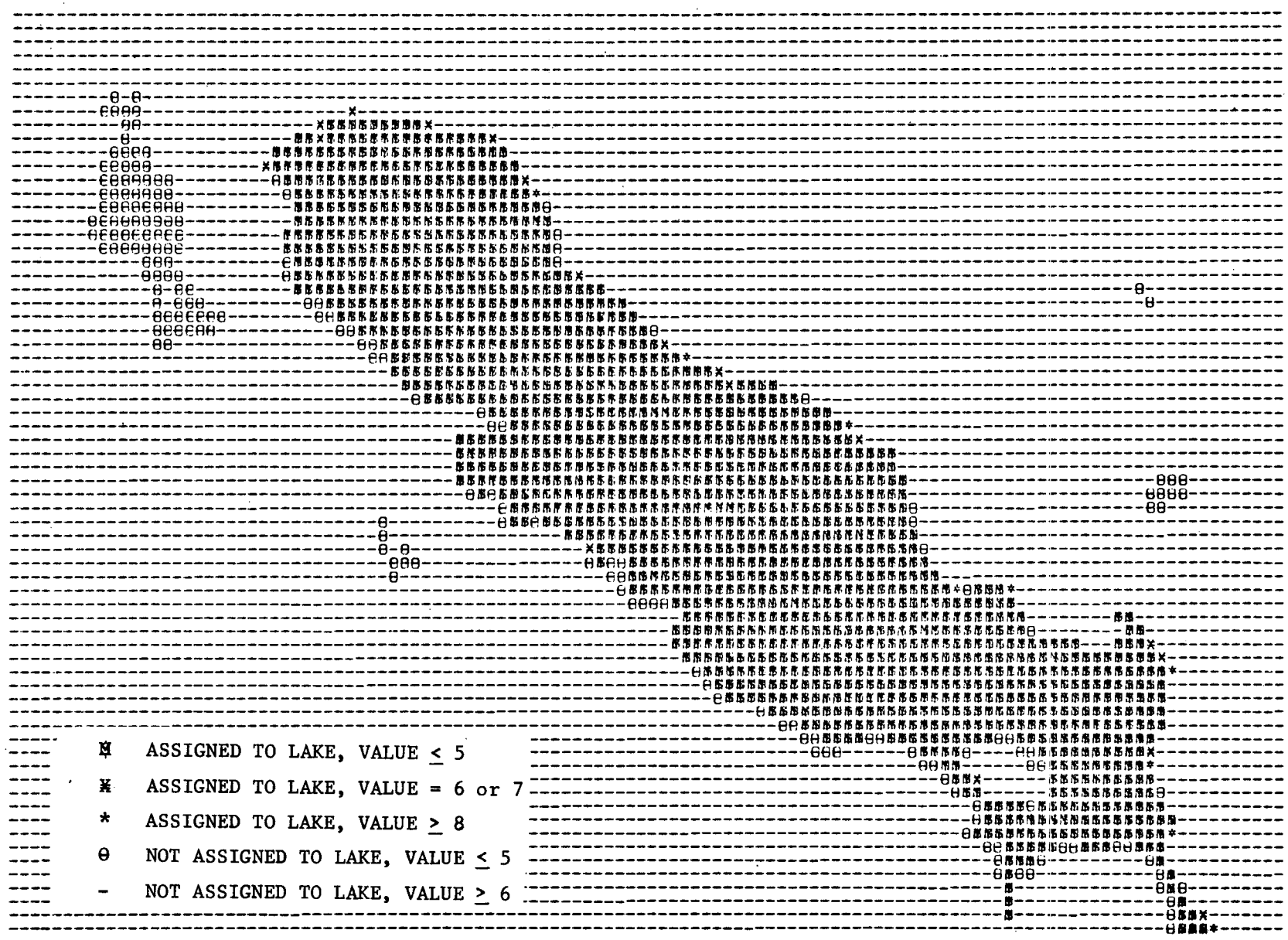

FIGURE 7 RESULTS OF COMPUTER-AIDED ASSIGNMENT OF ERTS PIXELS TO GULL LAKE

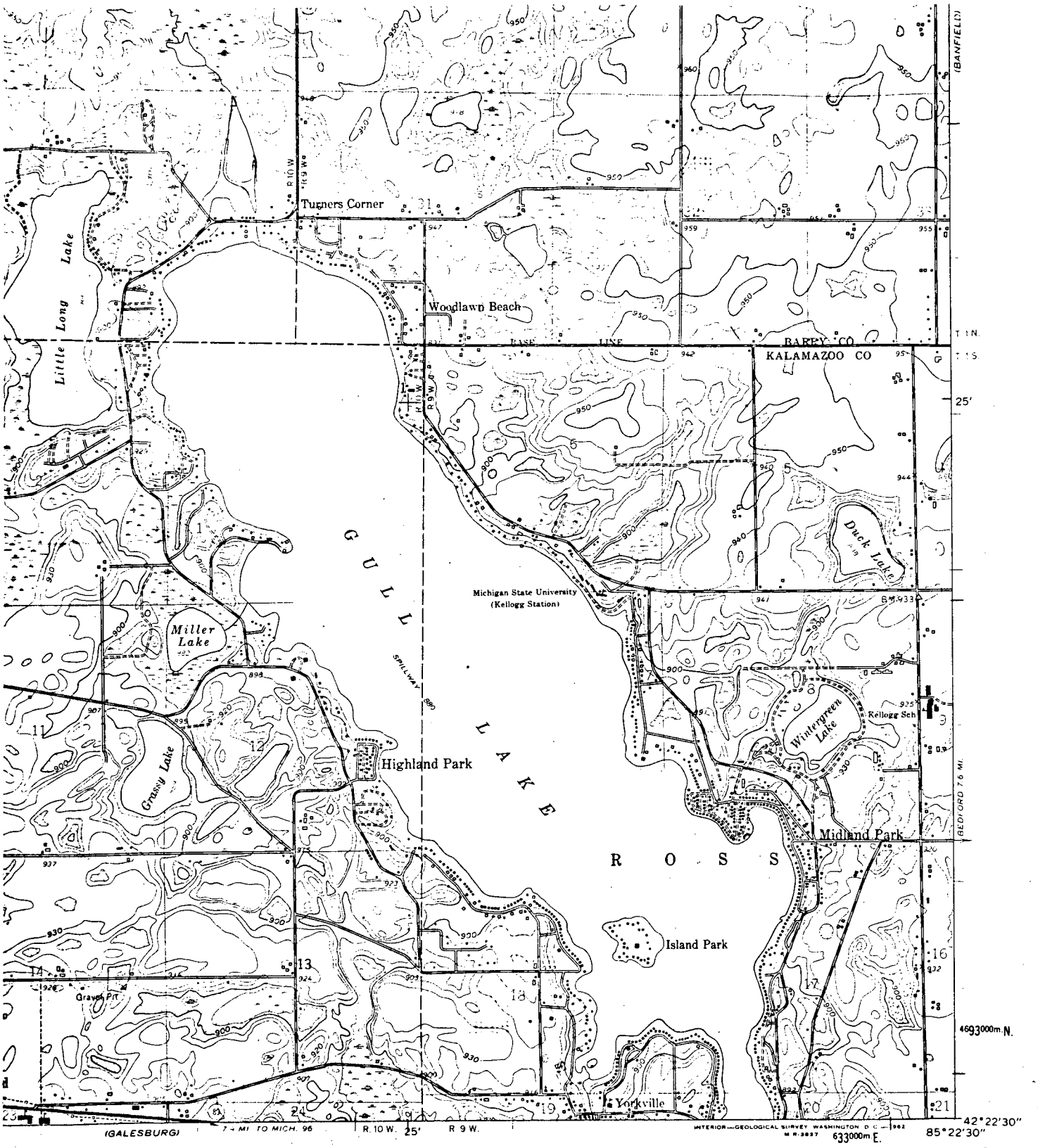

FIGURE 8

USGS TOPOGRAPHIC MAP OF GULL LAKE

Atmospheric Effects

The ERTS sensors detect radiation that passes through the Earth's atmosphere. Important questions for users of ERTS data are: (1) Does the atmosphere significantly degrade the quality or quantity of information that can be extracted from ERTS data and (2), if so, how and how much can these degrading effects be reduced? In this task, we are addressing these problems, primarily from the viewpoint of recognition processing of ERTS data on computers. Both empirical and theoretical analyses are being pursued.

Computer techniques for performing recognition operations on MSS data are susceptible to changes in atmospheric conditions because most use the absolute level of the received signals. Since atmospheric differences between training areas and areas to be recognized can cause changes in both magnitudes and spectral shapes of signals, automated recognition performance can be degraded and/or additional training can be required to maintain an acceptable level of performance. The same conditions might have less effect on a trained photo-interpreter; however, even he could be confused by substantial tonal and spectral changes.

One of our first steps in the analysis was to use the radiative transfer model developed at ERIM by Dr. Robert E. Turner (under NASA SR&T sponsorship through NASA/JSC) to predict the type of signal variations that could be induced by the atmosphere. Figure 9 presents several graphs that were included in the previously referenced paper that was presented at the "Symposium on Significant Results Obtained from ERTS-1", March 5-9, 1973. Without discussing the graphs in detail here, we note only that (1) extraneous path radiance constitutes a major part of the received signal, (2) the path radiance effect is greatest in ERTS Band 4 and least, but not negligible, in ERTS Band 7, (3) there is a strong dependence on both haze content (denoted by horizontal visual range at the ground) and background albedo, and (4) there is some dependence on scan angle, even though the ERTS-1 MSS scans $\pm 6°$ from nadir.

Another aspect of the atmospheric study presented in the first Type II Progress Report was a graphical comparison between ERTS-band radiance predictions made with the ERIM model and empirical measurements extracted from ERTS-1 data. Some errors in these preliminary graphs were subsequently determined, and corrected versions were presented in the Symposium paper. There still remains an unresolved difference in magnitude between the model calculations and the empirical results. The June 8th and 25th flights were to have helped resolve this difference.

Another investigation has been carried out during this reporting period to attempt to determine differences in signal levels throughout the Aug. 25th ERTS frame (1033-15580) and contributions of the atmosphere to these differences.

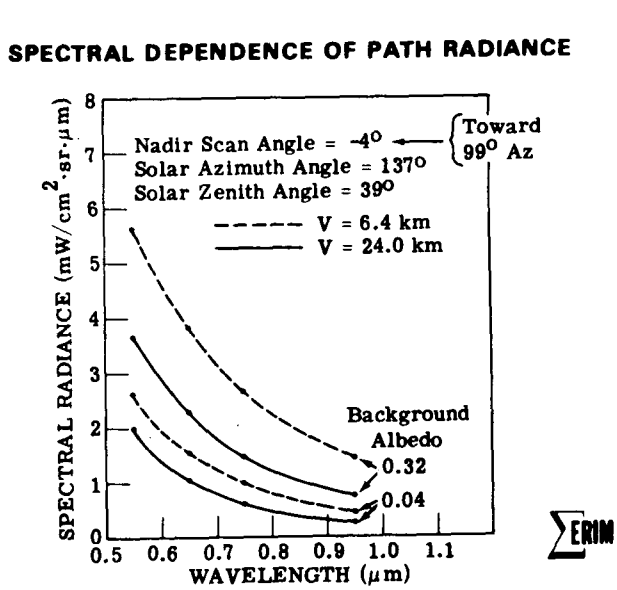

Part(a)

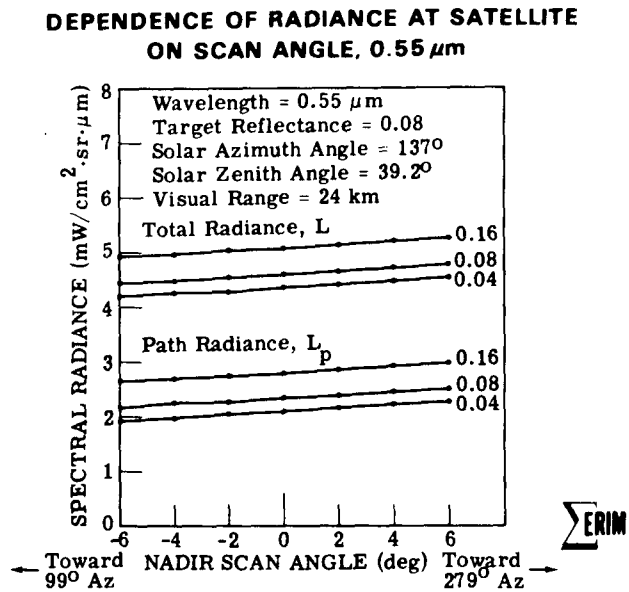

Part(b)

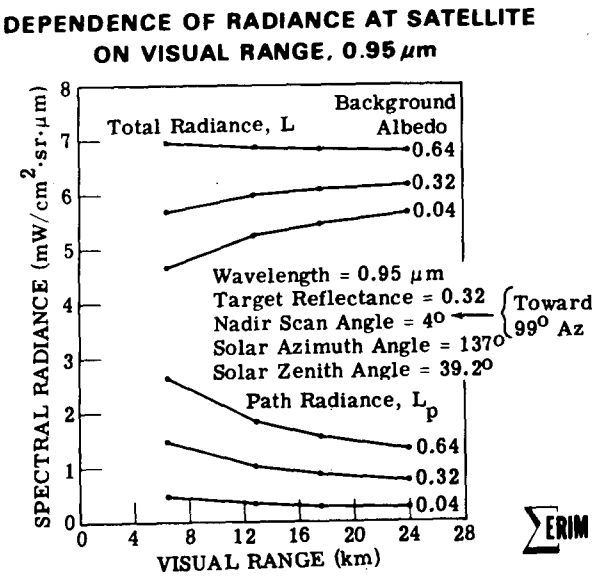

Part(c)

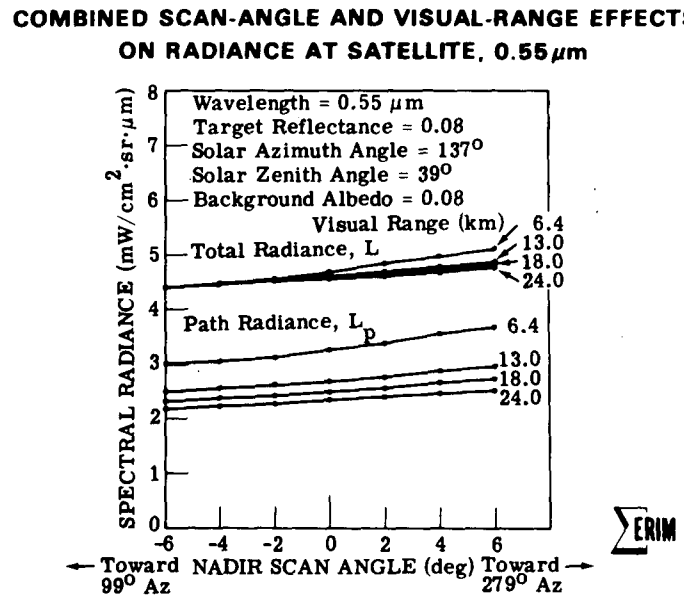

Part(d)

FIGURE 9 RADIATIVE TRANSFER MODEL CALCULATIONS OF ATMOSPHERIC EFFECTS IN ERTS DATA

Water was selected as the surface material for study since there are several relatively large lakes throughout the scene and water is easily identified in the data. Signal statistics (mean vector and covariance matrix) were determined for approximately 30 water bodies throughout the frame. Signal levels (in digital counts on the CCT) for each water body were placed on an overlay of the scene and contours of constant signal levels from water were produced manually. Figures 10 - 13 present the water signal-level contours for ERTS Bands 4-7, respectively. The contours generally reflect the weather pattern that existed at the time. A bank of clouds extended across the top left portion of the frame, while the center of the frame was relatively clear (especially Grand Rapids) and the bottom left half was hazy. The same general pattern applies to all four contour maps, i.e., lower signal values in the clear areas and higher signals in the hazy areas.

Information on the haziness of the atmosphere was obtained from National Weather Service (NWS) reports from five reporting stations within the frame --Muskegon, Grand Rapids, Kalamazoo, Battle Creek, and Lansing. Their reported horizontal visual ranges are listed at the bottom of Table 2. More discussion on the usefulness of such visibility reports is reserved for later in this subsection.

The reflectance of water is essentially zero in ERTS Bands 6 and 7, and a few percent in Bands 4 and 5 where it depends somewhat on the depth and turbidity of the water and the bottom color. Therefore, we believe that clear open-water signal levels in Bands 6 and 7 well represent path radiance and, in Bands 4 and 5, are still largely due to path radiance.

To study how much a signal from a low reflecting surface, like water, can vary across a frame with different amounts of haze in various portions, we made calculations with the radiative transfer model for the sun angle, scan angle, and visual range that existed for each of the five stations. A zero reflectance surface was assumed for water in Bands 6 and 7 and a 5% reflectance surface was assumed for Bands 4 and 5. The computed spectral radiances for three different background albedoes are listed in Table 2. The right-most column gives the maximum variation between stations, as a percentage of the minimum value for the given albedo. The variation ranges from 6 to 17% in Bands 4 and 5 and from 50 to 74% in Bands 6 and 7. Thus, it is seen that appreciable differences can exist due to atmospheric effects.

Empirical values in Bands 5 and 7 from lakes near four of the reporting stations are plotted versus location along a transect from Muskegon to Kalamazoo to Lansing; see Figure 14, Parts (a) and (b), respectively. Also, on the figures are corresponding computed values extracted from Table 2.

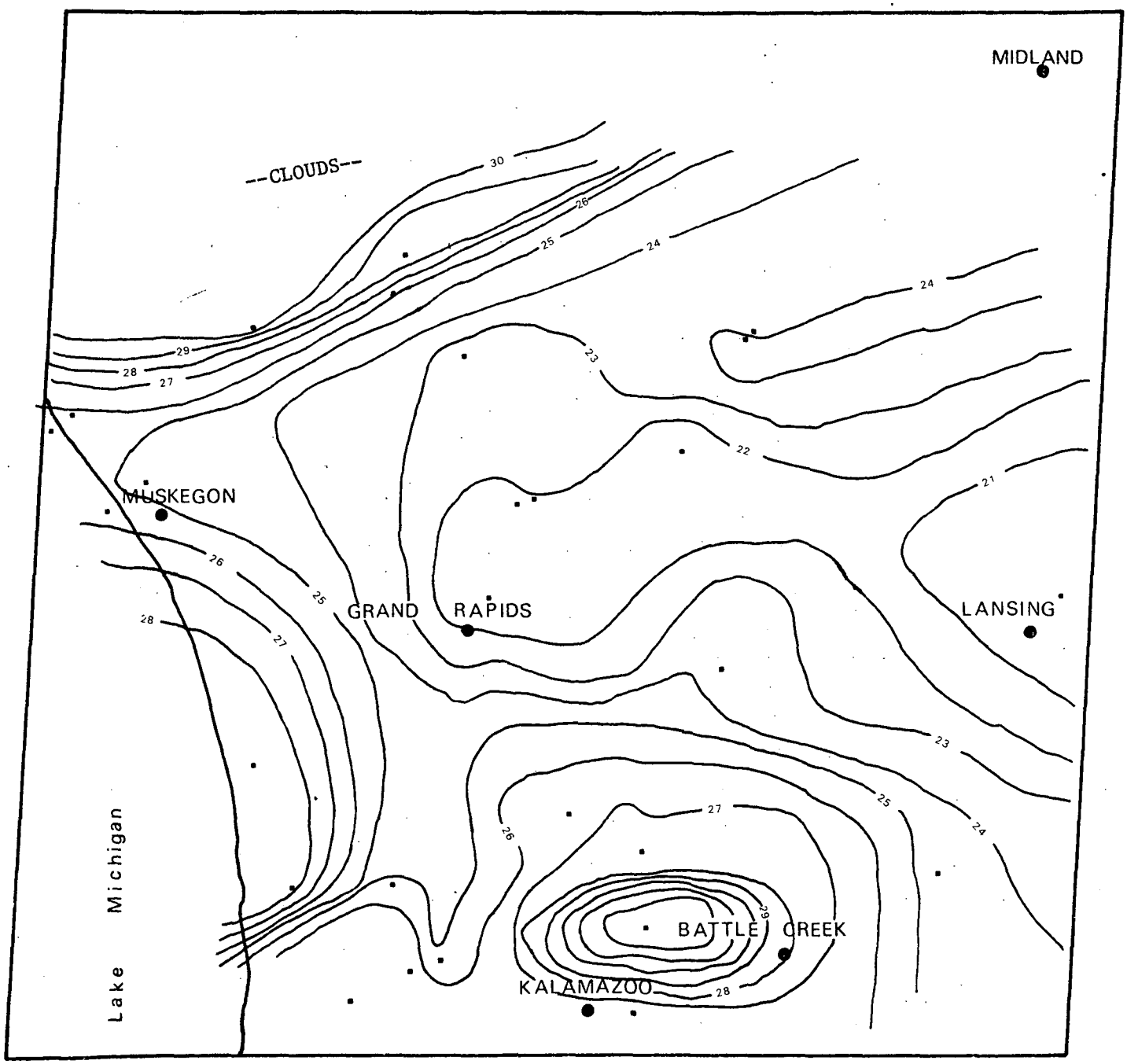

FIGURE 10. WATER SIGNAL CONTOURS, ERTS Band 4
(Frame 1033-15580)

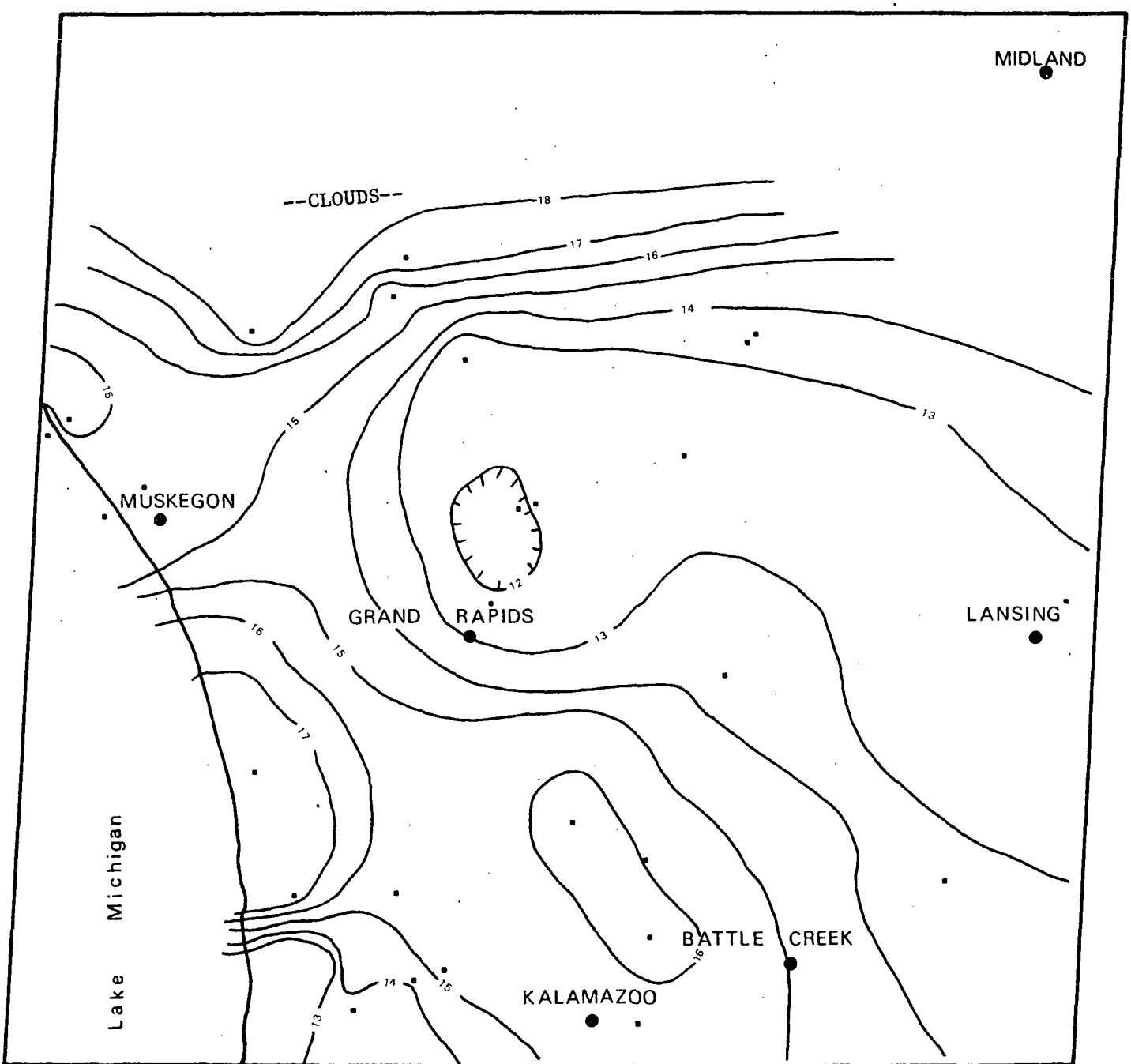

FIGURE 11. WATER SIGNAL CONTOURS, ERTS Band 5
(Frame 1033-15580)

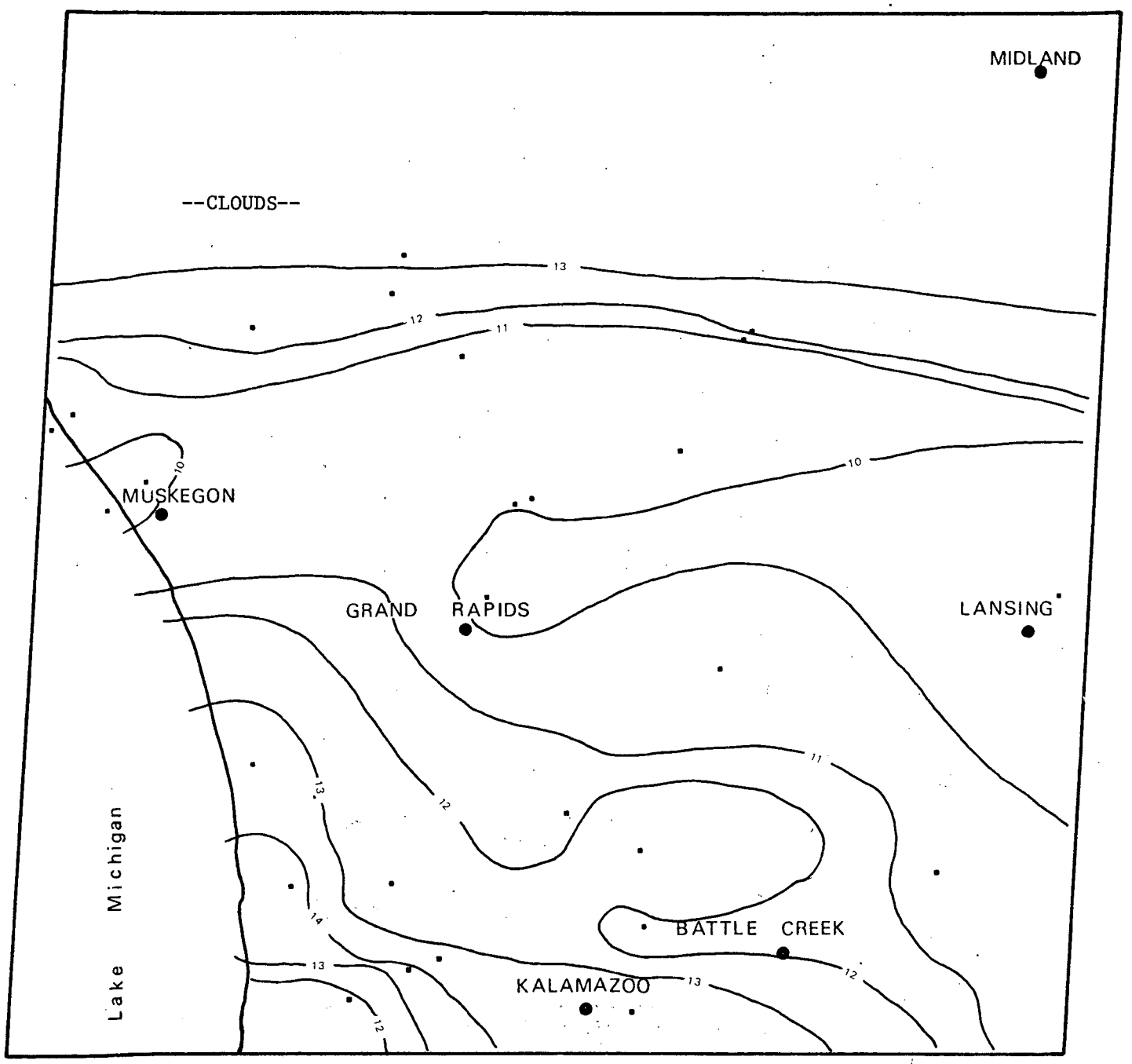

FIGURE 12. WATER SIGNAL CONTOURS, ERTS Band 6
(Frame 1033-15580)

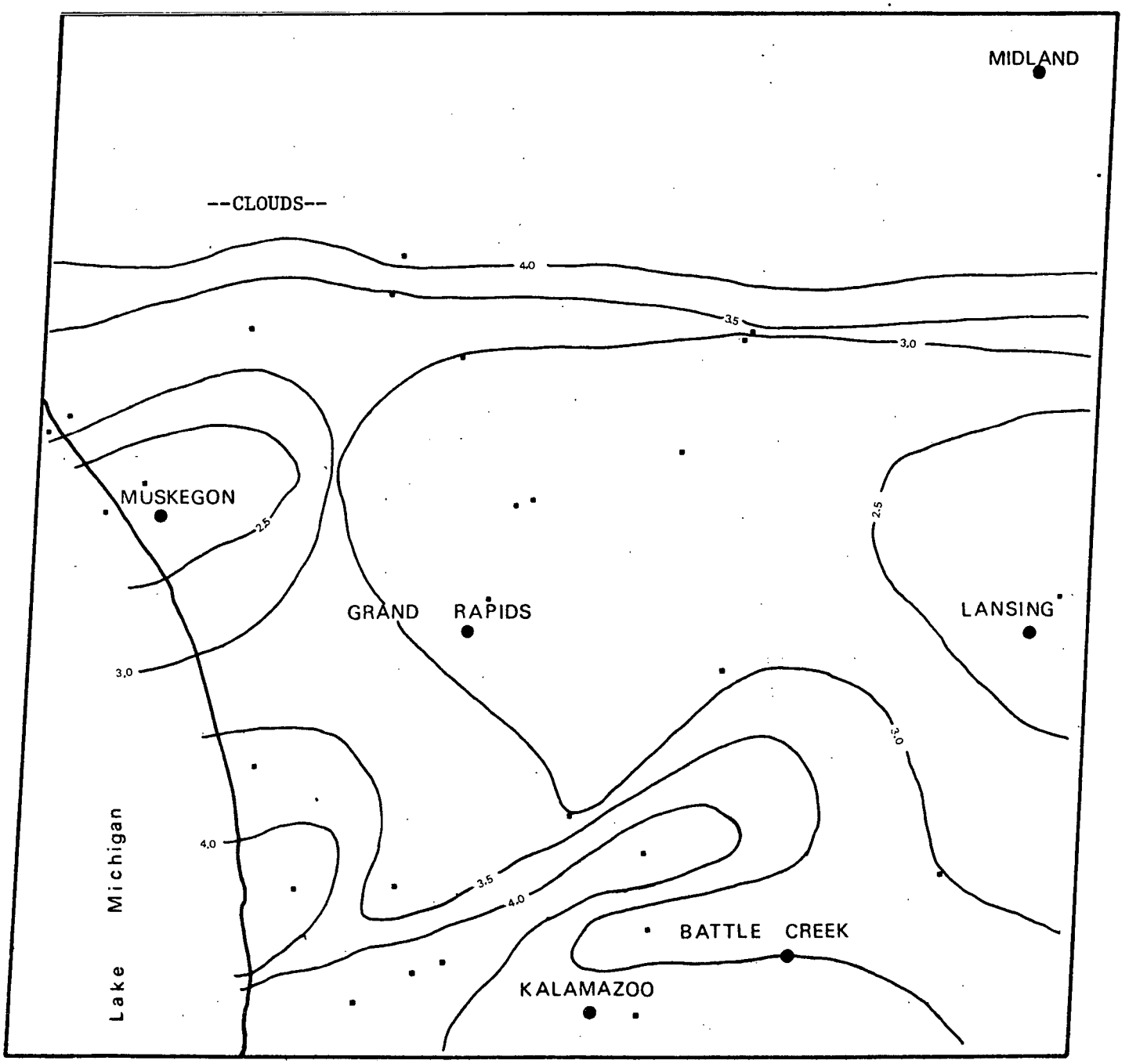

FIGURE 13. WATER SIGNAL CONTOURS, ERTS Band 7
(Frame 1033-15580)

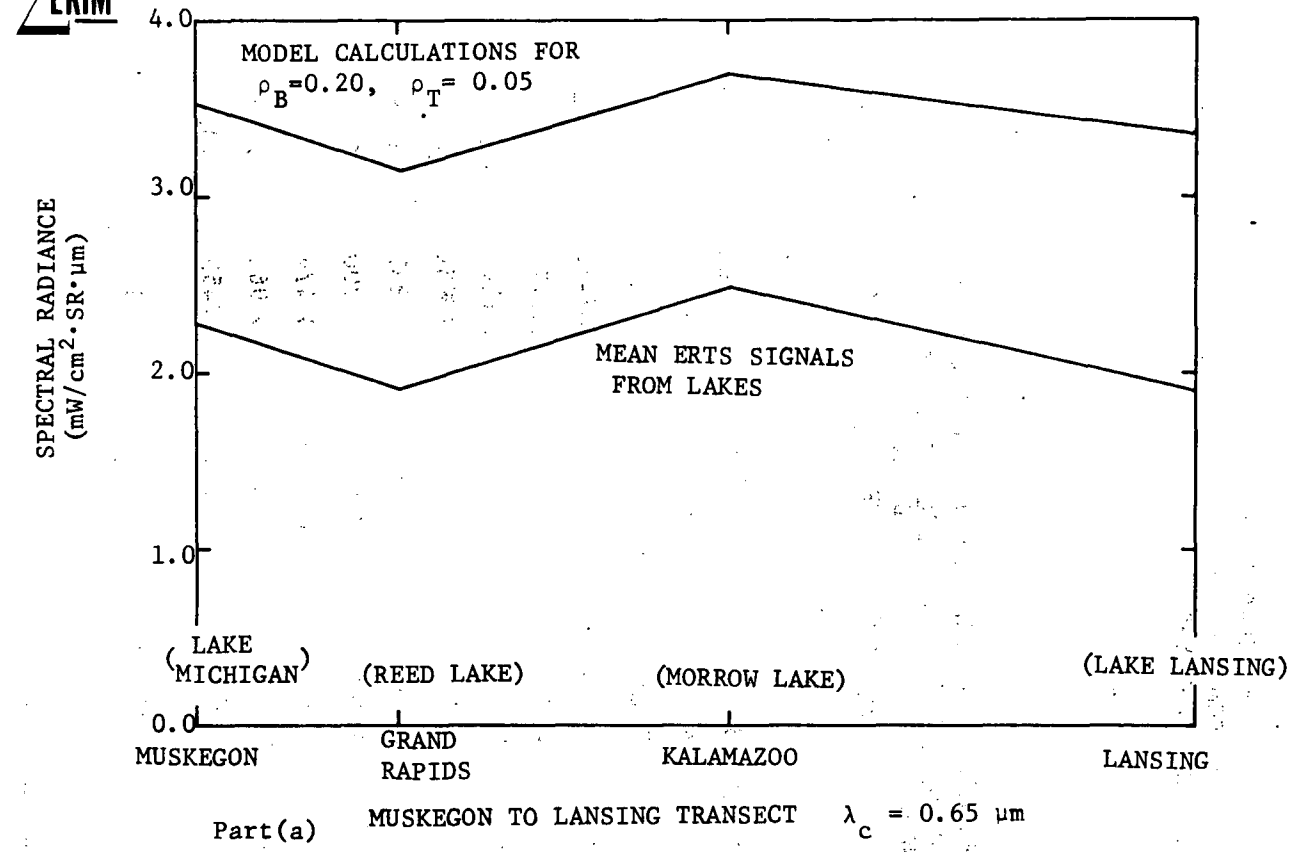

Part(a) MUSKEGON TO LANSING TRANSECT λ_c = 0.65 μm

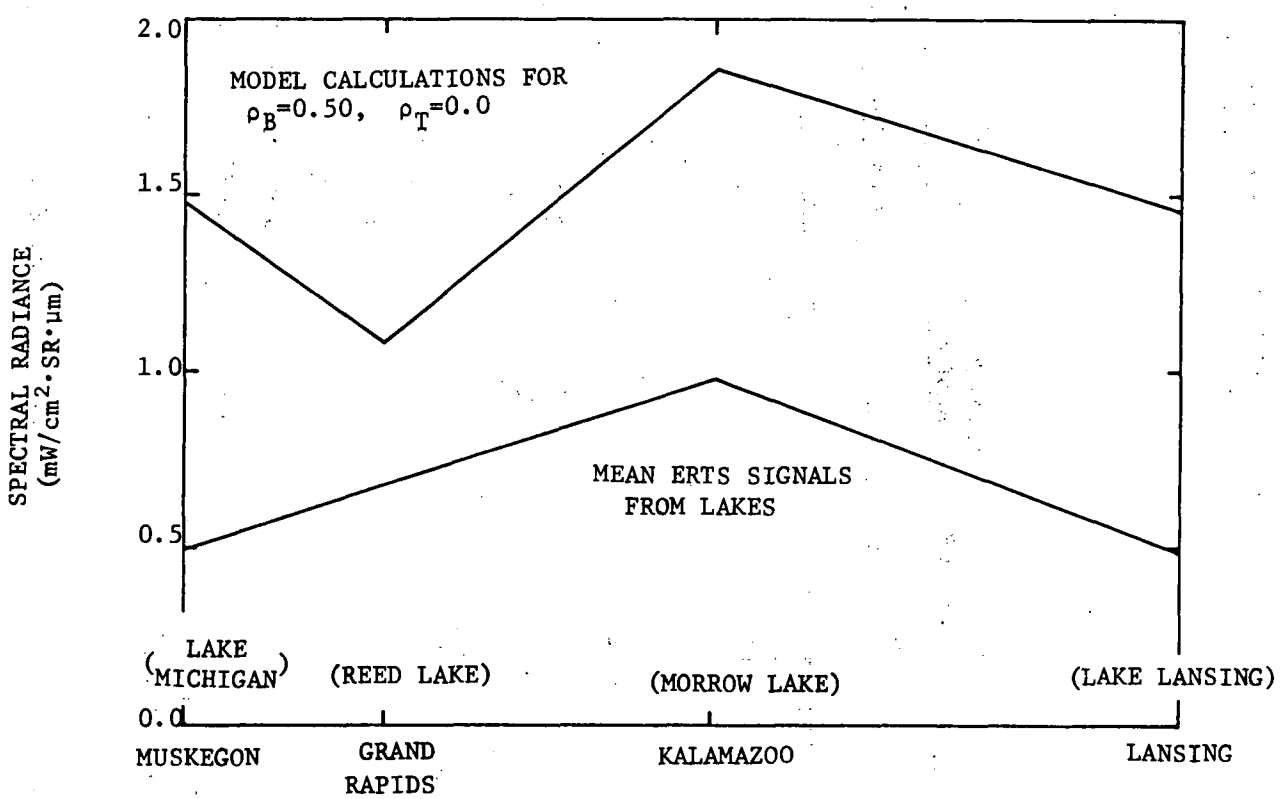

Part(b) MUSKEGON TO LANSING TRANSECT λ_c = 0.95 μm

FIGURE 14. COMPARISON OF MODEL CALCULATIONS WITH RADIANCES EXTRACTED FROM ERTS DATA FOR WATER BODIES

TABLE 2. MODEL CALCULATIONS OF TOTAL SPECTRAL RADIANCE AT SATELLITE FROM LOCATIONS THROUGHOUT FRAME 1033-15580

WAVELENGTH	TARGET REFLECTANCE	BACKGROUND ALBEDO	COMPUTED SPECTRAL RADIANCE AT VARIOUS REPORTING STATIONS ($mW/cm^2 \cdot Sr \cdot \mu m$)					MAXIMUM VARIATION ACROSS FRAME
λ	ρ_T	ρ_B	MUSKEGON	GRAND RAPIDS	KALAMAZOO	BATTLE CREEK	LANSING	Max-Min / Min
(μm)								(%)
.55	.05	.05	3.786	3.545	3.674	3.531	3.462	9.3
		.10	4.172	3.837	4.151	3.945	3.857	8.7
		.20	4.960	4.430	5.123	4.789	4.661	15.6
.65	.05	.05	2.640	2.514	2.600	2.517	2.485	6.2
		.10	2.926	2.726	2.962	2.825	2.777	8.6
		.20	3.506	3.153	3.694	3.449	3.368	17.1
.75	0	.10	1.074	0.815	1.222	1.045	0.981	49.9
		.30	1.907	1.417	2.290	1.943	1.831	61.6
		.50	2.759	2.030	3.386	2.863	2.700	66.8
.95	0	.10	0.509	0.370	0.607	0.506	0.474	64.0
		.30	0.988	0.716	1.223	1.022	0.963	70.8
		.50	1.474	1.065	1.851	1.546	1.459	73.8
REPORTING VISIBILITY (ST. MILES) @ 11 a.m. 8/25/72			8+	15	5* (Haze)	7	8	

*12 NOON REPORT SINCE NONE AVAILABLE @ 11 a.m.

The agreement between the shapes of the theoretical and empirical plots is striking. The one departure is the Band 7 value extracted from Reed Lake near Grand Rapids. This is a small lake; we are uncertain of its condition; and it was used only because no larger lakes exist nearby. The differences in magnitude between the two types of data are related to the unexplained difference discussed earlier and also are influenced by the particular target reflectance and/or background albedo selected for calculation and plotting.

From the foregoing, it would appear that a radiative transfer model and surface visual range estimates can be used to predict the general shape of variation that is present in ERTS data throughout a scene. However, further analysis and examples are needed to confirm this impression and to resolve the differences found between magnitudes of calculated and empirical radiances.

A word of caution is in order regarding the use of NWS visibility estimates. Aside from the facts that they indicate only ground-level conditions, depend upon the experience of the observer, and may not adequately characterize the entire atmospheric path, one must also understand the reporting procedures and be familiar with the visibility markers available at the stations of interest. Private conversations with NWS personnel have resulted in the following information: Seven miles is considered to be unlimited visibility as far as NWS and flight controllers are concerned; longer ranges depend on the reporting station having suitable markers at longer distances. The NWS observation manual states that "When the prevailing visibility is more than 7 miles and is also estimated to be more than twice the distance to the most distant marker visible, encode the visibility as twice the distance to that marker, rounded to the nearest reportable value, or 7 miles which ever is the greater, and if the visibility is estimated to be greater than the coded value, add a plus". Therefore, even on an exceptionally clear day a station with restricted view (e.g., because of trees and terrain) and an absence of suitable markers might never report a visibility greater than 7 miles, while another might have suitable markers at 30 miles or more distance and report corresponding values. In sum, ground visibility readings can provide useful information for analysis of ERTS data, but one can be misled if restrictions on the reporting stations are not known and considered.

Preprocessing for Improved Recognition Performance

In the atmospheric effects section, there is mention of the problems that can be encountered in recognition processing on computers when atmospheric conditions change. There also are other sources of signal change that can degrade recognition performance, e.g., changes in surface reflectance and sun and scan angle changes. Some of these sources are present to a greater extent in aircraft MSS data than in satellite data, but all potential sources should be considered here for ERTS data. ERIM's experience in processing aircraft MSS

data has led to the development over the past several years of preprocessing techniques to remove systematic variations from MSS data or to transform them in ways that minimize the effects of signal changes. Because these preprocessing techniques permit the use of signatures from localized areas to be applied to other locations and conditions, the preprocessing techniques are frequently called "signature extension" techniques.

A variety of preprocessing techniques have been developed for use on aircraft data, but thus far we have begun the investigation of only one of them on ERTS-1 data -- the ratioing of signals in various pairs of data channels. Multiplicative variation effects that are correlated between channels tend to cancel, especially if ratioing is performed after subtraction of terms which represent the additive path radiance component of the received signals.

Images of ratioed signals represent enhanced images which possibly can be more useful than single-band images in some applications. We produced ratio images for most non-redundant combinations of signal channels for that portion of ERTS frame 1033-15580 which contains the test area for this task. An example ratio image was presented in the Type I Progress Report for the period 1 March 73-30 April 73, ERIM Report No. 193300-13-L, dated 9 May 1973.

The ratioed signals also can be used as inputs to computers for automated decision making. Where scene materials have distinctive ratios, simple level gating can be used to decide which classes are present. In other instances they might be used as information inputs to more sophisticated recognition processors.

We are in the process of studying the usefulness of the ratio techniques for the agricultural data in our test area. The results of this work will be reported later.

Proportion Estimation

Another aspect of this investigation is concerned with testing the applicability of advanced information extraction techniques to ERTS-1 MSS data. (These techniques have been developed at ERIM with funding provided by the Supporting Research and Technology program of NASA-JSC under Contract NAS9-9784.) One technique addresses problems associated with accurately determining areas covered by features in the scene using scanners with limited spatial resolution, like ERTS-1 MSS. Clearly, there is a serious problem for features smaller than the instantaneous field of view of the scanner. In addition, problems exist even for larger features since many of the ERTS MSS pixels overlap the boundaries between these and adjoining features. As a result, the radiation represented in those pixels is a mixture of radiation reflected from two or more materials. Since the signals generated in such pixels are not characteristic of any one material, the pixels will generally be improperly classified. Therefore, the area assigned to each material class could seriously be in error. For example, at least 25% of the pixels covering a square field of 50 acres (20 hectares) will overlap its boundaries.

At ERIM we have developed a data processing technique* to estimate the proportions of materials contained within each pixel, by taking advantage of the fact that information is gathered in several spectral bands. This permits a more accurate determination of the area covered by each material; the greater the number of spectral bands used, the more materials can be considered. We next describe and evaluate the results of an initial test of this technique on ERTS-1 MSS data.

The goal of this initial test was to determine how accurately we could estimate the surface area of a number of lakes and ponds in a small portion of an ERTS frame. The region selected for processing is shown in Figure 15 a black and white aerial photograph of that region.

Using an enlargement of this photo, the surface area of the water bodies was determined. Two methods were used to determine area, dot grid and planimeter, with the results being calibrated by assuming a one mile separation between the section line roads apparent in the photo.

For purposes of comparison, the data were processed using two algorithms in addition to the proportion estimation algorithm. The first of these was the conventional recognition algorithm in which each pixel was assigned to one and only one class. In the second algorithm, a simple level slicing approach was used to estimate proportions using only one ERTS-MSS band.

*"Estimating the Proportions Within a Single Resolution Element of a Multispectral Scanner", by H.Horwitz, R.Nalepka, & J.Morgenstern, Proc. of 7th Internat'l Symp. on Remote Sensing of Environ., Willow Run Labs., The Univ. of Mich., Ann Arbor, 1971.

FIGURE 15. TEST AREA FOR PROPORTION ESTIMATION

In processing the data the first step was the establishment of training signatures for the major object classes in the scene. The primary scene components in this case were water, trees, and soil. A number of pixels containing pure samples of each of these classes was located and the mean signal vector and associated covariance matrix was determined for each class. Since there were some data quality problems with ERTS Band 6, only Bands 4, 5, and 7 were used to establish signatures and for the ensuing processing.

Having established the signatures, the three processing algorithms (proportion estimation, conventional recognition, and level slicing) were applied to the data. In order to meaningfully compare the results generated using these algorithms, threshold values were set in each case to eliminate water false alarms (i.e., non-water pixels classified as water). In the case of the proportion estimation algorithm the output is a set of proportions for each pixel. In order to eliminate water false alarms for this algorithm only pixels with proportions of water ≥ 0.4 were considered in the estimates of surface water area.

The level slicing approach which was suggested by someone outside of ERIM is similar to that used in the proportion estimation algorithm however the one major drawback is that it is limited to estimating the proportions of only two classes. Therefore only particular and limited problems may be handled using the level slicing approach. Basically, the approach assumes that only two classes exist in the scene and given the mean signal values in one spectral band for each of these classes one can determine the proportions of these classes in any pixel by the relationships

$$p_A = \frac{|\mu_B - X|}{|\mu_A - \mu_B|}$$

$$p_B = \frac{|\mu_A - X|}{|\mu_A - \mu_B|} \qquad \text{for} \quad \begin{matrix} \mu_B > \mu_A \\ \mu_A \leq X \leq \mu_B \end{matrix}$$

and

$$p_A = 1.0 \quad \text{for} \quad X < \mu_A$$

$$p_B = 1.0 \quad \text{for} \quad X > \mu_B$$

where μ_A and μ_B are the mean signal values of classes A and B, X is the signal value generated in the pixel being examined, and p_A and p_B are the proportions of class A and B, respectively.

It is clear that if more than two classes exist in the scene a signal value X between μ_A and μ_B could be generated by combinations of class A or class B and a third class. Also values of X smaller than μ_A or larger than μ_B might be a result of a pure sample of another class. Certainly one could place limits on the allowable values of X to reduce the effect of the latter problem however the former problem still would exist.

For this particular application where water was the primary class of interest it was not necessary to place limits on the allowable values of X since in ERTS Band 7 water generated the lowest signal values. Since many of the water bodies in the scene were surrounded by trees, the signatures for water and trees were used in the level slicing algorithm. In order to eliminate water false alarms for this algorithm only pixels with proportions of water ≥ 0.6 were considered in the estimates of surface water area.

For the conventional recognition algorithm all three signatures were used and the rejection threshold was set so that only a tiny fraction (<0.01%) of the pixels characterized by the water signature would be misclassified. The recognition map generated using this threshold contained no false alarms.

Before describing the test results we present here a brief discussion of the areas which were assigned to each pixel. The instantaneous field of view of the ERTS MSS is 79 m X 79 m but since the data are oversampled along the scan direction there is overlap in the ground patch covered by successive samples. Therefore in order that calculations of the total area of an ERTS frame not exceed the actual area viewed in that frame a smaller effective size has been used in the scan direction. However, for the problem being addressed here where the area for only one class in the scene is being estimated one needs to consider the actual ground area viewed by each pixel. In other words, if a pond smaller than 79 m X 79 m is contained within one pixel and that pixel is estimated to contain 50% water, the estimated area of the pond is 50% of 79 m X 79 m and not 50% of some smaller effective area. Now if this same pond was seen in the overlap area of two successive pixels it would be inaccurate to use the 79 m X 79 m area for each pixel since some portion of the pond would be counted twice.

In order to account for problems of this sort three separate pixel sizes were used in computing estimated area. If the pixel identified as containing some portion of water in excess of the threshold value fell between two pixels on the same scan line which also were identified as containing water, the pixel size for area estimates was assumed to be 79 m X 57 m (the 57 m size was computed based on the 100 nautical mile frame size and number of samples per scan line). "Water" pixels with one "water" neighbor along the scan line were assumed to be 79 m X 68 m and "water" pixels with no "water" neighbors were assumed to be 79 m X 79 m.

Test Results: Using the three processing algorithms described earlier, three water classification maps were generated. These are shown in Figures 16, 17, and 18 for the proportion estimation, level slicing, and conventional recognition algorithms, respectively. The proportion estimation and level slicing maps are printed with symbols whose density is related to the proportion of water estimated in each pixel while the conventional recognition map includes only a single symbol where water was detected implying that the entire ground area viewed in those pixels is covered with water.

Upon comparing Figures 16 through 18 with the aerial photograph in Figure 15 it is clear that the shape of the water bodies, more accurately reproduced on the proportion estimation map and that more of the small bodies of water are detected on this map. In fact only one of the bodies of water was totally undetected.

In order to compare the area estimation results achieved on individual water bodies using the three algorithms we present Figure 19. Here we plot on the vertical axis the ratio of area as measured from the photograph to the area determined by automatic processing. On the horizontal axis we plot the shape factor which we define as a constant times the area divided by the perimeter of the water body. Shape factor is used rather than area since water bodies with small shape factors (because of large perimeters or small size) can be expected to be less accurately estimated than those with large shape factors. This expectation is borne out on examining Figure 19 which shows that the spread in accuracy for the three methods is small for water bodies having large shape factors (relatively fewer boundary pixels) and generally increases for smaller shape factors.

The area estimate accuracies are better using the proportion estimate algorithm in almost every case. There are a small number of cases in which the area is slightly overestimated however it is possible that the areas measured from the aerial photograph were on the low side. In general, the results using the conventional recognition algorithm were much inferior, especially for the smaller shape factor water bodies.

A summary of the results for the entire test site is shown in Table 3. Here we see that roughly 97% of water measured from the photograph was detected using the proportion estimation algorithm while only 85% was detected using the other two algorithms. This difference would have been larger if fewer large lakes existed in the scene.

TABLE 3
SUMMARY OF WATER AREA ESTIMATION RESULTS

	Photointerpretation	Proportion Estimation	Level Slicing	Conventional Recognition
Number of Water Bodies Detected	19	18	14	13
Total Water Area (Meters^2)	1,041,958	1,006,739	892,118	879,120

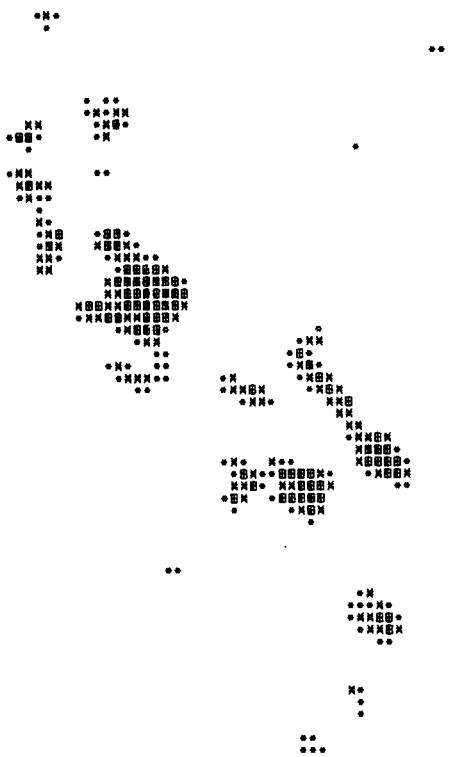

FIGURE 16.

PROPORTION ESTIMATE WATER RECOGNITION MAP

FIGURE 17.

LEVEL SLICE WATER RECOGNITION MAP

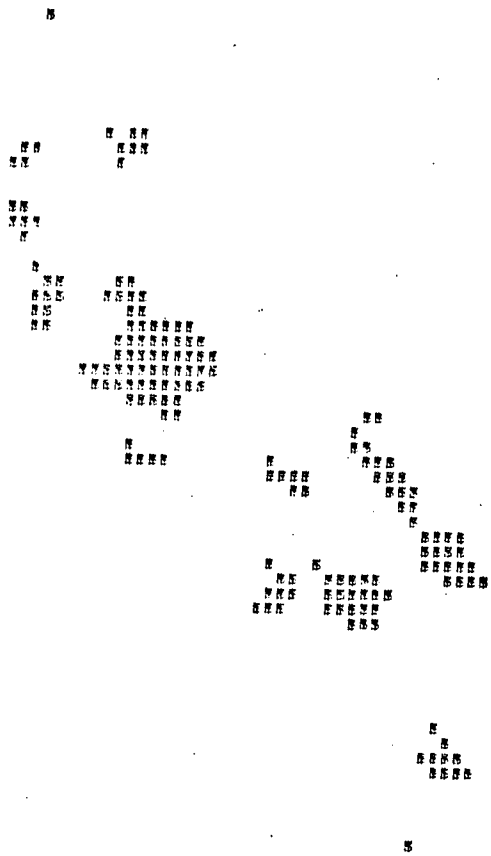

FIGURE 18.

CONVENTIONAL WATER RECOGNITION MAP

5 X 5 TO THE CENTIMETER 46 1610
10 X 24 CM. MADE IN U.S.A.
KEUFFEL & ESSER CO.

FIGURE 19 INDIVIDUAL WATER BODY AREA ESTIMATE ACCURACY VS. SHAPE FACTOR

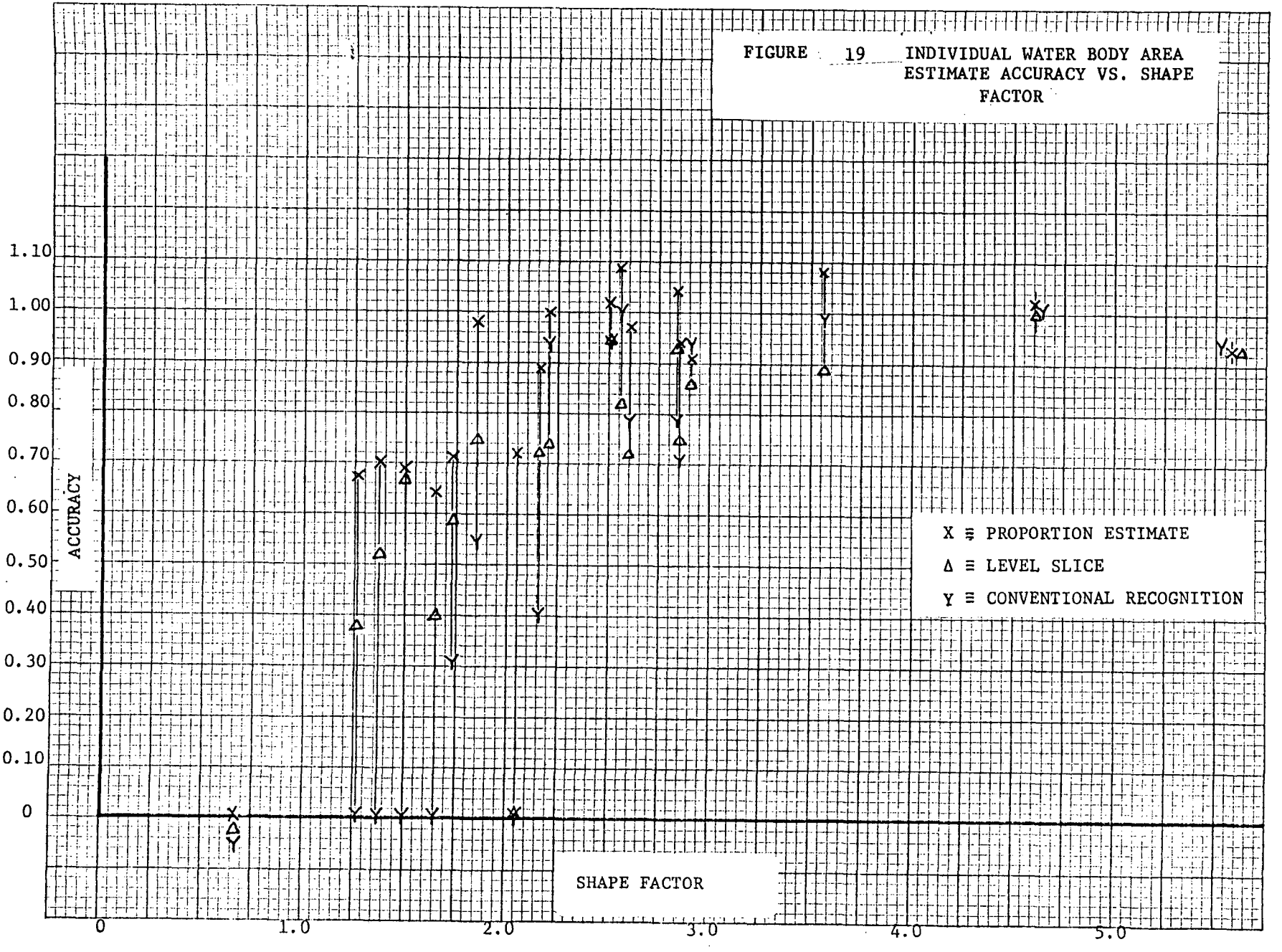

The results reported here for the conventional recognition algorithm differ from those reported at the Symposium on Significant Results Obtained from ERTS-1 in March of this year. Since that time we have had the opportunity to reexamine the initial outputs and have found that the rejection threshold used for this algorithm, while it would normally be proper, did not allow for a direct comparison between the conventional recognition results and those achieved with the other two algorithms. In any case, however, the conclusions to be drawn have not changed; that is, more accurate water surface area estimates are achieved by using the proportion estimates algorithm.

PROGRAM FOR NEXT REPORTING INTERVAL

During the next reporting period, work on all three tasks will be continued and completed, including support of the remaining aircraft underflight mission.

CONCLUSIONS

The strong influence of atmospheric effects in ERTS data has been shown. More analysis is required to demonstrate the severity of these effects in recognition processing and to apply techniques for reducing their influence.

The use of the ERIM proportion estimation technique produced more accurate estimates of surface water area in the test region than did more conventional techniques. The applicability of these techniques should be investigated for other problems.

The newly developed computer-aided procedure for assignment of ERTS pixels to ground features and test plots should facilitate our analysis of techniques for processing ERTS data.

RECOMMENDATIONS

None.

APPENDIX I

CORRELATION OF ERTS MSS DATA AND EARTH COORDINATE SYSTEMS*

William A. Malila
Ross H. Hieber
Arthur P. McCleer

ERIM, Environmental Research Institute of Michigan
P.O. Box 618
Ann Arbor, Michigan 48107

ABSTRACT

Experience has revealed a severe problem in the analysis and interpretation of ERTS multispectral scanner (MSS) data. The problem is one of accurately correlating ERTS MSS pixels with various Earth coordinate systems. The problem is caused primarily by the relatively large (∿ 80 m square) ground resolution element of ERTS. Analysis areas are usually specified on aerial photographs or topographic maps. It is difficult for an interpreter, examining a digital image display, to accurately identify which ERTS pixels (picture elements) belong to specific areas and test plots, especially when they are small. Therefore, we have developed a computerized procedure to correlate coordinates from topographic maps and/or aerial photographs with ERTS data coordinates. Application to data from other multispectral scanners is anticipated.

In the procedure, a map transformation from Earth coordinates (e.g., latitude and longitude, UTM grid, or relative grid on a photograph) to ERTS point and line numbers is calculated using selected ground control points and the method of least squares. The map transformation is then applied to the Earth coordinates of selected areas to obtain the corresponding ERTS point and line numbers. An optional provision allows moving the boundaries of the plots inwards by variable distances (typically half a resolution element) so the selected pixels will not overlap adjacent features.

Examples are presented to show improved accuracy, consistency, and efficiency over conventional procedures.

* This work was supported under ERIM Contract NAS5-21783 and an ERIM subcontract under Michigan State University Contract NAS5-21834.

Second Type II Progress Report
C. T. Wezernak, MMC 081
Task VIII, Water Quality Monitoring

INTRODUCTION

Presented in the sections which follow is a report on the technical progress of ERTS investigation MMC 081, Proposal to Determine Applicability of Satellite Remote Sensing to Water Quality Monitoring Using ERTS-A Data, for the period 1 January - 30 June 1973. During this time period, the major effort was directed towards analysis of data for the New York Bight, Tampa, and Lake Erie test sites.

The results indicate that major color and turbidity differences in water are detectable through an analysis of ERTS data. The results also indicate that this capability can be applied to the study of specific events such as ocean dumping of wastes, physical limnology of large lakes, and large scale pollution investigations.

PROGRESS

The sections which follow describe the field and analytical activities for the reporting period. Results are subdivided under the headings: New York Bight, Tampa Bay, Lake Erie, and other test locations.

NEW YORK BIGHT

General

The volume of waste disposed of by ocean dumping is increasing rapidly. Generally, ocean dumping is viewed as a convenient mechanism for the disposal of the more objectionable waste products of contemporary society, substances which are not readily amenable to treatment by means of existing techniques, or substances which are judged to be "too expensive" to treat. In the majority of cases, waste disposal takes place not in the deep ocean but rather in nearby coastal waters. Because of numerous environmental implications associated with the practice, ocean disposal of wastes has become a matter of national and international concern.

An important element in present and future programs for managing ocean disposal of wastes is the availability of a monitoring system (or systems) which will a) document authorized discharges to verify compliance in terms of discharge location, b) detect unauthorized dumps or accidental discharges, and c) provide data regarding the movement of wastes. Monitoring systems are required not only for the detection of small spills and discharges but also for monitoring large scale events.

The problem under investigation at this location is the practice of barge dumping of wastes into the sea. Specifically, the objectives of the investigation are:

1. Demonstrate the potential of satellite remote sensing for monitoring large scale waste disposal activities in the marine environment.

2. Provide data regarding the surface spread and movement of wastes discharged by barge dumping.

3. Provide data regarding surface circulation.

Information regarding the latter is vital for purposes of environmental impact assessment of existing waste disposal practices at this location.

Study Area

The coastal waters adjacent to the New York Metropolitan Region are the repository for substantial quantities of sewage sludge, industrial acid-waste, construction debris, and dredge spoils. The designated dumping areas are shown in Fig. 1.

Sewage sludge is normally disposed of at a location approximately 19 km. south of Long Island. At the present time, approximately 9,500 cu. m. per day are dumped at this location. In addition to nutrient enrichment of the overlying waters, the introduction of heavy metals, etc. at the immediate dump location, the practice often results in the formation of extensive surface films.

Acid-iron wastes are normally disposed of at a location approximately 20 km. east of New Jersey and 24 km. south of Long Island. The waste solution contains approximately 8.5% H_2SO_4, 10% $FeSO_4$, and small quantities of various metallic elements. The wastes are dispersed by barge over a hairpin-shaped course of approximately 8 km. in length. The subsequent oxidation of the iron from the ferrous to the ferric state produces a suspension which tends to remain in a distinct pattern for long periods after dispersal.

In addition to the above substances, dredging spoils from the New York metropolitan harbor area and construction debris are dumped in the New York Bight.

Field Activities and Aircraft Data Collection

Field data have been collected in support of the program at the locations shown in Fig. 2. The most recent efforts took place on 7 April 1973 and 25 April 1973. Typical surface water quality determinations are summarized in Table 1A - 1H. As expected, a sharp increase in total iron is found in the acid grounds area (800 µg/ℓ) as compared with adjacent ocean waters (20 µg/ℓ). Most of the iron is in the form of particulate iron.

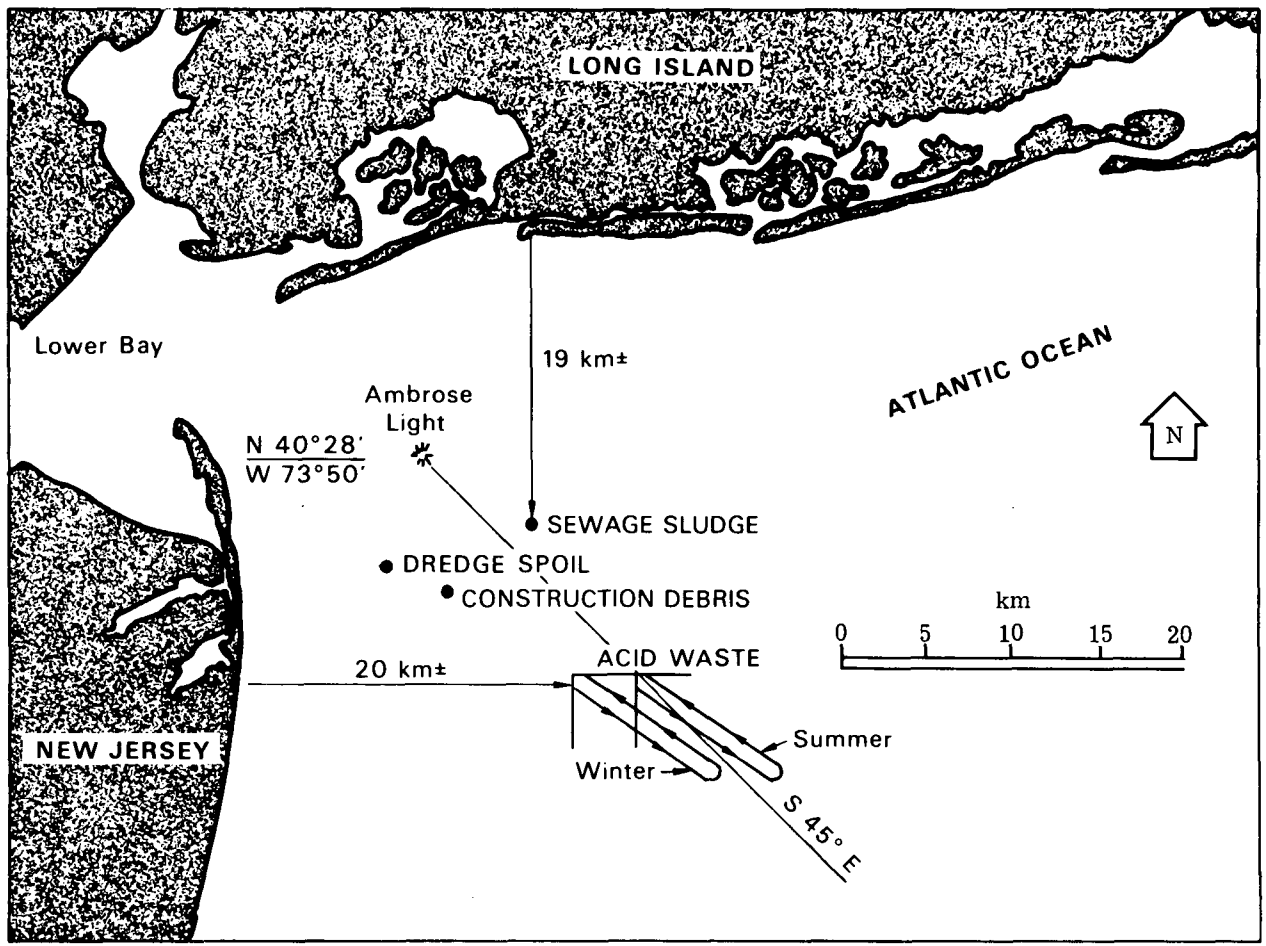

FIGURE 1. WASTE DISPOSAL SITES IN THE NEW YORK BIGHT

ERIM
FORMERLY WILLOW RUN LABORATORIES, THE UNIVERSITY OF MICHIGAN

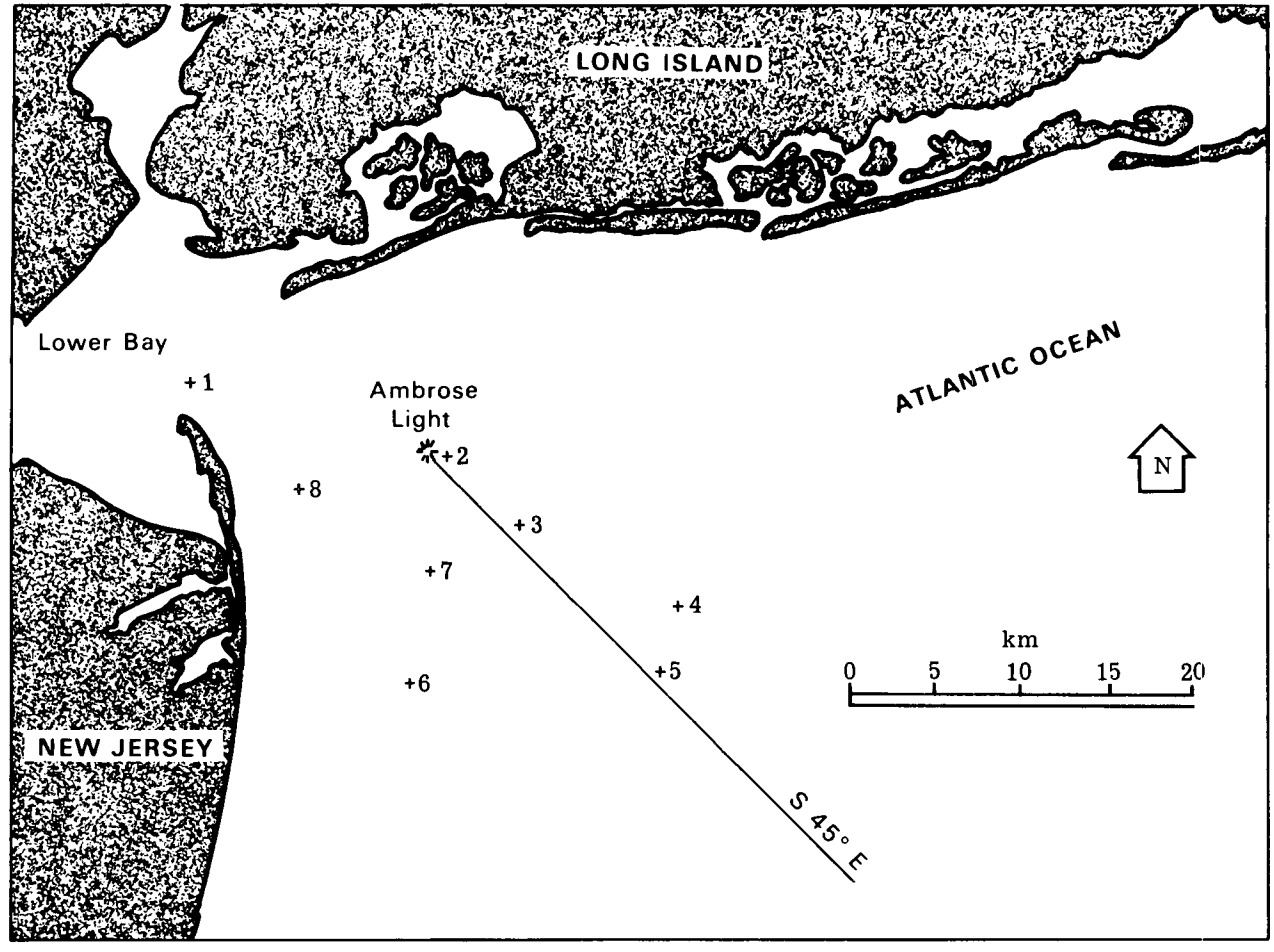

FIGURE 2. SAMPLING LOCATIONS

ERIM
FORMERLY WILLOW RUN LABORATORIES, THE UNIVERSITY OF MICHIGAN

TABLE 1A
WATER QUALITY DATA

Station 1 =	Buoy 12
pH =	8.0
turbidity =	6.6 FTU
Suspended solids =	13.7 mg/ℓ
Total solids =	18.4 gm/ℓ
Salinity 0/00 =	17.0 (outgoing tide)
chlorophyll "a" =	36 mg/m^3
PO_4 - P =	100 µg/ℓ
NO_3 - N =	
Total Fe =	
Secchi disk (50 cm):	white = 3.5' black = 2.0'

TABLE 1B
WATER QUALITY DATA

Station 2 =	Ambrose Tower
pH =	8.1
turbidity =	3.7 FTU
Suspended solids =	7 mg/ℓ
Total solids =	26 gm/ℓ
Salinity 0/00 =	24
chlorophyll "a" =	4 mg/m^3
PO_4 - P =	20 µg/ℓ
NO_3 - N =	0.10 mg/ℓ
Total Fe =	
Secchi disk (50 cm):	white = 10' black = 5'

TABLE 1C
WATER QUALITY DATA

Station 3 =	Sewage sludge dump area
pH =	8.0
turbidity =	7.0 FTU
Suspended solids =	31 mg/ℓ
Total solids =	31.7 gm/ℓ
Salinity 0/00 =	28
chlorophyll "a" =	1 mg/m^3
PO_4 - P =	140 µg/ℓ
NO_3 - N =	0.06 mg/ℓ
Total Fe =	
Secchi disk (50 cm):	white = 3.5' black = 1.5'
Comments:	Water mass black in color. Strong sludge supernatant odor.

TABLE 1D
WATER QUALITY DATA

Station 4 =	Ocean 29 km. E. of Sandy Hook
pH =	8.0
turbidity =	1.3 FTU
Suspended solids =	4.3 mg/ℓ
Total solids =	33.4 gm/ℓ
Salinity 0/00 =	31
chlorophyll "a" =	1.4 mg/m^3
PO_4 - P =	15 µg/ℓ
NO_3 - N =	
Total Fe =	20 µg/ℓ
Secchi disk (50 cm):	white = 21' black = 8'

TABLE 1E
WATER QUALITY DATA

Station 5 =	Oxidized acid-iron waste
pH =	
turbidity =	2.9 FTU
Suspended solids =	6.5 mg/ℓ
Total solids =	33.7 gm/ℓ
Salinity 0/00 =	30
chlorophyll "a" =	0.86 mg/m^3
PO_4 - P =	5 µg/ℓ
NO_3 - N =	
Total Fe =	700 µg/ℓ
Secchi disk (50 cm):	white = 8' black = 5'
Comment:	Typical oxidized acid-iron waste field. Large yellow water mass containing a fine suspension of particulate iron.

TABLE 1F
WATER QUALITY DATA

Station 6 =	Oxidized acid-iron waste
pH =	
turbidity =	3.6 FTU
Suspended solids =	7.5 mg/ℓ
Total solids =	31.4 gm/ℓ
Salinity 0/00 =	29
chlorophyll "a" =	0.87 mg/m^3
PO_4 - P =	5 µg/ℓ
NO_3 - N =	
Total Fe =	800 µg/ℓ
Secchi disk (50 cm):	white = 10' black = 5'
Comment:	Western edge of large yellow water mass (acid-iron waste)

TABLE 1G
WATER QUALITY DATA

Station 7 =	BA Buoy
pH =	8.1
turbidity =	3.2 FTU
Suspended solids =	10 mg/ℓ
Total solids =	29 gm/ℓ
Salinity 0/00 =	25
chlorophyll "a" =	14 mg/m^3
PO_4 - P =	20 µg/ℓ
NO_3 - N =	
Total Fe =	
Secchi disk (50 cm):	white = 10' black = 6'

TABLE 1H
WATER QUALITY DATA

Station 8 =	Scotland Light
pH =	8.15
turbidity =	1.9 FTU
Suspended solids =	7.8 mg/ℓ
Total solids =	27.2 gm/ℓ
Salinity 0/00 =	24
chlorophyll "a" =	3 mg/m^3
PO_4 - P =	12 µg/ℓ
NO_3 - N =	0.08 mg/ℓ
Total Fe =	
Secchi disk (50 cm):	white = 5' black = 3'

Aircraft multispectral missions were conducted by ERIM on 16 August 1972, 6 April 1973, and 7 April 1973. The 16 August and 7 April missions were conducted at a time coincident with the satellite pass over the area. Two missions were flown on 7 April 1973 in order to depict conditions during outgoing and incoming tides. All aircraft missions were successful.

Multispectral aircraft missions are included in the program in order to provide corrobative evidence for use in the analysis and interpretation of space data. The study area is large and includes low contrast phenomena of varying size and distribution. Hence aircraft data is utilized to identify features of interest in the study area and to evaluate ERTS-1 data. Analysis of aircraft data is limited to those features which are within the scope of the ERTS investigation.

Shown in Fig. 3 is photographic evidence of a typical acid-iron dumping operation and the subsequent oxidation and dispersion of the waste. The waste solution changes in appearances from a green-yellow color to orange as the material undergoes oxidation from the ferrous to ferric state. The orange water mass in the lower right-hand corner of Fig. 3 is a suspension of $Fe_2(SO_4)_3$ from an earlier dump. Figures 4 and 5 document the scene at the time of the ERTS pass over the study area on the 16 August 1972 and 7 April 1973 respectively. In both cases acid-iron waste is clearly evident in the scene.

An extensive field and aircraft remote sensing program was in progress in the area on 7 April 1973 under the direction of NOAA. The ERIM remote sensing aircraft was used to acquire multispectral scanner data at two stages in the tidal cycle. The scene depicted in Fig. 5 illustrates conditions in the dump area at approximately 1500 GMT, during the incoming portion of the tidal cycle at Sandy Hook; whereas Fig. 6 illustrates the waste field at approximately 2030 GMT, during an outgoing tide. Dye markers (see Fig. 6) depict a general southwesterly movement of the waste field. Additionally, dye markers over the entire area indicate an overall clockwise surface circulation pattern. The tendency for the waste field to move in a southwesterly direction (towards shore) was also supported by field observations on 25 April 1973. The westerly edge of a large dispersed yellow water mass (acid-iron waste) was located on that date at a position approximately 10 km. off the New Jersey coast (sta. 6, Fig. 2).

ERTS Data Analysis

Waste fields created by barge dumping are evident in all clear frames of the study area examined to date. Acid-iron waste in the process of being discharged (Fig. 7), recently dumped waste (Fig. 8), as well as relatively old waste suspensions (Fig. 9) have been detected. Also clearly visible are turbidity anomalies associated with variability in suspended solids concentration. The relatively high turbidity levels associated with water masses moving from the Lower Bay frequently mask the sewage sludge discharges and dredge spoil dumping. Under favorable conditions, however, sewage sludge is detectable (see Fig. 10).

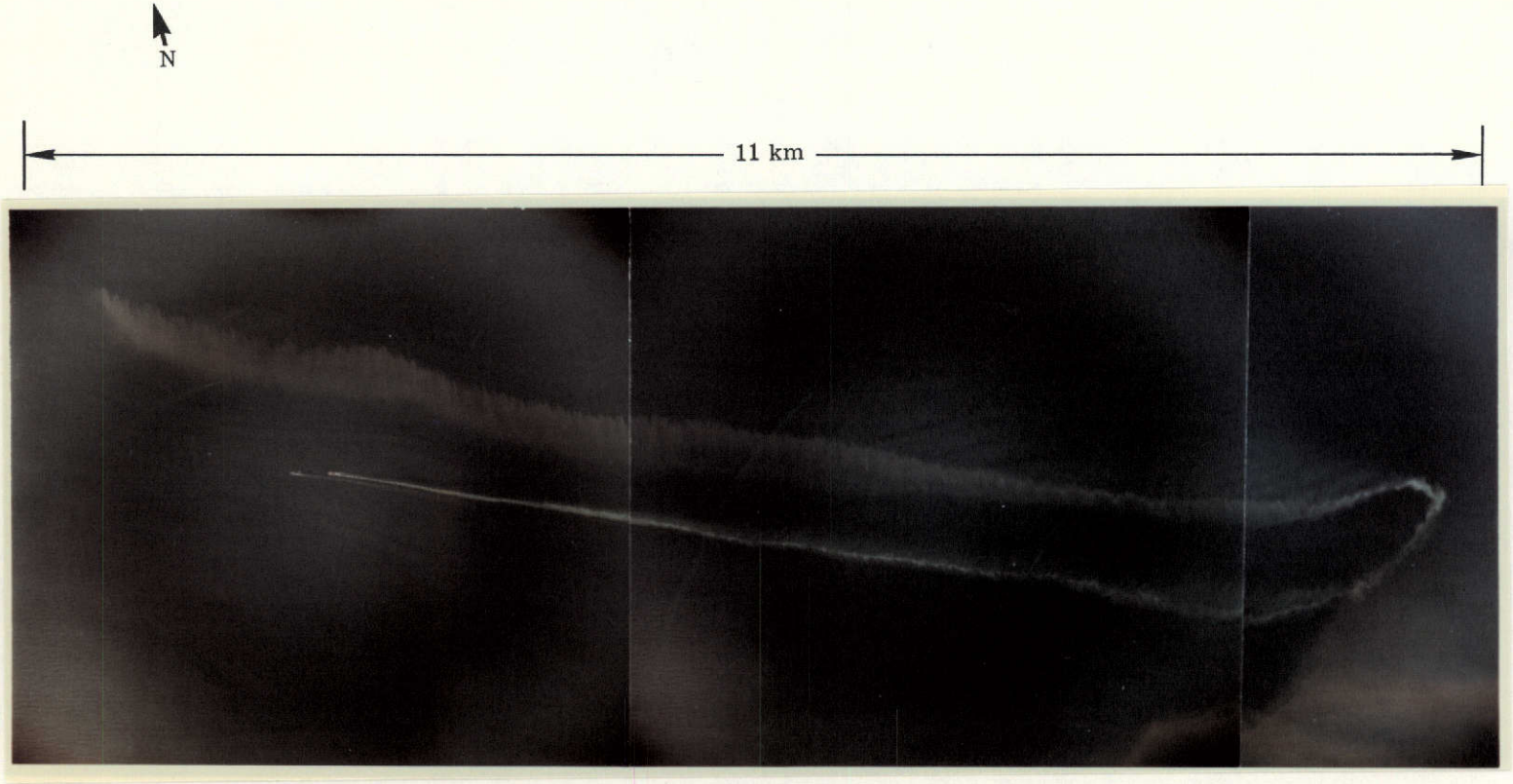

FIGURE 3. ACID WASTE, NEW YORK BIGHT, 7 APRIL 1973. Aircraft imagery, altitude 3048m.

ERIM
FORMERLY WILLOW RUN LABORATORIES, THE UNIVERSITY OF MICHIGAN

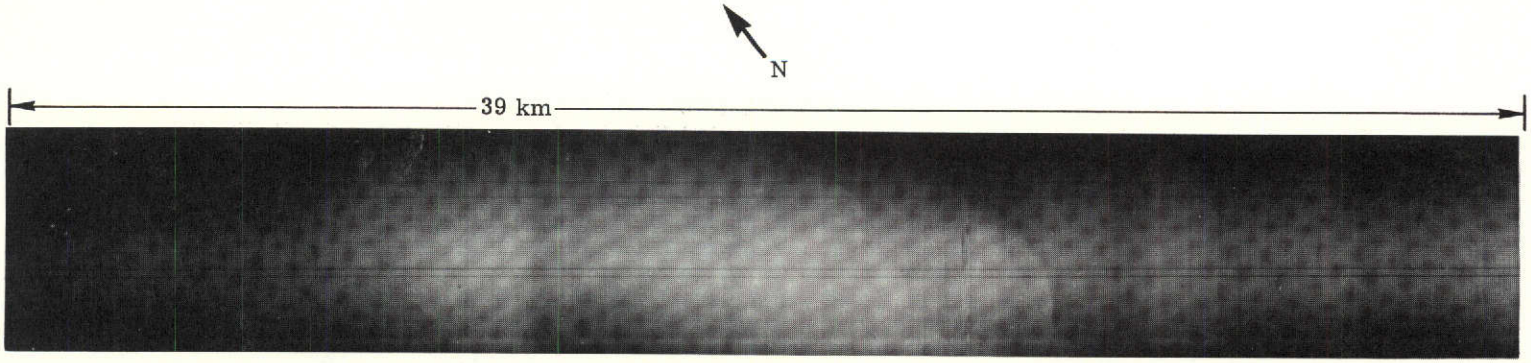

(a) 9.3-11.7 μm

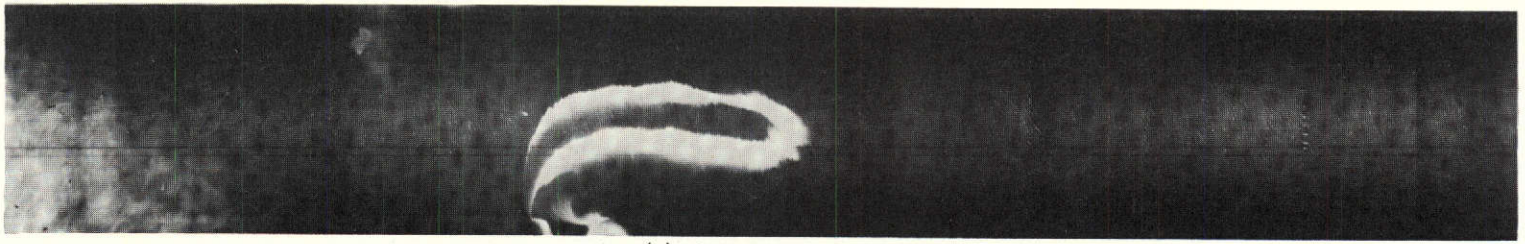

(b) 0.62-0.70 μm

FIGURE 4. NEW YORK BIGHT, 16 AUGUST 1972. Aircraft imagery, altitude 3048m.

ERIM
FORMERLY WILLOW RUN LABORATORIES, THE UNIVERSITY OF MICHIGAN

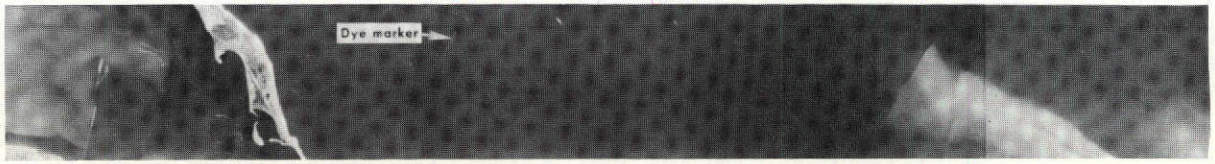

(a) 09:56:40-10:08:45 EST

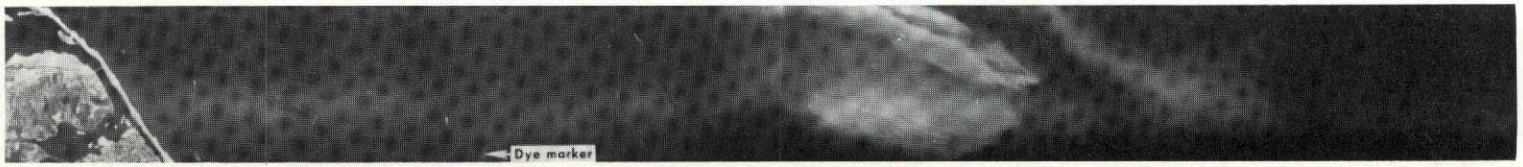

(b) 10:15:23-10:26:40 EST

FIGURE 5. ACID-IRON WASTE, NEW YORK BIGHT, 7 APRIL 1973. Aircraft imagery, altitude 3048m, 0.52-0.57 μm.

ERIM
FORMERLY WILLOW RUN LABORATORIES, THE UNIVERSITY OF MICHIGAN

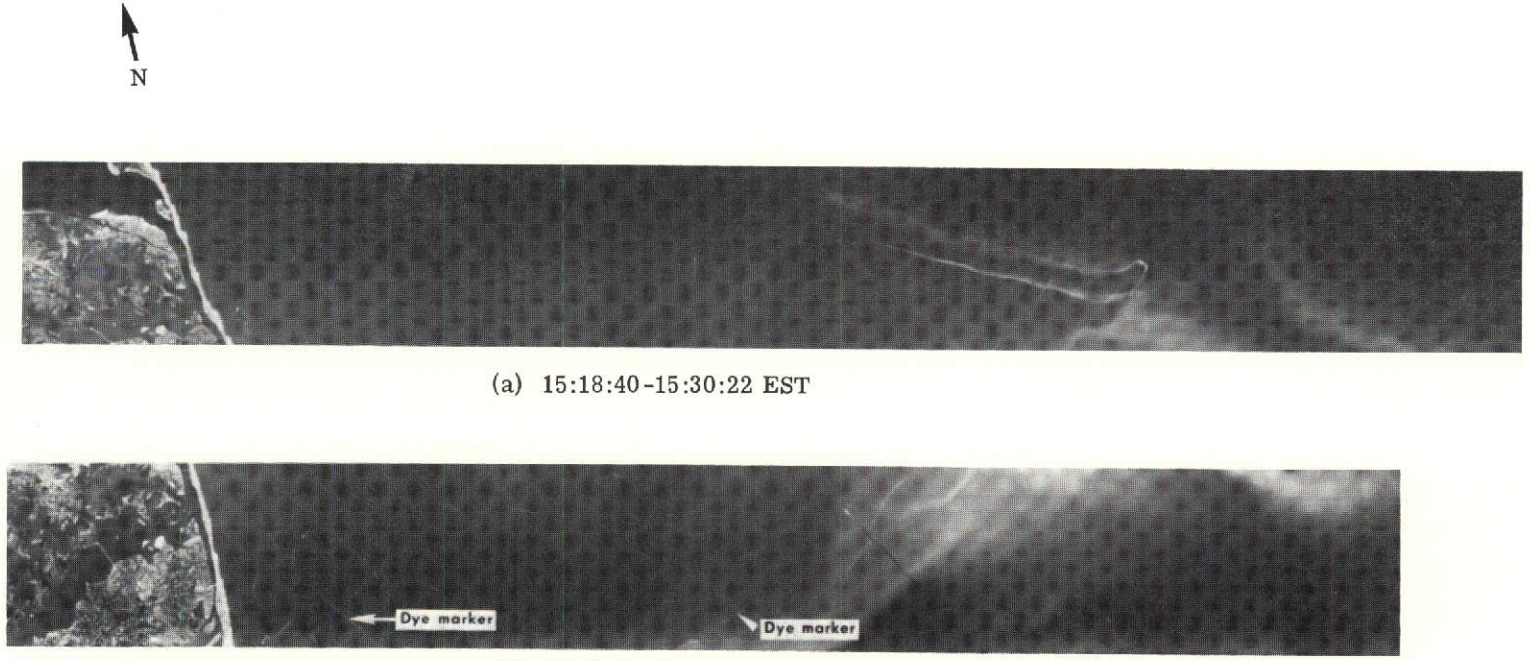

(a) 15:18:40-15:30:22 EST

(b) 15:33:28-15:44:28 EST

FIGURE 6. ACID-IRON WASTE, NEW YORK BIGHT, 7 APRIL 1973. Aircraft imagery, altitude 3048m, 0.52-0.57 μm.

ERIM
FORMERLY WILLOW RUN LABORATORIES, THE UNIVERSITY OF MICHIGAN

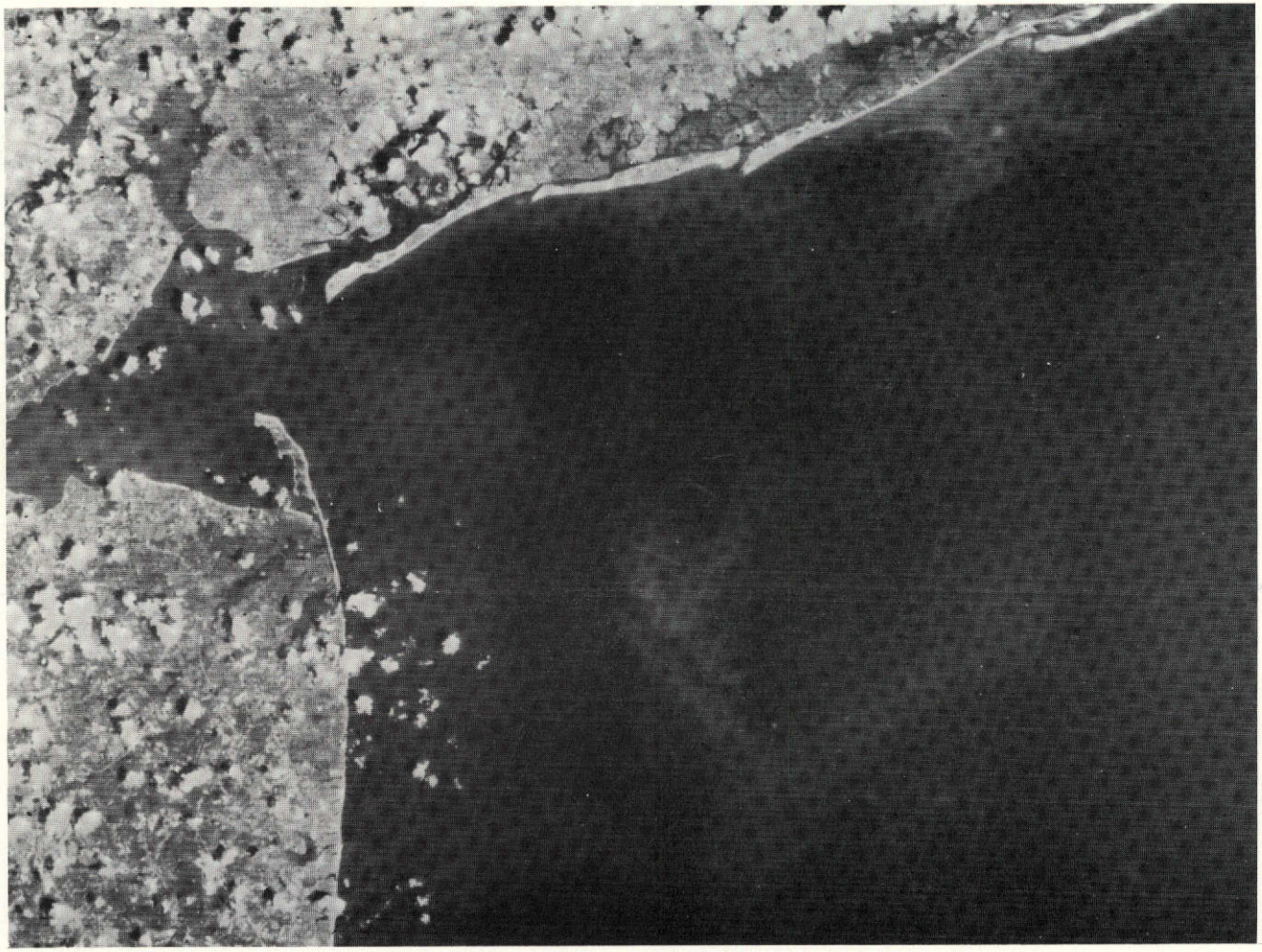

FIGURE 7. NEW YORK BIGHT, 13 MAY 1973. ERTS-1 data, MSS4 (0.5-0.6 μm) E-1294-15081.

ERIM
FORMERLY WILLOW RUN LABORATORIES, THE UNIVERSITY OF MICHIGAN

FIGURE 8. NEW YORK BIGHT, 7 APRIL 1973. ERTS-1 data, MSS5 (0.6-0.7 μm) E-1258-15082.

FIGURE 9. NEW YORK BIGHT, 9 OCTOBER 1972. ERTS-1 data, MSS5 (0.6-0.7 μm) E-1078-15072.

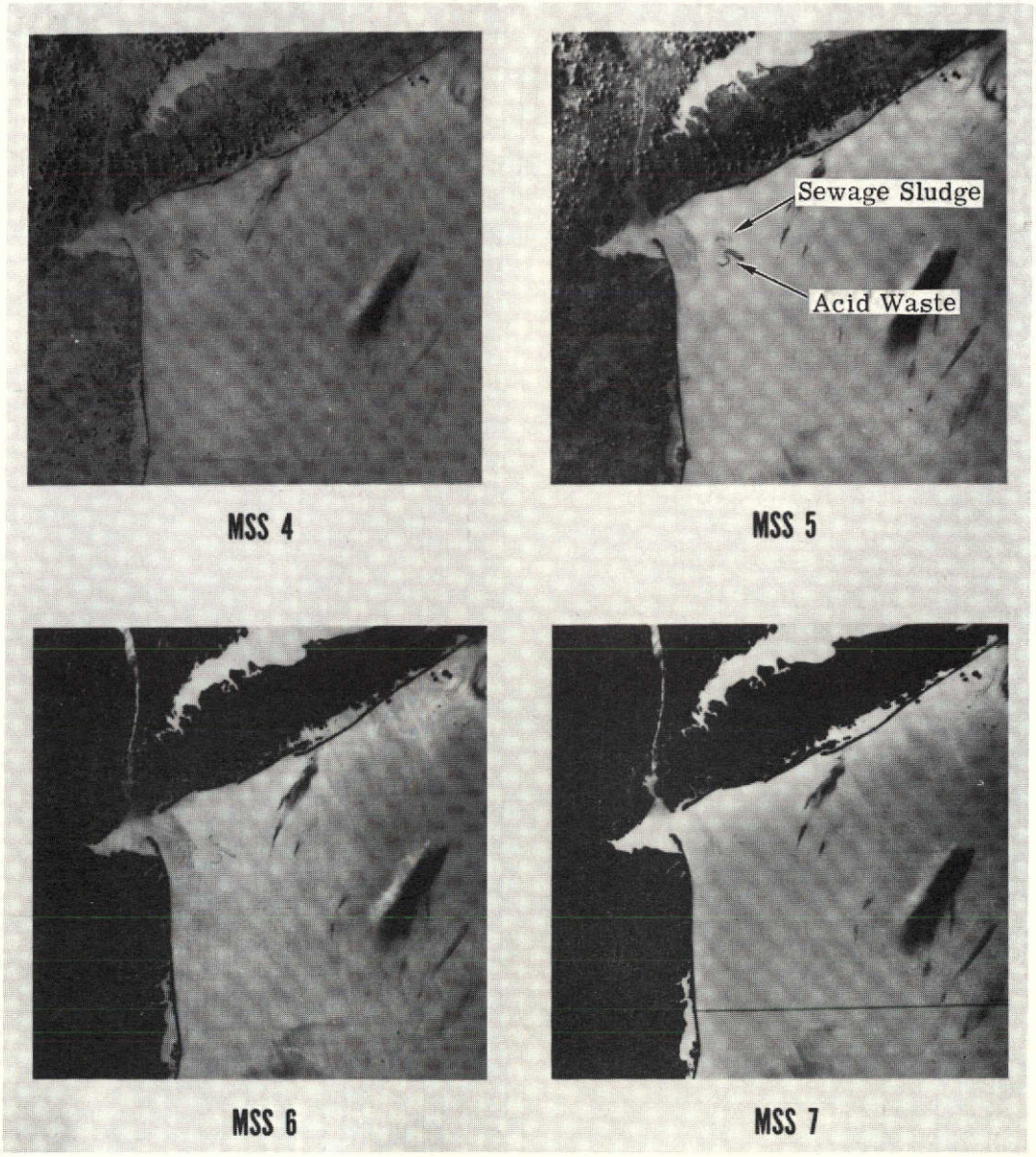

FIGURE 10. NEW YORK BIGHT, 16 AUGUST 1972. ERTS-1 data, E-1024-15071.

Figures 7-10 illustrate the kind of information which is obtainable by direct analysis of ERTS imagery. An attempt has been made to differentiate waste fields and water masses using digital ratioing techniques and densiotimetry (see Fig. 11). However, due to low signal levels and variability in the data, the results were unsatisfactory. An increase in scanner gain is clearly indicated over water areas.

A high-gain ERTS pass is reported to have been made on 13 May 1973. To date, digital tapes have not been received for this date.

Digital maps of the acid waste and sewage sludge have been generated (see Figs. 12, 13, 14). Digital techniques are being utilized to calculate the physical dimensions of waste fields and to determine their position relative to shore.

Publications and Seminars

The following publications and/or oral presentations have resulted from the present investigation, to date:

1. "Remote Sensing in the New York Bight". New York Bight Conference, NOAA, Rockville, Maryland, 12 September 1972. (A meeting of government agencies which have an interest in the New York Bight.)

2. "Barge Dumping of Wastes in the New York Bight". Goddard ERTS Seminar, 29 September 72. Report No. 011229-6-S, NASA-CR 128099, E 72-10084.

3. "Monitoring Ocean Dumping With ERTS-1 Data". NASA Symposium on Significant Results Obtained from ERTS-1, 5 March 1973, New Carrollton, Maryland.

4. "Monitoring of Ocean Dumping By Means of Satellite Remote Sensing". Accepted for publication in AMBIO, Journal of the Human Environment, Research and Management, The Royal Academy of Sciences, Sweden.

TAMPA BAY

General

Portions of Tampa Bay, particularly the Hillsborough Bay arm, have experienced serious water quality problems due to extremely high phosphorus levels, poor circulation features, and point sources of wastes. Excessive growths of phytoplankton and benthic growths in the Bay are primarily the result of existing high nutrient levels. The primary objective of the study at this location is to investigate the relationship between observed suspended solids and color anomalies and existing water quality.

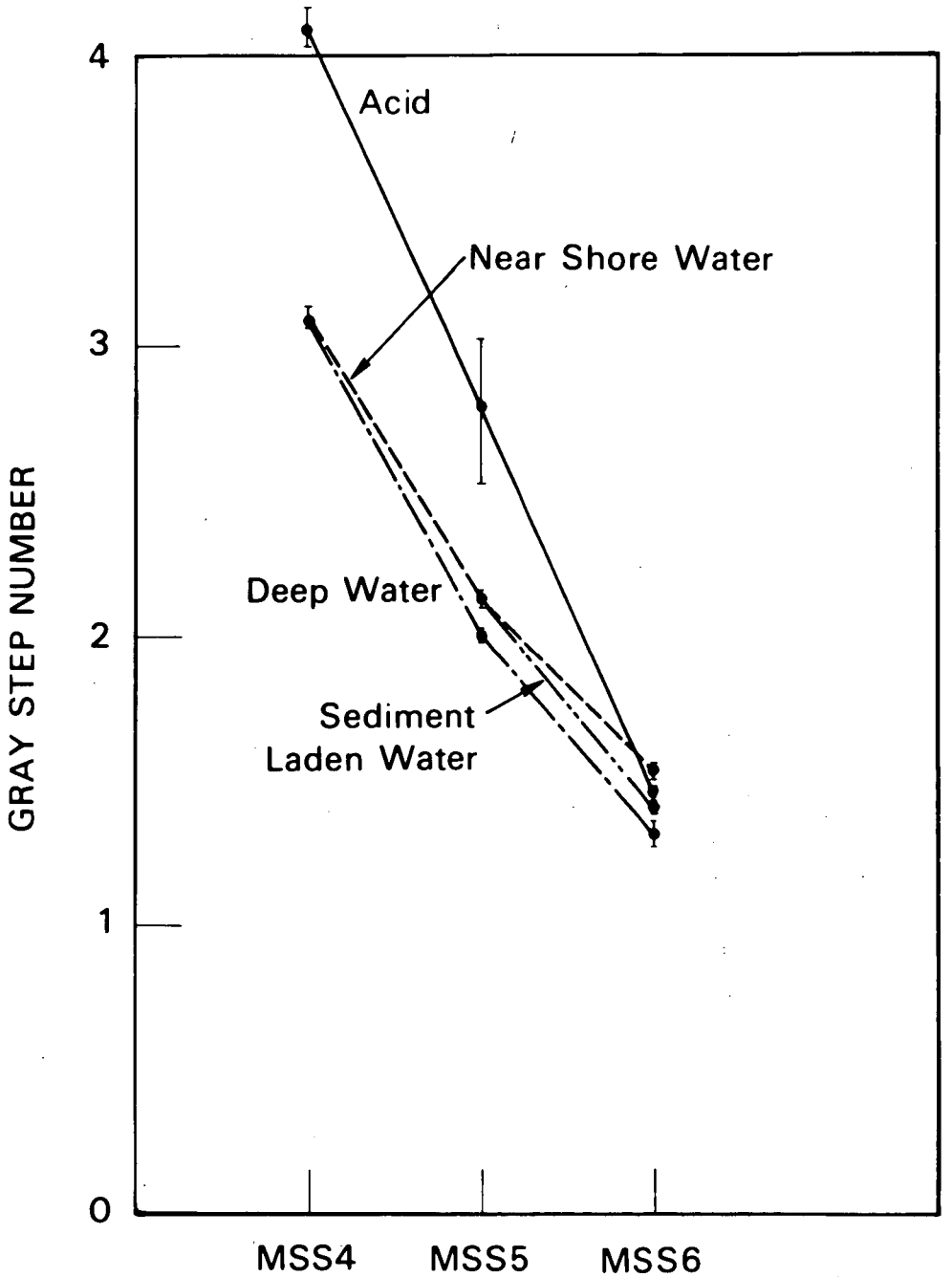

FIGURE 11. SIGNATURES OF NEW YORK BIGHT WATER AREAS, 16 AUGUST 1972. Deduced from ERTS-1 MSS data.

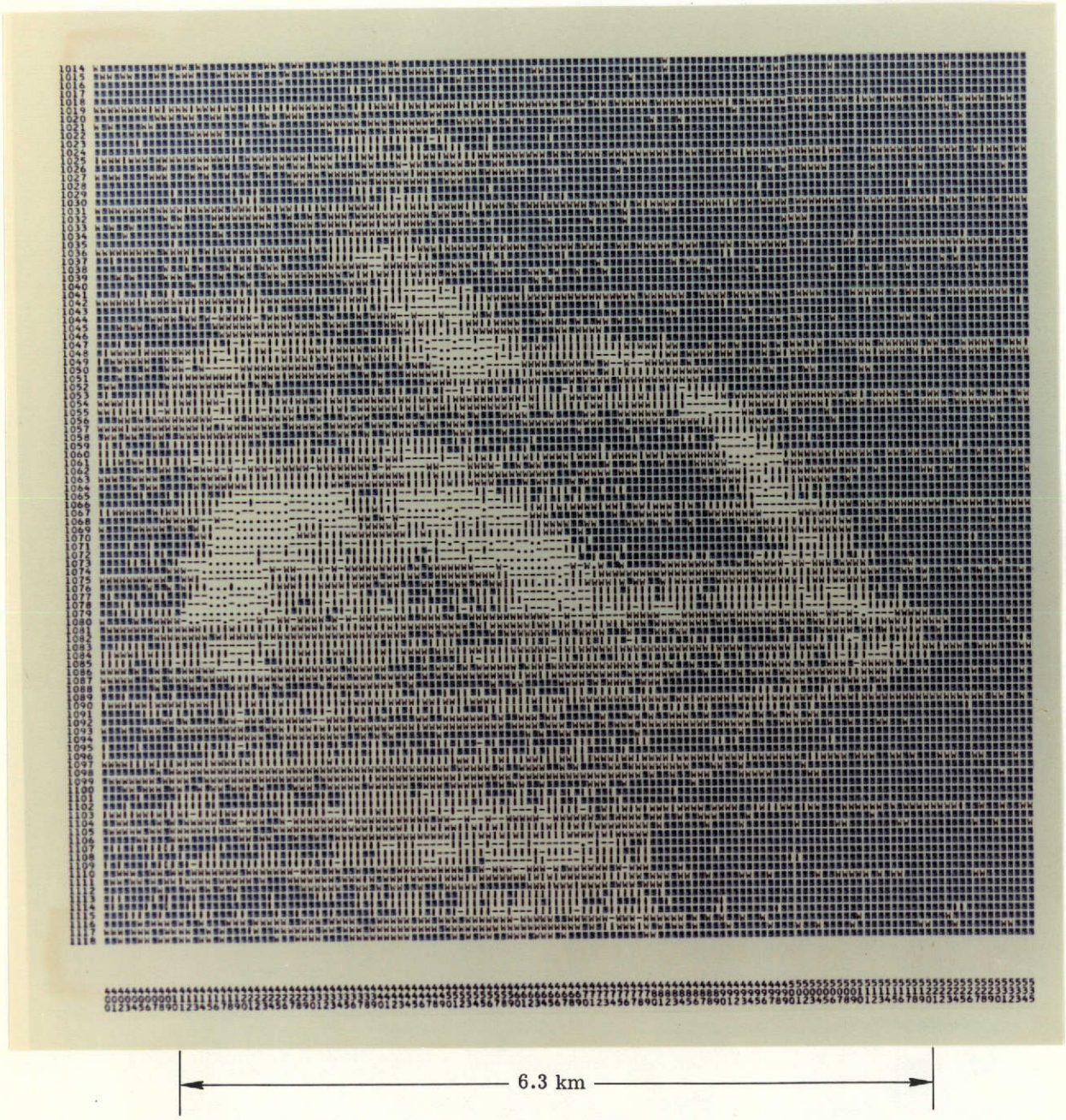

FIGURE 12. SEWAGE SLUDGE, NEW YORK BIGHT, 16 AUGUST 1972. ERTS-1 data, MSS5 (0.6-0.7 μm) E-1024-15071.

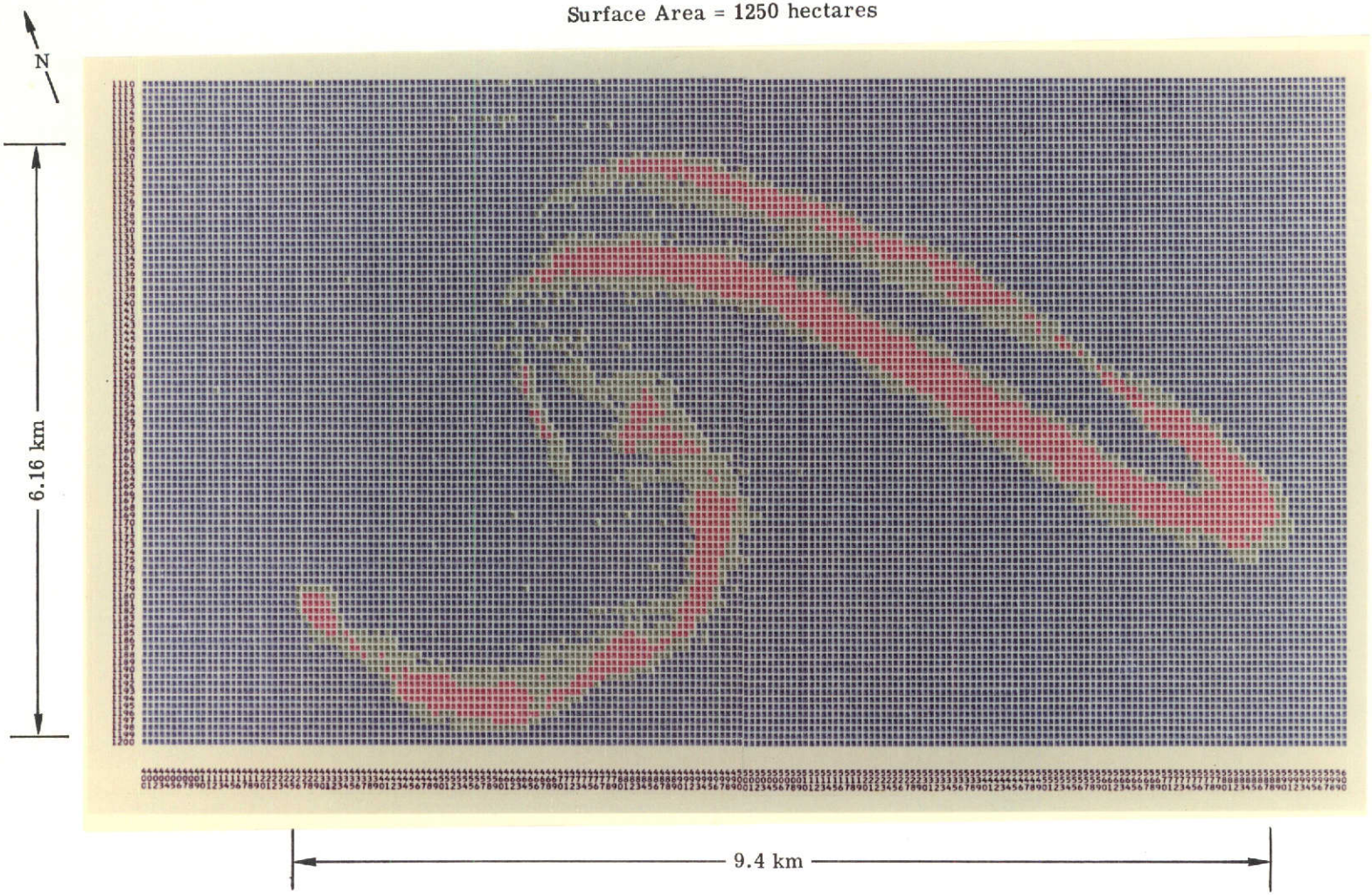

FIGURE 13. ACID WASTE, NEW YORK BIGHT, 16 AUGUST 1972. ERTS-1 data, MSS5 (0.6-0.7 μm) E-1024-15071.

ERIM
FORMERLY WILLOW RUN LABORATORIES, THE UNIVERSITY OF MICHIGAN

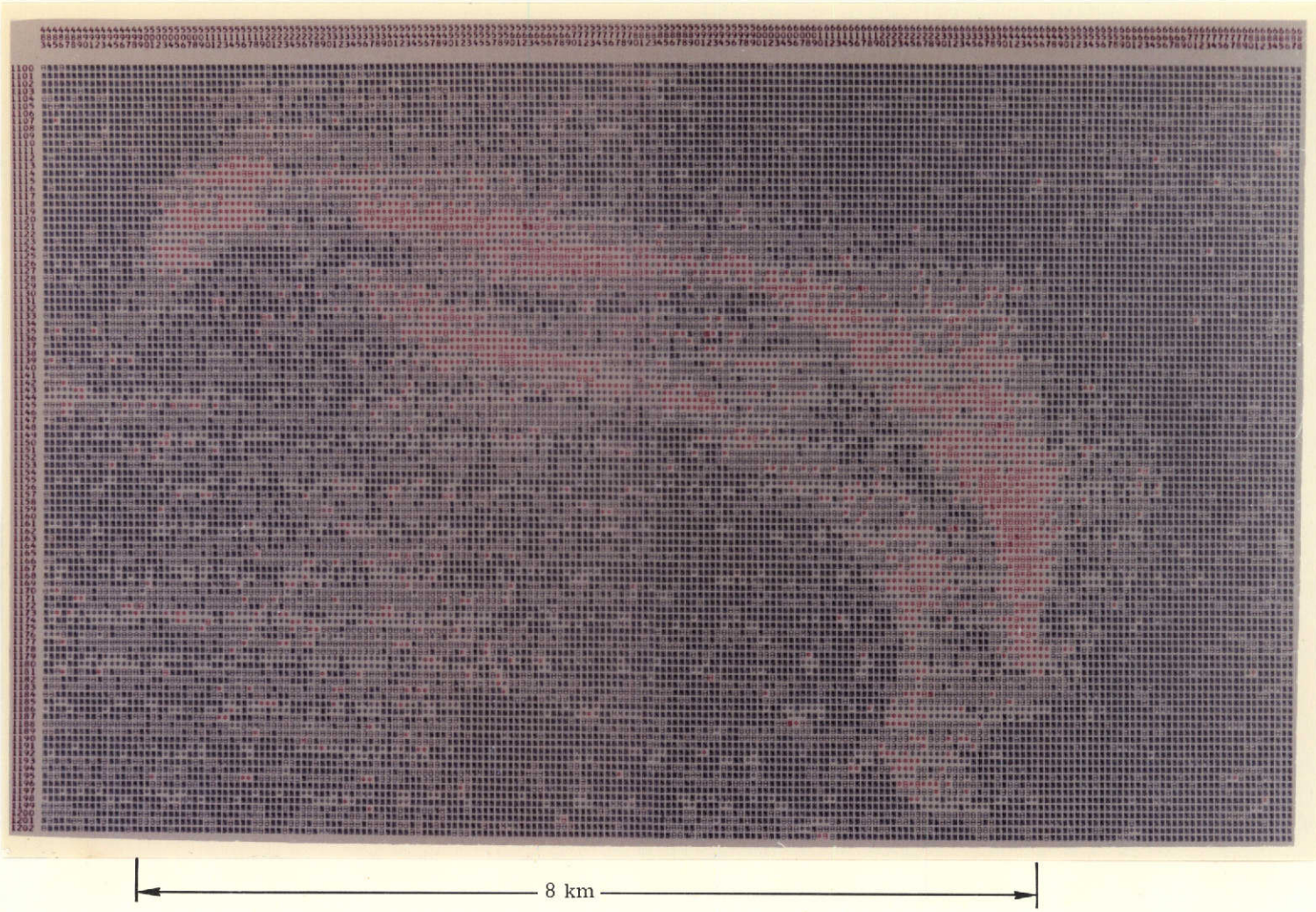

FIGURE 14. ACID WASTE, NEW YORK BIGHT, 9 OCTOBER 1972. ERTS-1 data, MSS5 (0.6-0.7 μm) E-1078-15072.

ERIM
FORMERLY WILLOW RUN LABORATORIES, THE UNIVERSITY OF MICHIGAN

Work performed during the period 1 January - 30 June, 1973 included field data collection, visual analysis of ERTS imagery and digital processing.

Field Activities

Water quality data were collected at the locations shown in Fig. 15 on 16 and 17 February 1973. Typical water quality characteristics of the surface waters of the Bay for these dates are tabulated in Tables 2A-2N. The data indicate that turbidity levels, phosphorus, and chlorophyll "a" levels are relatively high in the Hillsborough arm of the Bay.

ERTS Data Analysis

Imagery from a number of frames over the study area was received and screened. Several of the frames are considered suitable for purposes of this investigation, most notably 1100-15343 (31 October 1972), 1117-15285 (17 November 1972, 1136-15344 (6 December 1972), 1208-15345 (16 February 1973) and 1262-15350 (11 April 1973). Information of interest is largely contained in MSS 5, although under favorable conditions Band MSS 4 does provide useful information. During periods of high humidity, which is generally the case in the summer months at this location, the utility of MSS 4 is severely limited due to scattering.

ERTS frame 1117-15285 (17 November 1972) was selected for detailed processing. A color digital map was produced to display turbidity differences. The results are shown in Fig. 16. The differences in turbidity levels (and suspended solids) shown also serve to delineate the movement of water masses. The red plume near the center of the Bay was produced by dredging operations in the shipping channel. A similar digital map was prepared using data from 1099-15284 October 1972.

ERTS frame 1208-15345 (16 February 1973) is currently being processed. An attempt will be made to correlate color differences with phytoplankton levels.

Imagery of the study area for 11 April 1973 (Fig. 17) is of very good quality and appears to possess a higher dynamic range in terms of signal level than any of the frames received to date. Current plans call for processing this data using the ERIM Spectral Analysis and Recognition Computer.

LAKE ERIE

General

Many years of neglect by citizens and governments of the basin together with a lack of knowledge (and concern) regarding the dynamics of lake ecology and sources of pollution have accelerated the eutrophication processes in Lake Erie and diminished the beneficial uses of this resource.

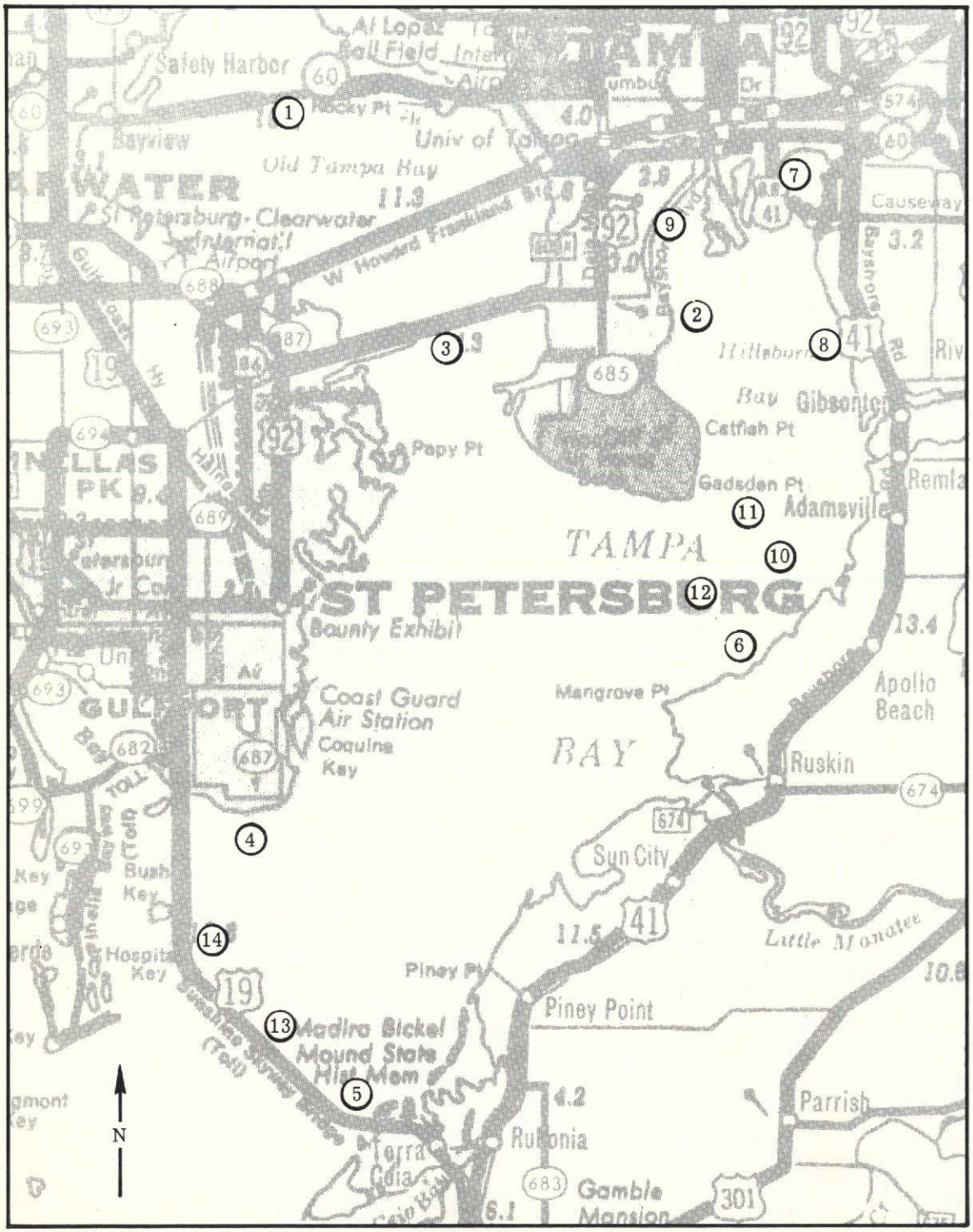

FIGURE 15. TAMPA BAY SAMPLING LOCATIONS

TABLE 2A
WATER QUALITY DATA

Station 1 =	Courtney Campbell	16 February 1973
Temperature =	16°C	
Forel Ule Color =	XIII	
turbidity =	4.2 FTU	
Suspended solids =	18.0 mg/ℓ	
Dissolved solids =	26.0 gm/ℓ	
Salinity 0/00 =	22	
chlorophyll "a" =	3.5 mg/m^3	
PO_4 =	2.4 mg/ℓ	
NO_3 - N =	< 0.1 mg/ℓ	
Coliforms =	800/100 mℓ	
Secchi disk (50 cm):	white = black =	

TABLE 2B
WATER QUALITY DATA

Station 2 =	Ballast Pt.	16 February 1973
Temperature =	18°C	
Forel Ule Color =	XVII	
turbidity =	6.2 FTU	
Suspended solids =	31 mg/ℓ	
Dissolved solids =	22 gm/ℓ	
Salinity 0/00 =	21.5	
chlorophyll "a" =	13 mg/m^3	
PO_4 =	4.6 mg/ℓ	
NO_3 - N =	< 0.1 mg/ℓ	
Coliforms =	2000/100 mℓ	
Secchi disk (50 cm):	white = 2.7' black = 1.5'	

TABLE 2C
WATER QUALITY DATA

Station 3 =	Gandy Bridge	16 February 1973
Temperature =	17°C	
Forel Ule Color =	X	
turbidity =	3.0 FTU	
Suspended solids =	18.0 mg/ℓ	
Dissolved solids =	29.5 gm/ℓ	
Salinity 0/00 =	25	
chlorophyll "a" =		
PO_4 =	2.6 mg/ℓ	
NO_3 - N =	< 0.1 mg/ℓ	
Coliforms =	1000/100 mℓ	
Secchi disk (50 cm):	white = 10.7' black = 6.0'	

TABLE 2D
WATER QUALITY DATA

Station 4 =	Pinellas Pt.	16 February 1973
Temperature =	17°C	
Forel Ule Color =	X	
turbidity =	3.8 FTU	
Suspended solids =	12.7 mg/ℓ	
Dissolved solids =	31.3 gm/ℓ	
Salinity 0/00 =	28	
chlorophyll "a" =		
PO_4 =	1.6 mg/ℓ	
NO_3 - N =	< 0.1 mg/ℓ	
Coliforms =	500/100 mℓ	
Secchi disk (50 cm):	white = black =	

Cr

TABLE 2E
WATER QUALITY DATA

Station 5 =	Sunshine Skyway E.	16 February 1973
Temperature =	17°C	
Forel Ule Color =	XII	
turbidity =	4.3 FTU	
Suspended solids =	18.8 mg/ℓ	
Dissolved solids =	33.4 gm/ℓ	
Salinity 0/00 =	28	
chlorophyll "a" =	1.8 mg/m^3	
PO_4 =	1.35 mg/ℓ	
NO_3 - N =	trace	
Coliforms =		
Secchi disk (50 cm):	white = 13.0' black = 6.0'	

TABLE 2F
WATER QUALITY DATA

Station 6 =	Apollo Beach	16 February 1973
Temperature =	19°C	
Forel Ule Color =	XVI	
turbidity =	7.0 FTU	
Suspended solids =	27.7 mg/ℓ	
Dissolved solids =	27.1 gm/ℓ	
Salinity 0/00 =	24	
chlorophyll "a" =	3 mg/m^3	
PO_4 =	4.4 mg/ℓ	
NO_3 - N =	0.1 mg/ℓ	
Coliforms =	1000/100 mℓ	
Secchi disk (50 cm):	white = 3.4' black = 1.8'	

TABLE 2G
WATER QUALITY DATA

Station 7 =	McKay Bay	16 February 1973
Temperature =	18°C	
Forel Ule Color =	XVII	
turbidity =	7.0 FTU	
Suspended solids =	28.2 mg/ℓ	
Dissolved solids =	23.6 gm/ℓ	
Salinity 0/00 =	22	
chlorophyll "a" =		
PO_4 =	5.0 mg/ℓ	
NO_3 - N =	0.1 mg/ℓ	
Coliforms =	3000/100 mℓ	
Secchi disk (50 cm):	white = 3.0' black = 1.5'	

TABLE 2H
WATER QUALITY DATA

Station 8 =	Alafia River	16 February 1973
Temperature =	18°C	
Forel Ule Color =	XVII	
turbidity =	6.3 FTU	
Suspended solids =	17.8 mg/ℓ	
Dissolved solids =	13.3 gm/ℓ	
Salinity 0/00 =	13.5	
chlorophyll "a" =		
PO_4 =	17.5 mg/ℓ	
NO_3 - N =	0.1 mg/ℓ	
Coliforms =	500/100 mℓ	
Secchi disk (50 cm):	white = 3.0' black = 1.5'	

TABLE 2I
WATER QUALITY DATA

Station 9 =	Davis Island	16 February 1973
Temperature =	16°C	
Forel Ule Color =	XVI	
turbidity =	4.3 FTU	
Suspended solids =	17.0 mg/ℓ	
Dissolved solids =	18.0 gm/ℓ	
Salinity 0/00 =	16	
chlorophyll "a" =	32.8 mg/m^3	
PO_4 =	3.7 mg/ℓ	
NO_3 - N =	0.1 mg/ℓ	
Coliforms =	1000/100 mℓ	
Secchi disk (50 cm):	white = black =	

TABLE 2J
WATER QUALITY DATA

Station 10 =		16 February 1973
Temperature =	18°C	
Forel Ule Color =	XVII	
turbidity =	6.7 FTU	
Suspended solids =	24.6 mg/ℓ	
Dissolved solids =	25.6 gm/ℓ	
Salinity 0/00 =	23	
chlorophyll "a" =		
PO_4 =	5.0 mg/ℓ	
NO_3 - N =	0.1 mg/ℓ	
Coliforms =		
Secchi disk (50 cm):	white = 3.3' black = 1.9'	

TABLE 2K
WATER QUALITY DATA

Station 11 =		16 February 1973
Temperature =	18°C	
Forel Ule Color =	XVII	
turbidity =	9.3 FTU	
Suspended solids =	34.4 mg/ℓ	
Dissolved solids =	24.9 gm/ℓ	
Salinity 0/00 =	21	
chlorophyll "a" =		
PO_4 =	5.0 mg/ℓ	
NO_3 - N =	0.1 mg/ℓ	
Coliforms =		
Secchi disk (50 cm):	white = 2.5'	black = 1.5'

TABLE 2L
WATER QUALITY DATA

Station 12 =		16 February 1973
Temperature =	15°C	
Forel Ule Color =	XVII	
turbidity =	5.8 FTU	
Suspended solids =	24.8 mg/ℓ	
Dissolved solids =	26.7 gm/ℓ	
Salinity 0/00 =	24.5	
chlorophyll "a" =		
PO_4 =		
NO_3 - N =		
Coliforms =		
Secchi disk (50 cm):	white = 4.7'	black = 2.5'

TABLE 2M
WATER QUALITY DATA

Station 13 =	Sunshine Skyway - Center	16 February 1973
Temperature =	17°C	
Forel Ule Color =	XII	
turbidity =	6.2 FTU	
Suspended solids =	26.2 mg/ℓ	
Dissolved solids =	33.8 gm/ℓ	
Salinity 0/00 =		
chlorophyll "a" =		
PO_4 =	1.0 mg/ℓ	
NO_3 - N =	trace	
Coliforms =		
Secchi disk (50 cm):	white = black =	

TABLE 2N
WATER QUALITY DATA

Station 14 =	Sunshine Skyway - W	16 February 1973
Temperature =	17°C	
Forel Ule Color =	XII	
turbidity =	5.7 FTU	
Suspended solids =	22.4 mg/ℓ	
Dissolved solids =	34.2 gm/ℓ	
Salinity 0/00 =		
chlorophyll "a" =		
PO_4 =	1.0 mg/ℓ	
NO_3 - N =	trace	
Coliforms =		
Secchi disk (50 cm):	white = black =	

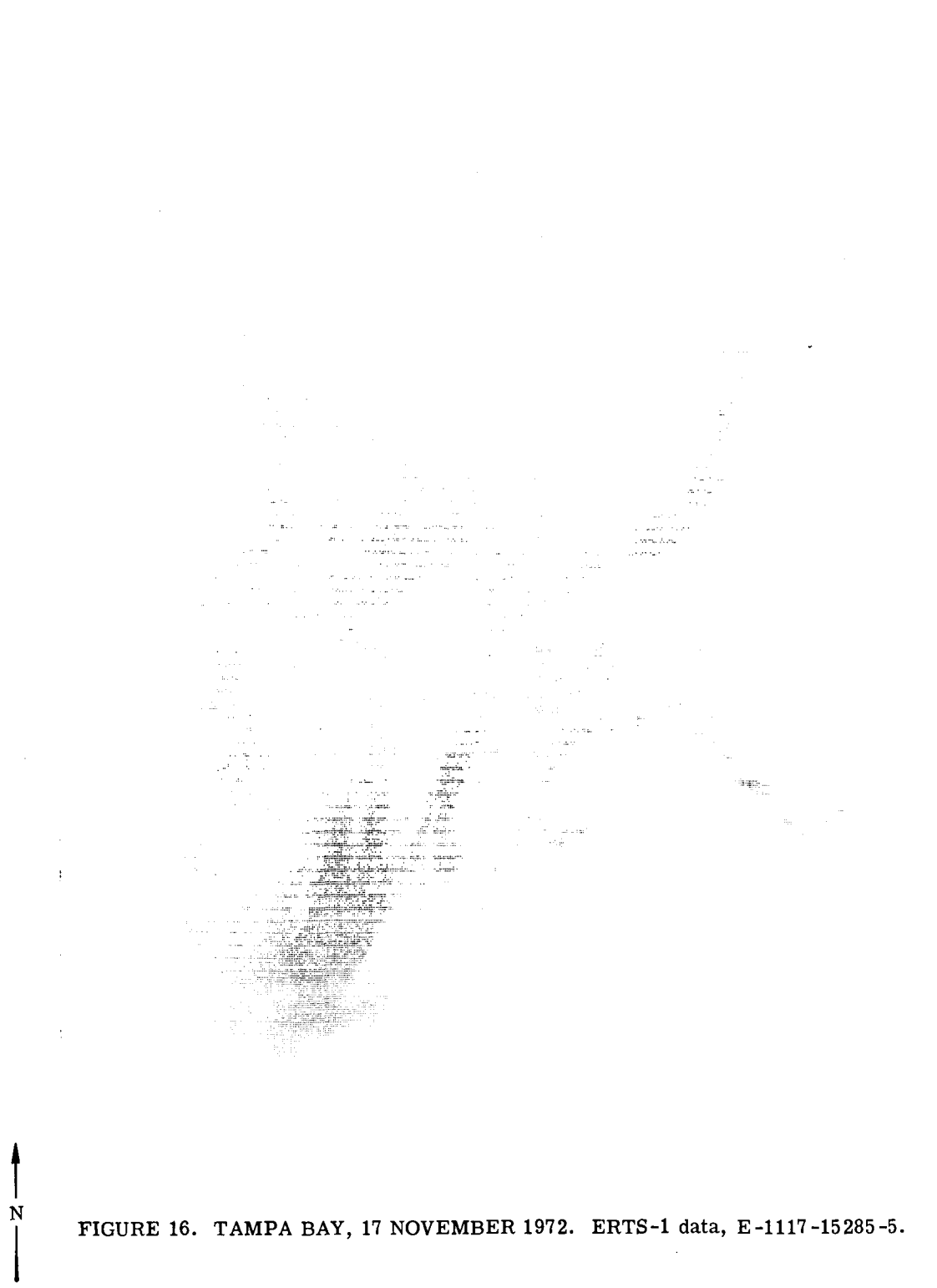

FIGURE 16. TAMPA BAY, 17 NOVEMBER 1972. ERTS-1 data, E-1117-15285-5.

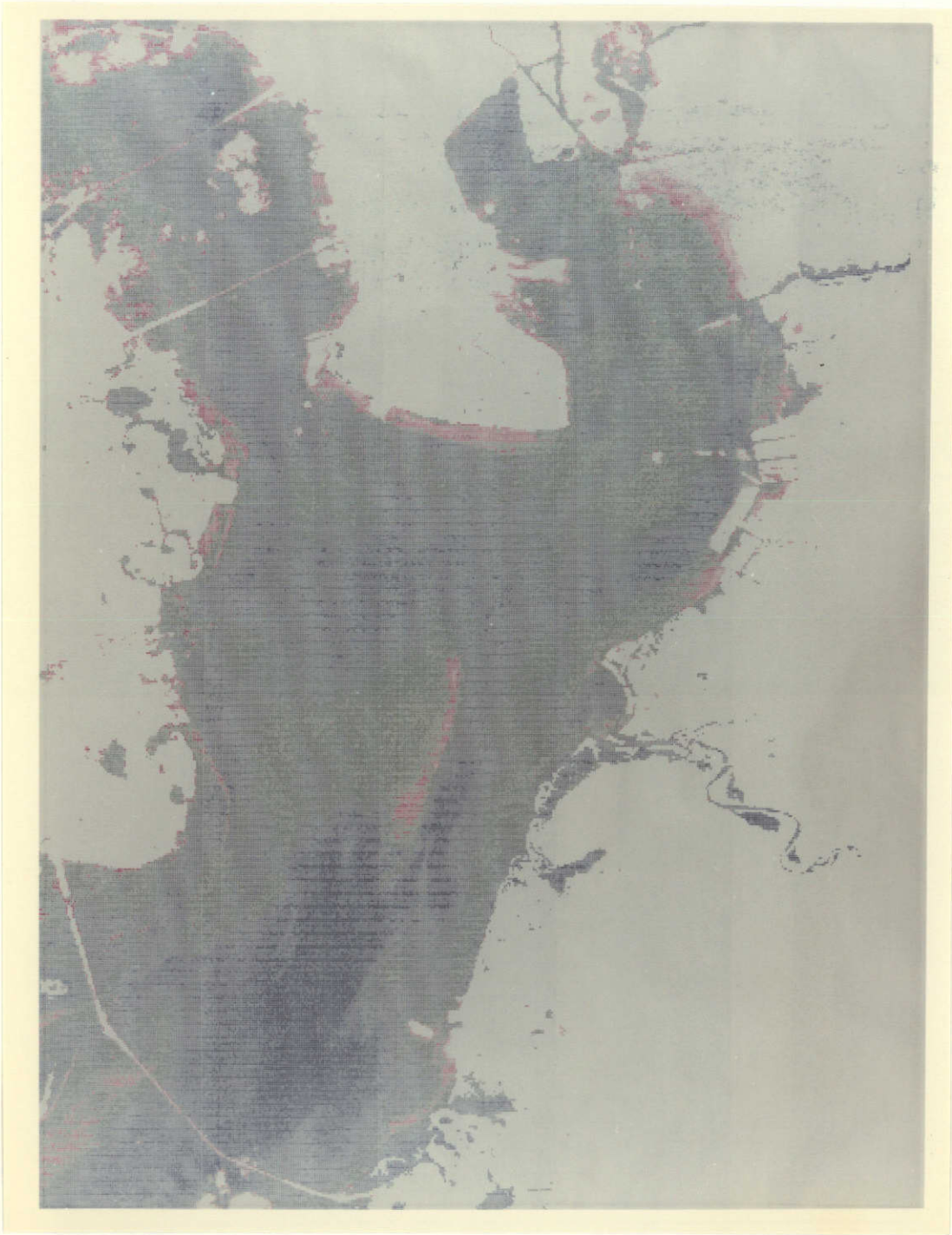

N

FIGURE 16. TAMPA BAY, 17 NOVEMBER 1972. ERTS-1 data, E-1117-15285-5.

FIGURE 17. TAMPA BAY, 11 APRIL 1973. ERTS-1 data, MSS5 (0.6-0.7 μm) E-1262-15350.

The major area of interest in this investigation is the western section of the lake; however, comparisons of the three sections of the lake would be highly desirable. The study proposes to investigate circulation dynamics and the spread and movement of major tributary sources, which are the major pollution sources. Phytoplankton dynamics are also an important part of this study.

Seasonal factors are important to this investigation. From the standpoint of phytoplankton distribution, the spring-summer-fall seasons are important. Winter lake ice conditions are of no interest to this investigation.

Work performed during the reporting period (1 January - 30 June 1973) included visual analysis of all ERTS imagery received to date, analysis of field data, and digital processing.

Of the ERTS frames examined to date, the following are considered most suitable for the purposes of the study:

1048-15405	9 September 1972
1247-15481	27 March 1973
1264-15422	13 April 1973
1265-15480	14 April 1973

Data from 27 March 1973 (see Fig. 18) is of excellent quality and is currently undergoing detailed processing.

Color digital displays of data from 9 September 1972 and 27 March 1973 have been prepared (Figs. 19 and 20). The displays show major circulation features, shore erosion processes, variations in turbidity levels and other water quality variability. Surface films also appear to be evident in the scene. Water quality data collected by the Environmental Protection Agency and other regulatory agencies is currently being analyzed for use in ERTS data interpretation.

OTHER TEST LOCATIONS

General

The status of the investigation at the Southeast Florida, S. California, and Lake Michigan test sites has been reviewed in the "Report on the Preliminary Data Analysis Phase", April 1973 submitted to NASA.

Studies at the Florida and California test locations deal with the discharge of wastewater into the coastal zone by means of ocean outfalls. As indicated in the "Report on the Preliminary Data Analysis Phase", this phase of the program is unlikely to be productive due to low scanner signal levels.

FIGURE 18. SOUTH LAKE HURON, LAKE ST. CLAIR, WEST LAKE ERIE, 27 MARCH 1973. ERTS-1 data, MSS5, E-1247-15474, E-1247-15481.

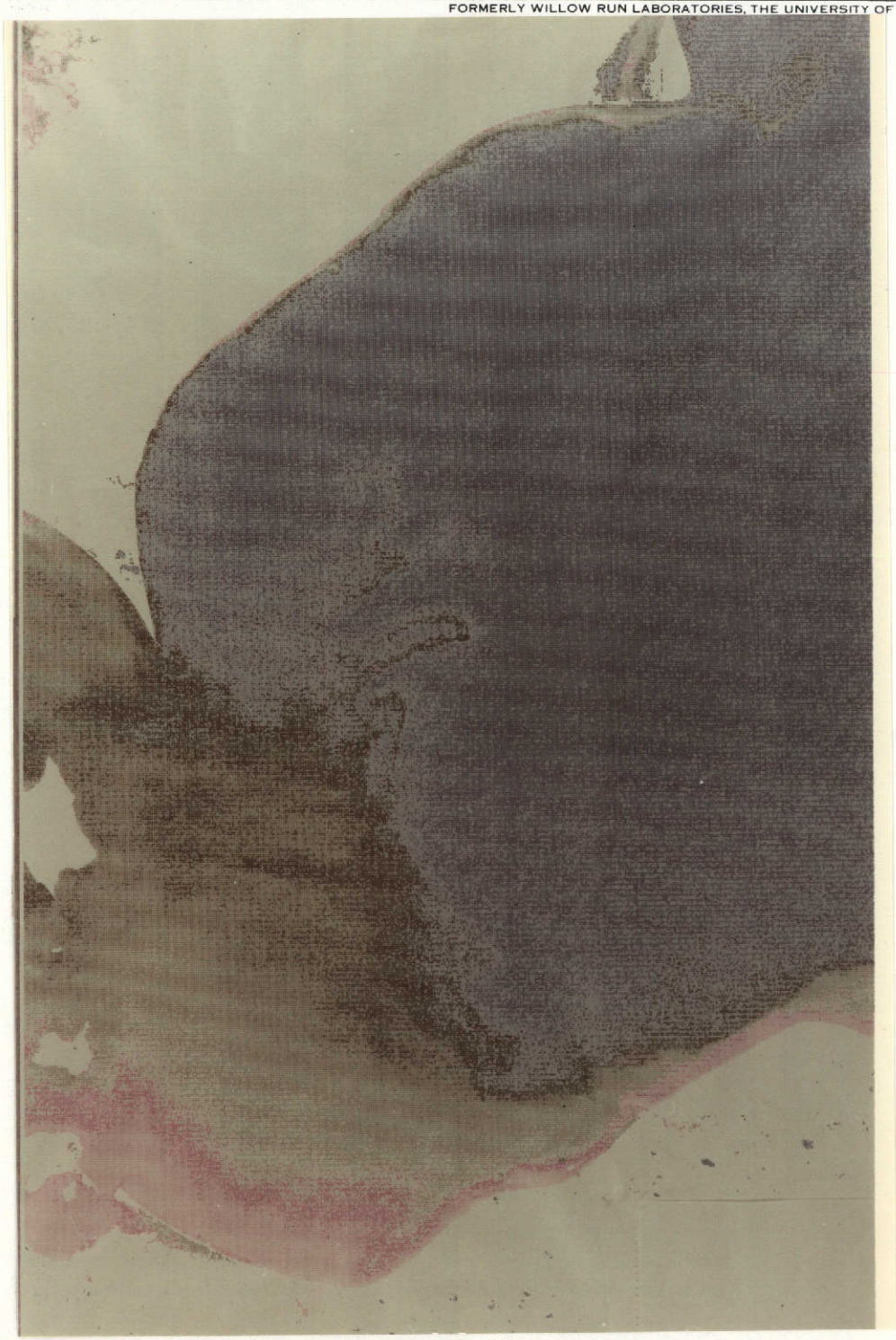

N

FIGURE 19. LAKE ERIE, 9 SEPTEMBER 1972. ERTS-1 data, E-1048-15404-5.

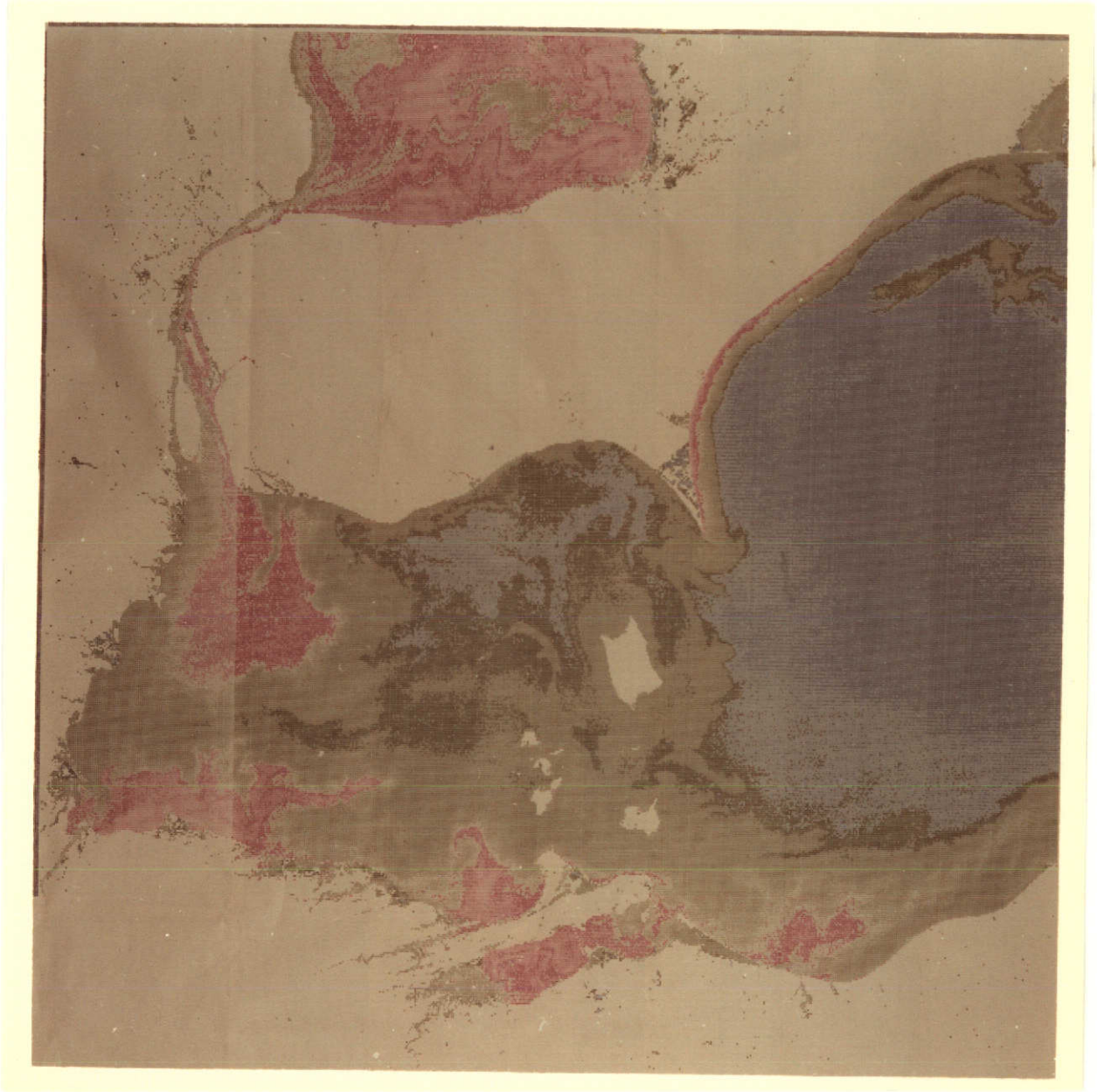

N

FIGURE 20. LAKE ERIE, 27 MARCH 1973. ERTS-1 data, E-1247-15481-5.

The Lake Michigan investigation has been hampered by a paucity of suitable data. A good data set, 1321-15584 and 1321-15590 9 June 1973, has been received recently and will be analyzed during the next reporting period. Visual examination shows pollution discharging from the Burns Harbor Area, tributary river discharges are visible, and an anomaly in the lake is discernible which appears to be related to the "thermal" bar. The "thermal" bar produces a color anomaly as well as a thermal anomaly. Aircraft coverage of this area was obtained on 11 June 1973 as part of work currently in progress for the State of Michigan.

Work performed during the period 1 January to 30 June 1973 has consisted of compilation and visual examination of all ERTS imagery received.

NEW TECHNOLOGY

None

PROGRAM FOR NEXT REPORTING INTERVAL

The following activities are planned for the next reporting interval:

1. Visual analysis of ERTS imagery, as received.

2. Digital processing of ERTS frames:

   a. 1258-15082 New York 7 April 1973
   b. 1294-15081 New York 13 May 1973
   c. 1208-15345 Tampa 16 February 1973

3. SPARC processing of ERTS frames

   a. 1262-15350 Tampa 11 April 1973
   b. 1321-15484 L. Michigan 9 June 1973
   c. 1321-15490 L. Michigan 9 June 1973

4. Water quality data collection and analysis -- Lake Erie

In the event that suitable data becomes available for the other test locations, computer processing of the data will be instituted. High-gain data is reported to have been collected on 13 May 1973 for the New York test locations. An attempt will be made to develop signatures for the various water masses (and waste fields) in the scene.

CONCLUSIONS

The investigation clearly demonstrates that major color and turbidity differences (due to suspended solids) are detectable through an analysis of ERTS data. Furthermore, the results indicate that this capability can be applied to the study of specific events such as ocean dumping of wastes, physical limnology of large lakes, and large scale pollution investigations. However, the investigation also indicates that the full capabilities of ERTS-1 are not being exploited. In general, the signal range over water is too small to detect the more subtle pollution events. Use of the high-gain mode for MSS 4 and MSS 5 can be expected to increase the utility of ERTS-1 data.

The objectives of the investigation at the New York, Tampa, and Lake Erie test sites are being realized. The phenomena under investigation are large in scale and exhibit a relatively high contrast as compared with background or adjacent waters. Studies at the above test locations are demonstrating the utility of satellite remote sensing for large scale water resource monitoring. At each test location, the program is providing specific information regarding the spread and movement of waste fields or water masses and providing information regarding surface circulation.

RECOMMENDATIONS

The full potential of ERTS-1 for water resource data collection should be determined. In this regard it is recommended that the high-gain option for Bands MSS 4 and MSS 5 be exercised on future orbits over the test site.

Second Type II Progress Report
R. Horvath, MMC 079
Task IX, Oil Pollution Detection

INTRODUCTION

The overall objective of this investigation is to determine the feasibility of using remote sensing from satellites or spacecraft in order to assist the U. S. Coast Guard in fulfilling its mission in the area of oil pollution detection and monitoring and law enforcement. The hypothesis involved is that the synoptic coverage of vast areas which is possible from spacecraft altitudes will provide an extra dimension and capability to the present Coast Guard program of surface monitoring and remote sensing from aircraft.

Three specific objectives can be defined. The first is to determine the detectability of "small scale" oil slicks associated with illegal dumping of contaminated ballast water, or inadvertant leakage of petroleum cargo, from ships operating in near-shore sea lanes. The most obvious method of "tagging" specific vessels to such occurrences is based upon proximity. However, the synoptic large area coverage capability of spacecraft remote sensing offers the possibility of "tagging" an offender hours after the occurrence by using the vessel's own wake to vector and track between the oil slick and the miles-distant vessel.

The second specific objective of this investigation is to determine the background level of oil pollution due to the presence of heavy industrialization near shipping lanes, and the masking effect of this upon detection of the shipping-associated pollution with which the Coast Guard is primarily concerned. Temporal variations in this background level can be studied by utilizing the repetitive nature of the ERTS coverage.

The third specific objective of this investigation is to demonstrate the utility of spaceborne remote sensing platforms in monitoring the extent and spread of oil slicks resulting from major pollution incidents, such as catastrophic shipping accidents or oil well blow-outs. The large areal extent of such occurrences severely strains the capability of surface and even airborne attempts to define the situation. Timely wide area coverage from a spaceborne sensor could significantly increase the effectiveness with which damage prevention and clean-up operations are deployed.

PROGRESS

ERTS-1 imagery of the Oakland, California area taken on 22 and 23 January 1973 has been received. Analysis of these images indicates the possible detection of the 120,000 gallon waste oil slick which was released from shore storage into the Oakland Inner Harbor on 19 January 1973. Detection on the images is severely hampered by the confinement of the very low oil/water contrast within the relatively narrow (200 to 400 m) channel which exhibits high water/land contrast at the edges. However, ERTS channels 5 and 6 do indicate a region of rather tenuous contrast whose apparent movement between 22 and 23 January coincides with the approximate position of the major oil concentration as reported by the U. S. Coast Guard on-scene commander. ERTS CCT's have been ordered for further analysis.

The general problems which have been encountered in attempting to acquire ERTS data suitable for this investigation are indicated in Table 1. This tabulation shows the relationship between major oil spill incidents and ERTS-1 overflights for the last eight months. These data show that the nature of the ERTS coverage, when combined with the vagueries of weather and the short-lived nature of most oil spills, has led to a rather exasperating combination of near misses.

PROGRAM FOR NEXT REPORTING INTERVAL

During the next reporting period, the CCT's of the Oakland oil spill will be analyzed in order to confirm (or deny) the possible detection seen on the imagery.

NEW TECHNOLOGY - None

CONCLUSIONS

None

RECOMMENDATIONS

None

TABLE 1. COINCIDENCE OF MAJOR SPILLS AND ERTS OVERFLIGHTS

Location	Oil Type	Quantity	Report Date	Clean Date	ERTS Date	Comments
Salem, Mass.	#2 and #5 Fuel Oil	29,500 gal.	2 Oct. 72	after 4 Oct.	8 Oct. 72	Good Data Too late
Barataria Bay, Louisiana	Crude	336,000 gal.	9 Oct. 72	Dissipated before 17 Oct.72	18/19 Oct. 72	Overcast
San Antonio, Texas	Diesel Fuel	678,000 gal.	11 Oct. 72	≈ 17-18 Oct. 72	24 Oct. 72	Too late
San Juan City, New Mexico	Crude	100,000 gal.	12 Oct. 72	≈ 1 Nov. 72	16/17 Oct. 72	Overcast
Lake Barre, Louisiana	Crude	700 bbl.	22 Nov. 72	≈ 24 Nov. 72	23/24 Nov. 72	Overcast
Albemarle Snd, N. C.	Bunker, C	1000 gal.	28 Nov. 72	29 Nov. 72	3 Dec. 72	Good Data Too late
Gulf Coast Penzoil rig J, Storm II	Gas and oil (burning)	?	4 Dec. 72	6 Dec. 72	11 Dec. 72	Overcast Too late
Timbalier Bay, La. (well blowout)	Gas, Light	(minor ?)	6 Dec. 72	?	12 Dec. 72	Overcast
Jennings, La. (Bayou Nezpique)	Crude	3720 bbls.	14 Dec. 72	?	12/13 Dec. 72	Too early
Alameda, Ca. (Naval Air Station)	10% diesel 20% solvent 70% 20/40 lube	>1400 gal.	22 Dec. 72	23 Dec. 72	17 Dec. 72	Too early
Fenwick, Conn. (L. I. Sound)	#6 Fuel Oil	12,000 gal.	26 Dec. 72	30 Dec. 72	7 Jan. 73	Too late
Gulf Coast, La. (Pltfm A West Delta 79, Signal Oil Co.)	Crude	400,000 gal.	10 Jan. 73	11 Jan. 73 (Dissipated)	15/16 Jan. 73	Too late

TABLE 1. COINCIDENCE OF MAJOR SPILLS AND ERTS OVERFLIGHTS (CONT.)

Location	Oil Type	Quantity	Report Date	Clean Date	ERTS Date	Comments
Oakland, Ca.	Waste Oil	~120,000 gal.	19 Jan. 73	Contained 24 Jan. Completed 4 Feb.	22/23 Jan. 73	Images Received Tapes Ordered
Vicksburg, Miss.	#2 Fuel Oil	4500 bbl.	31 Jan. 73	3 Feb. 73 (Dissipated)	4 Feb. 73	Too late
Baton Rouge, La.	Crude	500,000 gal.	1 Mar. 73	Before 13 Mar. 73	12 Mar. 73	Too late
Bellingham, Wash.	?	est. 1000 gal. (7 sq. mi. slick)	2 Mar. 73	?	3 Mar. 73	Overcast
Cold Bay, Alaska	Diesel and Gasoline	235,000 gal.	9 Mar. 73 (start 8 Mar.)	18 Mar. 73	14/15 Mar. 73	Overcast
Houston, Texas	Oil and Diesel	420,000 gal.	12 Mar. 73 (start 9 Mar.)	19 Mar. 73	15 Mar. 73	Overcast
LaParguera, Puerto Rico	Crude	38,000 bbl.	19 Mar. 73	After 5 April 1973	29 Mar. 73	No Data Taken
Baton Rouge, La.	Slop Oil	40,000 gal.	28 Mar. 73	After 29 Mar. 73	30 Mar. 73	Overcast
Providence, R. I.	#6 Fuel Oil	50,000 gal.	12 Apr. 73	Before 20 Apr. 73	24 Apr. 73	Too late
Norfolk, Va.	Navy Distillate	30,000 gal.	27 Apr. 73	?	26 Apr. 73	Too early
Grand Isle, La.	Crude	240,000 gal.	11 May 73	?	22 May 73	Too late

Second Type II Progress Report
R. K. Vincent, MMC 075
Task X, Mapping Iron Compounds

INTRODUCTION

In previous reports on this task a ratio method has been described which is designed to map geologic targets, particularly iron compounds, with consistent results for data gathered under different atmospheric and illumination conditions. The method involves the subtraction of the radiance of the darkest object in the scene from every other point in the scene for each MSS channel, to correct for atmospheric path radiance, the ratioing of the resulting radiances from several pairs of MSS channels, and the normalization of these ratios to a known reference point in the scene to correct for atmospheric transmission and solar illumination variations.

The data processing technique for implementing this method has been successfully employed for a small portion of a single ERTS frame for the southern end of the Wind River Range, Wyoming. These results were shown at the ERTS Symposium in March. Once the technique had been implemented, the need arose to test whether the corrective measures for atmospheric and solar illumination effects were working and to theoretically test the usefulness of the ratio method for discriminating iron oxides from each other and from other natural targets. Those were the principal goals of this reporting period.

PROGRESS

During this reporting period the efforts of this task were directed toward the following:

(1) Evaluating the effectiveness of the ratio method described in the Type I report for suppressing atmospheric effects.

(2) Determining expected ratio signatures of iron oxides from laboratory data and determining how unique they are, compared with other natural targets.

To investigate the effectiveness of the dark object subtraction and ratio normalization corrections of the ratio method described in prior reports, digital temporal ratio maps were produced in the following manner. Spectral ratio maps (R_{75}, for example) of two different ERTS passes were produced, with dark object subtraction and ratio normalization to correct for atmospheric effects. The two spectral ratio maps were then merged by computer software such that they spatially coincided, and then

one spectral ratio map was divided by the other to produce a temporal ratio map. Theoretically, only those objects on the ground which have changed will have a temporal ratio appreciably different from 1.0, if the empirical atmospheric corrections are accurate. A temporal ratio map was produced over the test area (Atlantic City District, Wyoming). The two ERTS passes used to produce the temporal ratio were in August and October 1972; during the latter pass, the test site was half-covered by cumulus clouds. The path radiance, as determined from dark object subtraction, was approximately the same for both passes, even though the August frame was cloud free. Most non-vegetative targets were found to have a temporal ratio within 10% of 1.0 in this first attempt. The normalization area was restricted to a portion of the iron mine (non-vegetative and not cloud covered); hence, the ground in the normalization area could have changed slightly in spectral properties in the two months between frames. Three similar temporal ratio maps were produced of the same area from the same two ERTS frames, except no dark object subtraction and no ratio normalization were made. In one case, the straight R_{75} spectral ratio (uncorrected for atmospheric effects) was the subject of the temporal ratio. In the second case, the single-channel radiance of channel 5 was temporally ratioed, i.e., channel 5 in August divided by channel 5 in October, with no dark object subtraction or normalization procedures. In the third case, the same procedure was repeated for channel 7. In each of these three cases the ground changes, both vegetative and non-vegetative, appeared considerably greater than the temporal ratio produced from the atmospherically corrected R_{75} ratio. The next bimonthly report will give quantitative results comparing these three temporal ratio maps. This indicates that the dark object subtraction and ratio normalization are reducing the atmospheric effects, as they were designed to do. The degree to which the atmospheric effects are removed will be reported in the next bimonthly report. This procedure for atmospheric corrections may help other ERTS investigators to improve their change-detection maps for phenology studies.

The second achievement of this reporting period was the preparation and use of laboratory reflectance spectra from the NASA Earth Resources Spectral Information System for determining the ratio signatures of iron oxides and for identifying other natural targets which will be confused with iron oxides in ratio processing from ERTS data. Compression of the laboratory data into a shorter, more useable format was made desirable by the requirement that the resulting data types must be searched at least once for each geological target of interest. Hence, the following procedure was initiated.

The curves (approximately 750 of them) used from ERSIS were initially selected on the basis of being continuous through the range .4 to 1.1 microns, except that many of the vegetation curves which met this criterion were

omitted because this ERTS experiment deals primarily with non-vegetative targets. After being called from the data bank, the curves were run through a computer program (DATFIX) that produced equal spacing between data points. This placed the data into the proper format for another computer program (ERAGAL), which calculated the average reflectance in the four ERTS multispectral scanner channels for each curve. A 50% sine filter was used to approximate the spectral shapes of the ERTS scanner channels. ERAGAL also calculated the six non-redundant ratios from the four channels. If the symbol for the i^{th} channel reflectance divided by the j^{th} channel reflectance is taken to be R_{ij}, these six ratios were R_{76}, R_{75}, R_{74}, R_{65}, R_{64}, and R_{54}, where channel 7 is .8 - 1.1 μm, 6 is .7 - .8 μm, 5 is .6 - .7 μm, and 4 is .5 - .6 μm.

Each ratio was divided into ten intervals, each containing approximately 10% of the 750 spectral curves taken from ERSIS, as determined from a histogram plot of R_{ij} versus the number of curves having an R_{ij} in a given interval ΔR_{ij}. Each of the ten ΔR_{ij} intervals was then assigned a digit from 0 to 9. Table 1 shows the ten intervals, with their assigned digits, for each of the six ratios. In this manner a six-digit number, one digit for each R_{ij}, with the order of ratio digits from left to right as shown in Table 1, was created for each of the 750 curves. For example, the limestone spectrum in ERSIS has the following reflectance ratios: $R_{76} = 1.16$, $R_{75} = 1.38$, $R_{74} = 1.55$, $R_{65} = 1.20$, $R_{64} = 1.34$, $R_{54} = 1.12$. [Note: The single channel reflectances from which these were derived were $\rho_4 = 28.92\%$, $\rho_5 = 32.44\%$, $\rho_6 = 38.82\%$, and $\rho_7 = 44.92\%$.] Therefore, the R_{76} value falls into the interval assigned to the digit 5, R_{75} and R_{74} into the digit 4 intervals, etc. For this limestone spectrum the resulting six-digit number, which will be hereafter referred to as the ERTS MSS ratio code, is 544348. Thereby, the entire limestone spectrum in the 0.5 to 1.1 μm wavelength region is reduced to a six-digit number, the ratio code. Note that the intervals for each R_{ij} ratio are approximately 5% or less of the R_{ij} ratio value, except for the broad end intervals, to which the digits 0 and 9 are assigned.

Table 2 gives the ratio codes for 54 soil types (129 spectra), 82 minerals (181 spectra), 17 rock types (25 spectra), and 15 types of vegetation (18 spectra), calculated from ERSIS spectra. The documents from which these spectra originate, listed in Table 3, provide more information about these data. Although ratio codes for mineral and rock powders of 0 - 74 μm and 0 - 5 μm grain sizes were calculated, they are not reported here because they are unrealistic for most rocks and minerals in the natural state.

Although the data in Table 3 are still being studied, several searches of the data have been made already. Searches are made by specifying the ranges of each digit of the ratio code and examining the data for materials whose ratio codes fall within those limits. For instance, the ratio codes for the 74 - 250 μm grain size sample of goethite is 114249. Therefore, a search was made where the first digit ranged from 1 to 2, the second digit was 1, the third digit was 3 to 4, the fourth was 1 to 2, the fifth was 3 to 4, and the sixth digit was 9. With these ratio ranges, the results of the search are shown in Table 4. A computer program was used to perform these searches automatically, but they can be done simply enough by inspection of Table 2. Also shown in Table 4 are searches with other iron oxides as subjects.

Generally speaking, most soils have a sixth digit of 9, unlike most other materials; and the ERTS MSS ratios seem to be less dependent than single channel reflectances on soil moisture. For spectrally flat materials, dark materials cannot be discriminated by the ratios from bright ones, as evidenced by the confusion between dark magnetite and some of the bright carbonate minerals. However, the ability to discriminate the iron oxides from all except the materials listed in Table 4 is encouraging, from the standpoint of mineralogical exploration. More searches and study will be made concerning the use of these ratio codes in the next few months and their impact on geochemical remote sensing.

NEW TECHNOLOGY

Temporal ratio maps of spectral ratios corrected for effects of atmospheric and solar illumination variations were made for the first time. These should be useful for change detection in a number of disciplines, especially phenology.

Ratio codes for laboratory data were created and used for the first time. These ratio codes are a form of data compression, which tell (within 5% for most cases) in just six digits what ratios can be expected for a given material from ERTS MSS data. These ratio codes are the forerunners of an on-board data bank in an Earth resources satellite package of the future.

PROGRAM FOR NEXT REPORTING INTERVAL

During the next reporting period it is planned that automatic recognition maps will be produced of the entire ERTS frame by two methods. First, the traditional statistical likelihood ratio decision rule (using in-scene training sets) will be implemented with the six non-redundant ratios as inputs, instead of the single channel radiances usually input for that method. The ratio means and variances will be measured for each of the planned eight training sites, which will be compared with ratios calculated from

lab data for the targets expected to be found in each test site. Second, ratios from laboratory data will be used as training sets to make automatic recognition maps by either a Euclidean distance or ratio gating logic method. This will be an attempt to practically eliminate in-scene training sets from the data processing procedure.

Also, during the coming period a field trip will be conducted to evaluate automatic recognition maps and ratio images for geochemical mapping. Finally, the effectiveness of the atmospheric and solar illumination corrections will be quantitatively assessed.

CONCLUSIONS AND RECOMMENDATIONS

The dark object subtraction and ratio normalization procedures used for atmospheric corrections are reducing the effects of atmosphere and solar illumination variations on the ratioed images. The degree of their effectiveness will be determined in the next reporting period. Those investigators making phenological studies would probably benefit from making temporal ratio maps of an R_{75} or R_{74} ratio, corrected with dark object subtraction and ratio normalization.

Laboratory data indicate that the iron oxides of hematite, goethite, magnetite, ilmenite, and limonite (actually a goethite with more water in the cavities) can be discriminated from one another. The other materials which look like these iron oxides are given in Table 4, which shows that all of the above iron oxides except magnetite are fairly unique, i.e., they should be confused with only five or less of the approximately 165 natural materials in the studied subset of ERSIS data. These findings should have a significant impact on mineralogical exploration and general geologic mapping, if these laboratory spectra results can be reproduced with ERTS scanner data. During the next three months, we should know approximately to what degree the laboratory data results can be translated into geologic automatic recognition maps from ERTS data.

Table 1. Ratio Intervals for Six-Digit ERTS MSS Ratio Code

Code	Ratio Intervals					
	1st Digit (R_{76})	2nd Digit (R_{75})	3rd Digit (R_{74})	4th Digit (R_{65})	5th Digit (R_{64})	6th Digit (R_{54})
0	0- .914	0- .949	0- .949	0- .999	0- .999	0- .849
1	.915- .969	.950-1.049	.950-1.024	1.000-1.049	1.000-1.049	.850- .924
2	.970-1.029	1.050-1.134	1.025-1.124	1.050-1.149	1.050-1.149	.925- .929
3	1.030-1.084	1.135-1.324	1.125-1.224	1.150-1.249	1.150-1.299	.930- .934
4	1.085-1.144	1.325-4.499	1.225-1.599	1.250-1.499	1.300-1.499	.935- .939
5	1.145-1.199	4.500-5.199	1.600-2.499	1.500-2.499	1.500-2.499	.940- .949
6	1.200-1.249	5.200-5.899	2.500-3.499	2.500-3.499	2.500-3.499	.950- .999
7	1.250-1.299	5.900-6.599	3.500-4.499	3.500-4.499	3.500-4.499	1.000-1.049
8	1.300-1.399	6.600-7.499	4.500-5.499	4.500-5.499	4.500-5.499	1.050-1.149
9	1.400-90.0	7.500-90.0	5.500-90.0	5.500-90.0	5.500-90.0	1.150-90.0

ERIM
FORMERLY WILLOW RUN LABORATORIES, THE UNIVERSITY OF MICHIGAN

TABLE 2. ERTS Multispectral Scanner Ratio Codes For Selected Laboratory Data from the NASA Earth Resources Spectral Information System (ERSIS)

Category	Name and Description	ERSIS Curve Number	ERTS MSS Ratio Code
Soils	Clay Alonso type (Puerto Rico, dry)	B00830203	235459
	" " (Puerto Rico, wet)	B00830205	246469
	Matanzas type (Cuba, dry)	117	447479
	" " (Cuba, wet)	118	347479
	Oriente type (Cuba, dry)	101	223238
	" " (Cuba, wet)	102	224249
	Orman type (N. Carolina, dry)	097	645349
	" " (N. Carolina, wet)	099	545349
	Quibdo (Gravelly, dry)	001	235259
	" (Gravelly, wet)	003	235359
	Loam (Unspecified)		
	Akron type (Alabama, dry)	075	346469
	" " (Alabama, wet)	076	247469
	Albion type (Kansas, dry)	082	846459
	" " (Kansas, wet)	084	946459
	Blakely type (Georgia, dry)	062	446359
	" " (Georgia, wet)	064	446359
	Clarion (Iowa, dry)	017	845459
	" (Iowa, wet)	019	946459
	Colt's Neck type (New Jersey, dry)	049	235359
	" " " (New Jersey, wet)	051	125359
	" " " (New Jersey, dry)	059	135469
	" " " (New Jersey, wet)	060	035469
	" " " (New Jersey, dry)	141	236469
	" " " (New Jersey, wet)	142	035469
	Greenville type (Louisiana, dry)	159	347479
	" " (Louisiana, wet)	161	236469
	Hamakua, Heavy type (Hawaii, dry)	079	135359
	" " " (Hawaii, wet)	080	025359
	Onomea type (Hawaii, dry)	131	114249
	" " (Hawaii, wet)	132	113139
	Weld type (Colorado, dry)	133	645459
	" " (Colorado, wet)	134	545459

Category	Name and Description	ERSIS Curve Number	ERTS MSS Ratio Code
Soils	Loam (Clay Type)		
	Aiken Clay (Oregon, dry)	B00830029	235359
	" " (Oregon, wet)	031	025359
	Blakely Clay (Georgia, dry)	183	345459
	" " (Georgia, wet)	185	445359
	Clareville Clay (Texas, dry)	105	434249
	" " (Texas, wet)	106	435359
	Dublin Clay (California, dry)	125	745349
	" " (California, wet)	126	544238
	Moaula Light Clay (Hawaii, dry)	037	345459
	" " " (Hawaii, wet)	039	446469
	" " " (Hawaii, dry)	127	346469
	" " " (Hawaii, wet)	128	146469
	Naalehu Heavy Clay (Hawaii, dry)	061	345459
	" " " (Hawaii, wet)	063	246469
	" " " (Hawaii, dry)	151	345459
	" " " (Hawaii, wet)	153	446469
	Ookala Clay (Hawaii, dry)	109	035469
	" " (Hawaii, wet)	110	125359
	" " (Hawaii, dry)	113	135459
	" " (Hawaii, wet)	114	135359
	Pierre Clay (Wyoming, dry)	071	334249
	" " (Wyoming, wet)	072	334249
	Loam (Silt Type)		
	Aguan Silt (Honduras, dry)	025	235359
	" " (Honduras, wet)	027	234359
	Alamance Silt (S. Carolina, dry)	123	334249
	" " (S. Carolina, wet)	124	335359
	Decatur Silt (Tennessee, dry)	089	546359
	" " (Tennessee, wet)	091	646459
	Guthrie Silt (Kentucky, dry)	149	445359
	" " (Kentucky, wet)	150	545459
	Herradura Pure Silt (Cuba, dry)	021	235259
	" " " (Cuba, wet)	023	335259
	Marshall Silt (Iowa, dry)	119	946459
	" " (Iowa, wet)	120	946459

Category	Name and Description	ERSIS Curve Number	ERTS MSS Ratio Code
Soils	Loam (Silt Type)		
	Maury Silt (Tennessee, dry)	B00830081	546459
	" " (Tennessee, wet)	083	646469
	Penn Silt (N. Carolina, dry)	098	545459
	" " (N. Carolina, wet)	100	746459
	Tilsit Silt (Indiana, dry)	143	334259
	" " (Indiana, wet)	145	235359
	Zanesville Silt (Indiana, dry)	041	434249
	" " (Indiana, wet)	043	335259
	Loam (Sandy Type)		
	Barnes Fine Sandy (S. Dakota, dry)	087	946459
	" " " (S. Dakota, wet)	088	945459
	Black Volcanic Sandy (Guatemala, dry)	191	645459
	" " " (Guatemala, wet)	193	745459
	Gooch Fine Sandy (Oregon, dry)	144	234249
	" " " (Oregon, wet)	146	335359
	Grady Sandy (Georgia, dry)	121	845349
	" " (Georgia, wet)	122	945359
	Greenville Sandy (Georgia, dry)	057	025359
	" " (Georgia, wet)	058	015359
	Hall Very Fine Sandy (Nebraska, dry)	066	845459
	" " " " (Nebraska, wet)	068	845459
	Orangeburg Fine Sandy (Louisiana, dry)	147	336359
	" " " (Louisiana, wet)	148	236469
	Putnam Fine Sandy (Oklahoma, dry)	085	846459
	" " " (Oklahoma, wet)	086	946459
	Ruston Sandy (Georgia, dry)	053	336369
	" " (Georgia, wet)	055	336469
	" " (Georgia, dry)	093	235359
	" " (Georgia, wet)	095	025459
	" " (Georgia, dry)	129	224249
	" " (Georgia, wet)	130	125259
	Santa Barbara Gravelly Fine Sandy (Cuba, dry)	069	124259
	(Cuba, wet)	070	015359
	" " (Cuba, dry)	163	235259
	" " (Cuba, wet)	165	125359

Category	Name and Description	ERSIS Curve Number	ERTS MSS Ratio Code
Soils	Loam (Sandy Type)		
	Tifton Sandy Type (Georgia, dry)	B00830077	125359
	" " " (Georgia, wet)	078	025359
	Tillman Fine Sandy (Oklahoma, dry)	073	647469
	" " " (Oklahoma, wet)	074	447479
	Vernon Very Fine (Texas, dry)	103	446459
	" " " (Texas, wet)	104	546469
	Weld Fine Sandy (Colorado, dry)	137	645459
	" " " (Colorado, wet)	138	545459
	Joplin Stony (Montana, dry)	090	445359
	" " (Montana, wet)	092	445459
	Sand		
	Colt's Neck Loamy (New Jersey, dry)	111	135359
	" " " (New Jersey, wet)	112	015359
	Orangeburg (N. Carolina, dry)	115	236369
	" (N. Carolina, wet)	116	136369
	Rubicon (Michigan, dry)	005	435359
	" (Michigan, wet)	007	445459
	Ruston Fine Type (N. Carolina, dry)	139	125359
	" " " (N. Carolina, wet)	140	015359
	Windthorst Type (Oklahoma, dry)	107	546469
	" " (Oklahoma, wet)	108	547469
	" " (Oklahoma, dry)	199	545359
	" " (Oklahoma, wet)	201	646459
	Light Tan Sand with Some Grass (Fort Walton, Florida)	A02010101	746459
	Gray Sand (Fort Walton, Florida)	A02012101	435349
	Gray, Washed Pit Sand (Ann Arbor, Michigan)	A02013101	334239
Minerals	Silicates		
	Amphibole (Tremolite, St. Lawrence Cty, N.Y.)		
	74 - 250 µm	B09000003	000007
	250 - 1200 µm	4	000017
	74 - 250 µm	7	000006
	250 - 1200 µm	8	000017

C

Category	Name and Description		ERSIS Curve Number	ERTS MSS Ratio Code
Minerals	Silicates			
	Amphibole (Actinolite, Chester, Vermont)			
		74 - 250 μm	B09000011	000101
		250 - 1200 μm	12	010215
	Amphibole (Actinolite, San Bernardino, Calif)			
		74 - 250 μm	B09000015	000001
		250 - 1200 μm	16	000001
	Amphibole (Hornblende, Brewster, N.Y.)			
		74 - 250 μm	B09000019	434337
		250 - 1200 μm	20	311006
	Amphibole (Hornblende, Clintonville, N.Y.)			
		74 - 250 μm	B09000023	100006
		250 - 1200 μm	24	111017
	Amphibole (Hornblende, Gore Mts, N.Y.)			
		74 - 250 μm	B09000027	323238
		250 - 1200 μm	28	212127
	Andalusite (Australia)			
		74 - 250 μm	B09000031	334249
		250 - 1200 μm	32	334249
	Anorthoclase (Larvik, Norway)			
		74 - 250 μm	B09000035	334238
		250 - 1200 μm	36	434238
	Beryl (Maine)			
		74 - 250 μm	B09000039	500002
		250 - 1200 μm	40	800000
	Biotite (Bancroft, Ontario, Canada)			
		250 - 1200 μm	B09000043	212018
	Chabazite (Colorado)			
		74 - 250 μm	B09000045	223238
	Chlorite (Colorado)			
		74 - 250 μm	B09000048	324128
	Chlorite (Calaveras County, California)			
		74 - 250 μm	B09000052	400000
		250 - 1200 μm	B09000050	200000
	Danburite (New York)			
		74 - 250 μm	B09000055	101018
		250 - 1200 μm	56	213128

Category	Name and Description		ERSIS Curve Number	ERTS MSS Ratio Code
Minerals	Silicates			
	Dumortierite (Pershing County, Nevada)			
		74 - 250 μm	B09000059	435359
		250 - 1200 μm	60	545459
	Kaolinite (Mesa Alta, New Mexico)			
		74 - 250 μm	B09000062	212128
		250 - 1200 μm	63	212128
	Kaolinite (Macon, Georgia)			
		74 - 250 μm	B09000070	223238
		250 - 1200 μm	71	223238
	Montmorillorite (Polkville, Mississippi)			
		74 - 250 μm	B09000073	124359
		250 - 1200 μm	74	024359
	Montmorillonite(Amory, Mississippi)			
		74 - 250 μm	B09000077	114249
		250 - 1200 μm	78	002039
	Muscovite (Effingham Township, Ontario, Canada)			
		74 - 250 μm	B09000081	222127
	Olivine (Forsterite, Crestmore, California)			
		74 - 250 μm	B09000089	111127
		250 - 1200 μm	90	113238
	Olivine (Fayalite, Jackson County, North Carolina)			
		74 - 250 μm	B09000093	000006
		250 - 1200 μm	94	000006
	Orthoclase (Ruggles Mine, New Hampshire)			
		74 - 250 μm	B09000102	213238
		250 - 1200 μm	103	223238
	Plagioclase (Albite, Amelia, Virginia)			
		74 - 250 μm	B09000106	212128
		250 - 1200 μm	107	212127
	Plagioclase (Oligoclase, Norway)			
		74 - 250 μm	B09000110	212127
		250 - 1200 μm	111	212128
	Plagioclase (Andesine, Montana)			
		74 - 250 μm	B09000114	224238
		250 - 1200 μm	115	213139
	Plagioclase (Labradorite, New York)			
		74 - 250 μm	B09000118	111117
		250 - 1200 μm	119	100007

Category	Name and Description		ERSIS Curve Number	ERTS MSS Ratio Code
Minerals	Silicates			
	Plagioclase (Bytownite, Minnesota)			
		74 - 250 µm	B09000122	210006
		250 - 1200 µm	123	100001
	Pyroxene (Augite, Canada)			
		74 - 250 µm	B09000126	100005
		250 - 1200 µm	127	200001
	Pyroxene (Diopside, New York)			
		74 - 250 µm	B09000130	000000
		250 - 1200 µm	131	000000
	Pyroxene (Hedenburgite, Montana)			
		74 - 250 µm	B09000134	323228
		250 - 1200 µm	135	213138
	Pyroxene (Hypersthene, Canada)			
		74 - 250 µm	B09000137	014359
		250 - 1200 µm	138	000249
	Pyroxene (Bronzite, North Carolina)			
		74 - 250 µm	B09000141	000008
		250 - 1200 µm	142	000029
	Quartz			
		250 - 1200 µm	B09000145	211117
	Quartz (Milky)			
		149 - 250 µm	B09000146	323228
		250 - 420 µm	147	323128
	Serpentine (Missouri)			
		250 - 1200 µm	B09000155	000001
	Talc (North Carolina)			
		74 - 250 µm	B09000066	101018
		250 - 1200 µm	67	000006
	Oxides and Hydroxides			
	Brucite (Lodi, Nevada)			
		74 - 250 µm	B09005003	112128
		250 - 1200 µm	04	000018
	Cassiterite (Nigeria)			
		74 - 250 µm	B09005007	024359
		250 - 1200 µm	08	013239
	Chrysoberyl (South Dakota)			
		74 - 250 µm	B09005011	223228
		250 - 1200 µm	12	324238

Category	Name and Description		ERSIS Curve Number	ERTS MSS Ratio Code
Minerals	Oxides and Hydroxides			
	Corundum (Transvaal, Africa)			
		74 - 250 μm	B09005017	434238
		250 - 1200 μm	18	544348
	Cuprite (Butte, Montana)			
		74 - 250 μm	B09005019	746459
		250 - 1200 μm	20	746459
	Diaspore (Rosebud, Missouri)			
		74 - 250 μm	B09005024	545349
		250 - 1200 μm	25	434249
	Gibbsite (Brazil)			
		74 - 250 μm	B09005028	334249
		250 - 1200 μm	29	234249
	Goethite (Biwabik, Minnesota)			
		74 - 250 μm	B09005032	003249
		250 - 1200 μm	33	113139
	Hematite (Irontown, Minnesota)			
		74 - 250 μm	B09005036	546459
	Ilmenite (Norway)			
		74 - 250 μm	B09005039	434238
	Limonite			
		74 - 250 μm	B09004003	015359
	Limonite (Sawed Plate)			
			B09004004	014259
	Limonite			
		250 - 1200 μm	B09004005	125359
	Limonite (Tuscaloosa County, Alabama)			
		250 - 1200 μm	B09005042	025459
	Magnetite (Farmington County, Colorado)			
		74 - 250 μm	B09005045	323127
	Magnetite (Michigan)			
		74 - 250 μm	B09005048	200006
	Psilomelane (Magdalena, New Mexico)			
		74 - 250 μm	B09005050	212117
		250 - 1200 μm	51	100006
	Pyrolusite (Villa Grove, Colorado)			
		74 - 250 μm	B09005053	534128
		250 - 1200 μm	54	534238

Category	Name and Description		ERSIS Curve Number	ERTS MSS Ratio Code
Minerals	Oxides and Hydroxides			
	Pyrolusite(Brazil)			
		74 - 250 μm	B09005057	545359
		250 - 1200 μm	58	845459
	Rutile (Mexico)			
		74 - 250 μm	B09005060	646459
		250 - 1200 μm	61	846459
	Rutile (Georgia)			
		74 - 250 μm	B09005063	746459
		250 - 1200 μm	64	645459
	Zincite (Plus Franklinite, New Jersey)			
		74 - 250 μm	B09005067	345459
		250 - 1200 μm	68	324249
	Carbonates			
	Azurite (Bisbee, Arizona)			
		74 - 250 μm	B09008003	830000
		250 - 1200 μm	4	930000
	Calcite (Mexico)			
		74 - 250 μm	B09008006	211117
		250 - 1200 μm	8	211117
	Calcite (Cherokee Co., Kan.)			
		74 - 250 μm	B09008010	111117
		250 - 1200 μm	12	100006
	Dolomite (Mass.)			
		74 - 250 μm	B09008015	111117
		250 - 1200 μm	16	100117
	Dolomite (New York)			
		74 - 250 μm	B09008019	111117
		250 - 1200 μm	20	111117
	Magnesite (California)			
		74 - 250 μm	B09008023	212127
		250 - 1200 μm	24	212127
	Magnesite (Norway)			
		74 - 250 μm	B09008026	000117
		250 - 1200 μm	27	000117
	Malachite (Arizona)			
		74 - 250 μm	B09008030	400000
		250 - 1200 μm	31	600000

Category	Name and Description		ERSIS Curve Number	ERTS MSS Ratio Code
Minerals	Carbonates			
	Rhodochrosite (Argentina)			
		74 - 250 μm	B09008033	013349
		250 - 1200 μm	34	003359
	Siderite (Conn.)			
		74 - 250 μm	B09008036	000359
		250 - 1200 μm	37	004359
	Smithsonite (New Mexico)			
		74 - 250 μm	B09008039	000001
		250 - 1200 μm	40	000000
	Strontianite (Westphalia)			
		74 - 250 μm	B09008041	322127
		250 - 1200 μm	42	322127
	Witherite	74 - 250 μm	B09008044	212117
		250 - 1200 μm	45	212128
	Sulphur, Sulfates, and Sulfides			
	Alunite (Utah)			
		74 - 250 μm	B09009003	224249
		250 - 1200 μm	4	235359
	Arsenopyrite (Utah)			
		74 - 250 μm	B09009007	212117
		250 - 1200 μm	8	211117
	Barite (Colorado)			
		74 - 250 μm	B09009011	334249
		250 - 1200 μm	12	335359
	Celestite (Mexico)			
		74 - 250 μm	B09009015	334238
		250 - 1200 μm	16	444348
	Chalcocite (Montana)			
		74 - 250 μm	B09009020	200001
		250 - 1200 μm	21	200001
	Chalcopyrite (Canada)			
		74 - 250 μm	B09009024	113139
		250 - 1200 μm	25	200005
	Cinnabar (Nevada)			
		74 - 250 μm	B09009027	336369
		250 - 1200 μm	28	336369

Category	Name and Description		ERSIS Curve Number	ERTS MSS Ratio Code
Minerals	Sulphur, Sulfates, and Sulfides			
	Cobaltite (Canada)			
		74 - 250 μm	B09009031	212117
		250 - 1200 μm	32	222128
	Enargite (Peru)			
		74 - 250 μm	B09009035	734228
		250 - 1200 μm	36	533127
	Galena (Kansas)			
		74 - 250 μm	B09009039	100006
	Gypsum (Italy)			
		74 - 250 μm	B09009042	111117
		250 - 1200 μm	43	111117
	Gypsum (Utah)	74 - 250 μm	B09009046	111117
		250 - 1200 μm	47	111117
	Gypsum (New York)			
		74 - 250 μm	B09009050	212127
		250 - 1200 μm	51	112127
	Jamesonite (Bolivia)			
		74 - 250 μm	B09009058	434249
		250 - 1200 μm	59	544249
	Jarosite (Nevada)			
		Rough Surface	B09009060	004149
	Marcasite (Oklahoma)			
		74 - 250 μm	B09009063	212117
		250 - 1200 μm	64	111006
	Molybdenite (Utah)			
		74 - 250 μm	B09009066	945348
		250 - 1200 μm	67	945348
	Niccolite (Canada)			
		74 - 250 μm	B09009069	434238
		250 - 1200 μm	70	434238
	Proustite (Colorado)			
		74 - 250 μm	B09009072	845459
		250 - 1200 μm	73	545459
	Pyrargyrite (Nevada)			
		74 - 250 μm	B09009075	333228
		250 - 1200 μm	76	323228

Category	Name and Description		ERSIS Curve Number	ERTS MSS Ratio Code
Minerals	Sulphur, Sulfates, and Sulfides			
	Pyrite (Colorado)			
		74 - 250 μm	B09009079	002139
		250 - 1200 μm	80	002128
	Pyrrhotite (Canada)			
		74 - 250 μm	B09009083	645349
		250 - 1200 μm	84	745459
	Realgar (Nevada)			
		74 - 250 μm	B09009086	447479
		250 - 1200 μm	87	446469
	Sphalerite (Colorado)			
		74 - 250 μm	B09009089	324138
	Stibnite (Mexico)			
		74 - 250 μm	B09009092	969559
		250 - 1200 μm	93	979558
	Sulphur (Nevada)			
		74 - 250 μm	B09009096	334238
		250 - 1200 μm	97	334249
	Thenardite (California)			
		74 - 250 μm	B09009101	222228
		250 - 1200 μm	102	223228
Rocks	Igneous			
	Andesite (Hornblende, California)			
		420 - 500 μm	B09012026	000028
	Andesite (Porphyry, Colorado)			
		420 - 500 μm	B09012021	112128
	Basalt (Oregon)			
		420 - 500 μm	B09012028	000106
	Basalt		B14004091	110100
	Basaltic Lava			
		Broken Surface	B09004013	111226
	Basaltic Lava			
		Iron Oxide Stained	B09004010	223238
	Basaltic Lava		B14004084	000128
	Basaltic Lava		A01697001	000007

Category	Name and Description	ERSIS Curve Number	ERTS MSS Ratio Code
Rocks	Igneous		
	Diorite (Hornblende, Mass.)		
	420 - 500 μm	B09012016	000007
	Diorite (Porphyry, Canada)		
	420 - 500 μm	B09012018	001128
	Gabbro (Bytownite, Minn.)		
	420 - 500 μm	B09012024	110006
	Granite (Biotite, Rhode Island)		
	420 - 500 μm	B09012029	334239
	Granite (Hornblende, Mass.)		
	420 - 500 μm	B09012020	212127
	Granite Potash	B14004095	221212
	Granodiorite (Minn.)		
	420 - 500 μm	B09012017	223238
	Obsidian (Oregon)		
	420 - 500 μm	B09012022	000006
	Peridotite (Mica-augite, Arkansas)		
	420 - 500 μm	B09012023	100006
	Peridotite (Serpentinite, New York)		
	420 - 500 μm	B09012030	000006
	Pumice Broken Surface	B09004011	334249
	Rhyolite (Grey, Colorado)		
	420 - 500 μm	B09012019	212228
	Rhyolite (Pink, Colorado)		
	420 - 500 μm	B09012027	224249
	Sedimentary and Metamorphic		
	Chert	A00263001	434239
	Flint	B14004096	445359
	Greenstone	A00261001	000101
	Limestone	B14004087	544348
	Marble	B14004094	110105
	Sandstone (Red)	B14004090	000000
	Sandstone (Yellow)	B14004088	434349
	Shale	B14004086	212117

Category	Name and Description	ERSIS Curve Number	ERTS MSS Ratio Code
Vegetation	Grass and Moss		
	Clover	B09004008	899980
	Grass (Swamp, green)	B01176007	489980
	Grass (Coarse)	B09004007	778870
	Grass (Dead)	B01176048	945459
	Moss (Healthy - non-fruiting)	B20000391	799999
	Moss (Sphagnum)	B03333001	356760
	Straw (Dead)	B01176046	545459
	Coniferous Trees		
	Pine (Needles)	B09004009	357870
	Pine (Black, Needles)	B01176006	357871
	Pine (Ponderosa, healthy needles)	B03333012	467870
	Pine (White, needles)	B03070003	478970
	Pine (Red, needles)	B03559007	948579
	Pine (Jack, bark)	B01818027	947459
	Deciduous Trees		
	Ash (American, new leaf)	B00829128	599990
	Dogwood (new leaf)	B00829152	489980
	Maple (Red. new leaf)	B00829138	499980
	Oak (green leaf)	B01176003	599980
	Sycamore(green leaf, upper surface)	B04803003	448778

Table 3. Source Documents for ERSIS Laboratory Spectra

Document Number	Reference
B00830	Hopkins: Reflectance Curves of Various Soils, USAERDL, Ft. Belvoir, Virginia, ca. 1955 (unpublished).
B09000	Hunt, Salisbury: "Visible and Near-Infrared Spectra of Minerals and Rocks: I. Silicate Minerals," Mod. Geol., Vol. I, 1970, pp. 283-300.
B09004	Hunt, Ross: "A Bidirectional Reflectance Accessory for Spectroscopic Measurements," Appl. Opt., Vol. 6, No. 10, October 1967, pp. 1687-1690.
B09005	Hunt, Salisbury: "Visible and Near-Infrared Spectra of Minerals and Rocks: III. Oxides and Hydroxides," Mod. Geol., Vol. II, 1971, pp. 195-205.
B09008	Hunt, Salisbury: "Visible and Near-Infrared Spectra of Minerals and Rocks: II. Carbonates," Mod. Geol., Vol. II, 1971, pp. 23-30.
B09009	Hunt, Salisbury: "Visible and Near-Infrared Spectra of Minerals and Rocks: IV. Sulphides and Sulphates," accepted by Mod. Geol. for 1971.
B09012	Ross, Adler, Hunt: "A Statistical Analysis of the Reflectance of Igneous Rocks from 0.2 to 2.65 Microns," Icarus, Vol. 11, 1969, pp. 46-54.
B14004	Williamson: Night Reconnaissance Subsystem (U), (Final Technical Documentary Report), Martin-Marietta Corp., Orlando, Florida, November 1964, AD 355 324 (CONFIDENTIAL).
B01176	Wright: Spectral Reflectance Characteristics of Camouflage Greens Versus Camouflage Detection, IRMA III Report No. 1281, USAERDL, Ft. Belvoir, Virginia, March 1953.
B03333	Infrared Optical Measurements, Report No. 8626, NBS, Washington, D.C., December 1964.
B03070	Gates et al.: Spectral Properties of Plants, Appl. Opt., Vol. 4, No. 1, 1965.

Document Number	Reference
B20000	Reflectance of Target and Background Materials, unpublished data from the Air Force Target Signature Measurement Program, Willow Run Laboratories, Institute of Science and Technology, The University of Michigan, Ann Arbor, 1967.
B03559	Barbrow: Calibration on the Spectral Directional Reflectance of Six Samples of Red Pine Needles, NBS, Test No. G-35201-1, Agricultural Research Center, Belleville, Maryland, November 1964, (unpublished).
B01818	Kronstein: Research, Studies, and Investigations on Spectral Reflectances and Absorption Characteristics of Camouflage Paint Materials and Natural Objects, Final Report, Contract DA-44-009 ENG-1447, New York University, New York, March 1955.
B00829	Hopkins: Reflectance Curves of Various Leaves, USAERDL, Ft. Belvoir, Virginia, ca. 1955 (unpublished).
B04803	Cooper, Derksen: Spectral Reflectance and Transmittance of Forest Fuel Materials (Final Report), Material Lab, New York Naval Shipyard, Brooklyn, New York, March 1952.
A00263	Measured at Environmental Research Institute of Michigan.
A00261	Measured at Environmental Research Institute of Michigan.
A01697001	Measured at Environmental Research Institute of Michigan.
A02010	Measured at Environmental Research Institute of Michigan.
A02012	Measured at Environmental Research Institute of Michigan.
A02013	Measured at Environmental Research Institute of Michigan.

Table 4. Results of Searches for Materials Which Are Inseparable from Several Iron Oxides by ERTS MSS Ratio Methods

Subject of the Search			Materials With Which the Oxides Can Be Confused	
Name	Curve No.	Ranges of 6-Digit Ratio Code	Name	Curve No.
Goethite (Minn.)	B09005032	1-2, 1, 3-4, 1-2, 3-4, 9	Montmorillonite (Amory, Miss.)	B09000077
(Minn.)	B09005033		Cassiterite (Nigeria)	B09005008
			Chalcopyrite (Canada)	B09009024
			Jarosite (Nevada)	B09009060
Hematite (Minn.)	B09005036	6, 4, 6, 4, 5, 9	Loam, Weld Type (Colorado, wet)	B00830134
			Loam, Weld Fine Sandy Type (Colorado, wet)	B00830138
Magnetite (Colorado)	B09005045	2-3, 0-2, 0-3, 0-1, 0-2, 6-7	Amphibole (Hornblende, NY)	B09000023
			Amphibole (Hornblende, NY)	B09000024
			Amphibole (Hornblende, NY)	B09000028
			Danburite (New York)	B09000055
			Talc (North Carolina)	B09000066
			Muscovite (Canada)	B09000081
			Olivine (Forsterite, Calif.)	B09000089
			Plagioclase (Albite, Virginia)	B09000107
			Plagioclase (Oligoclase, Norway)	B09000110
			Plagioclase (Labradorite, NY)	B09000118

Name	Curve No.	Ranges of 6-Digit Ratio Code
Plagioclase (Labradorite, NY)	B09000119	
Plagioclase (Bytownite, Minn.)	B09000122	
Quartz	B09000145	
Psilomelane (New Mexico)	B09005050	
Psilomelane (New Mexico)	B09005051	
Calcite (Mexico)	B09008006	
Calcite (Mexico)	B09008008	
Calcite (Kentucky)	B09008010	
Calcite (Kentucky)	B09008012	
Dolomite (Massachusetts)	B09008015	
Dolomite (Massachusetts)	B09008016	
Dolomite (New York)	B09008019	
Dolomite (New York)	B09008020	
Magnesite (California)	B09008024	
Magnesite (California)	B09008023	
Witherite (England)	B09008044	
Arsenopyrite (Utah)	B09009007	
Arsenopyrite (Utah)	B09009008	
Cobaltite (Canada)	B09009031	

Name	Curve No.	Ranges of 6-Digit Ratio Code
Ilmenite (Norway)	B09005039	4, 3, 4, 2, 3, 8

Name	Curve No.
Galena (Kansas)	B09009039
Gypsum (Italy)	B09009042
Gypsum (Italy)	B09009043
Gypsum (Utah)	B09009046
Gypsum (Utah)	B09009047
Gypsum (New York)	B09009050
Gypsum (New York)	B09009051
Marcasite (Oklahoma)	B09009063
Marcasite (Oklahoma)	B09009064
Diorite (Hornblende, Mass.)	B09012016
Granite (Hornblende, Mass.)	B09012020
Peridotite (Mica-Augite, Ark.)	B09012023
Gabbro (Bytownite, Minn.)	B09012024
Shale	B09012086
Chrysoberyl (South Dakota)	B09005012
Celestite (Mexico)	B09005015
Niccolite (Canada)	B09005069
Niccolite (Canada)	B09005070
Sulphur (Nevada)	B09005096

Name	Curve No.	Ranges of 6-Digit Ratio Code
Limonite (Alabama)	B09005042	0-1, 1-2, 5, 3-4, 5, 9
Limonite (Alabama)	B09004003	
Limonite (Alabama)	B09004004	

Name	Curve No.
Montmorillonite (Mississippi)	B09000073
Montmorillonite (Mississippi)	B09000074
Pyroxene (Canada)	B09000137
Cassiterite (Nigeria)	B09005007